

Investigating the Effects of Variable Water Chemistry on Bacterial Transport during Stormwater Infiltration

A Thesis

Submitted to the Faculty

of

Drexel University

by

Haibo Zhang

in partial fulfillment of the

requirements for the degree

of

Doctor of Philosophy

January 2013

ACKNOWLEDGEMENTS

This work would not have been accomplished without the help and support of my family, friends, advisors and colleagues. I would like to take this opportunity to express my sincere gratitude to the following people.

My thanks go first to my advisor, Dr. Mira S. Olson, for her clear guidance and encouragement throughout my study at Drexel University. Thank you for providing professional advice on both my research and my future careers.

I also thank my committee members, Dr. Charles Haas, Dr. Patrick Gurian, Dr. Franco Montalto, Dr. Patricia Gallagher, Dr. Susan Kilham for their comments and suggestions on this work. I also thank Dr. Diederik Jacques for his generous help and advice on programming in HP1.

Appreciation is also given to Tatiana Morin and Jeff Gu for preparing sampling sites at New York City and taking water samples. I also thank Nahjan Amer Nordin for her hard work on column transport experiments. Working with You guys was a fun and unforgettable experience.

To my friends and colleges at Drexel, Suting Hong, Dr. Jingjie Teng , Dr. Tao Hong, Ziwen Yu, Dr. Rajveer Singh, Dr. Michael Ryan, Neha Sunger, Dr. Joanna Pope and Dr. Shamia Hoque and many more. You made my time at Drexel enjoyable and memorable.

I am deeply grateful to my family for their endless love, support and encouragement to further my education.

TABLE OF CONTENTS

LIST OF TABLES	vii
LIST OF FIGURES	viii
ABSTRACT.....	xi
CHAPTER 1. INTRODUCTION	1
1.1 Motivation and Significance of Research	1
1.2 Objectives.....	3
1.3 Dissertation Structure.....	4
CHAPTER 2. BACKGROUND	6
2.1 Introduction	6
2.2 Stormwater Runoff Pollutants.....	6
2.3 Potential Microbial Contamination to Groundwater	9
2.4 Factors Affecting Microbial Deposition and Transport	9
2.4.1 Chemical factors	11
2.4.2 Physical factors.....	11
2.4.3 Biological factors.....	12
2.5 Microbial Transport Modeling	13
2.5.1 The governing solute transport equation	13
2.5.2 Reactive transport modeling.....	15
2.5.3 Laboratory method	17
2.6 Stormwater Best Management Practices (BMPs)	17
2.6.1 Bioretention systems.....	18
2.6.2 Bacterial removal in bioretention systems.....	23
2.7 Knowledge Gap.....	24
CHAPTER 3. THE EFFECTS OF HEAVY METAL ON BACTERIAL TRANSPORT IN THE SUBSURFACE.....	26
3.1 Introduction	27
3.2 Materials and Methods	28
3.2.1 Soil characteristics	28

3.2.2 Solution chemistry	29
3.2.3 Bacterial growth and quantification	29
3.2.4 Live-dead bacterial viability assay	30
3.2.5 Zeta potential measurement.....	30
3.2.6 Metal-bacteria batch adsorption experiments.....	31
3.2.7 Bacteria-soil batch adsorption experiments.....	32
3.2.8 Column transport experiments.....	33
3.3 Results	36
3.3.1 Soil elemental coverage.....	36
3.3.2 Bacterial characteristics	38
3.3.3 Metal adsorption to bacteria	39
3.3.4 Bacterial adsorption to soil	42
3.3.5 Column transport experiments.....	43
3.4 Discussion	45
CHAPTER 4. EVALUATING THE EFFECTS OF VARIABLE WATER CHEMISTRY ON BACTERIAL TRANSPORT DURING INFILTRATION.....	49
4.1 Introduction	51
4.2 Material and Methods.....	53
4.2.1 Development of rate equation to predict attachment at the soil-water interface (SWI)	53
4.2.2 Sensitivity analysis of bacterial attachment rate at the SWI	57
4.2.3 Modeling approach	61
4.2.4 Model application to lab data	67
4.3 Results	73
4.3.1 Validation of rate equations used to predict bacterial attachment rate at the SWI	73
4.3.2 Profile of attachment rate to SWI under two scenarios simulated	75
4.3.3 Sensitivity analysis of SWI attachment rate	77
4.3.4 Inverse modeling of soil hydraulic parameters and dispersivity	80
4.3.5 Application of semi-reactive microbial transport model to bacterial transport data.....	80
4.4 Discussion	83

CHAPTER 5. FIELD EVALUATION AND MODELING OF MICROBIAL POLLUTANT REMOVAL IN BIORETENTION SYSTEMS USING A SEMI-REACTIVE MICROBIAL TRANSPORT MODEL.....	84
5.1 Introduction	86
5.2 Methods	88
5.2.1 Site description	88
5.2.2 Soil characterization	91
5.2.3 Water sampling	91
5.3 Data Analysis	92
5.4 Application of the Semi-reactive Microbial Transport Model.....	93
5.5 Results	94
5.5.1 Soil properties.....	94
5.5.2 Storm event characteristics.....	96
5.5.3 Water quality analysis	96
5.5.4 Application of the semi-reactive microbial transport model	107
5.6 Discussion	115
5.6.1 The effect of antecedent conditions on bacterial removal.....	115
5.6.2 The effect of preferential flow paths on bacterial removal	116
CHAPTER 6. CONCLUSIONS AND FUTURE RESEARCH	121
6.1 Conclusions	121
6.2 Future Research.....	123
LIST OF REFERENCES.....	127
Appendix A: List of Symbols	140
Appendix B: List of Abbreviation and Acronyms.....	143
Appendix C: Experimental Protocols	144
Appendix D: PHREEQC Programming for the Semi-reactive Microbial Transport Model	146
VITA.....	157

LIST OF TABLES

Table 2-1. The percent removal of pollutants by bioretention systems in laboratory and field studies	21
Table 3-1. Synthetic stormwater and nutrient solution composition	32
Table 3-2. Summary of parameters used to calculate single collector contact efficiency and attachment efficiency of <i>E. coli</i> in soil.....	36
Table 4-1. Summary of input variables in rate prediction	60
Table 4-2. Summary of constant parameters used in rate prediction.....	61
Table 4-3. Summary of column transport scenarios	67
Table 4-4. The fitted soil hydraulic parameters, soil properties and bacterial properties.	70
Table 5-1. The soil properties at Nashville bioretention area.....	95
Table 5-2. Characteristics of storm events.....	96
Table 5-3. Concentrations of total nitrogen and total phosphorous in stormwater runoff and lysimeter effluent samples collected from the Nashville bioretention area for all sampled storm events	102
Table 5-4. Initial soil moisture profile for the lysimeter at Nashville bioretention area on August 15 th , 2012.....	108
Table 5-5. The surface flux to the lysimeter at Nashville bioretention area on August 15 th , 2012.....	109
Table 5-6. Fitted soil hydraulic parameters for Nashville bioretention area	110

LIST OF FIGURES

Figure 2-1. Illustration of DLVO theory including total interaction energy (Φ_T), the electrostatic interaction energy (Φ_{el}) and the van der Waals forces (Φ_{vdw}).....	10
Figure 2-2. Schematic of a typical bioretention system (Roy-Poirier, Champagne et al. 2010)	19
Figure 3-1. SEM images of soil equilibrated with synthetic stormwater (A); quantitative histogram for all elements present on soil surfaces before (B) and after (C) equilibrated with synthetic stormwater. The presence of carbon is from carbon coating during sample preparation to prevent surface charging up.....	38
Figure 3-2. Adsorption of copper, zinc and lead to <i>E. coli</i> K12 cells in synthetic stormwater. Solid lines represent linear isotherms fitted with $K_d = 0.235 \text{ L}/10^9 \text{ cells}$ ($R^2 = 0.83$) for copper, $K_d = 0.616 \text{ L}/10^9 \text{ cells}$ ($R^2 = 0.97$) for zinc and $K_d = 4.34 \text{ L}/10^9 \text{ cells}$ ($R^2 = 0.88$) for lead.....	41
Figure 3-3. Isotherms of bacteria-soil batch adsorption experiments. Solid lines show linear isotherms fitted with $K_d = 0.0100 \text{ mL}/\text{mg}$, $R^2 = 0.91$ (BNS-U), $K_d = 0.0119 \text{ mL}/\text{mg}$, $R^2 = 0.83$ (BNS-T), $K_d = 0.0229 \text{ mL}/\text{mg}$, $R^2 = 0.89$ (BSS-U), and $K_d = 0.0338 \text{ mL}/\text{mg}$, $R^2 = 0.86$ (BSS-T).....	43
Figure 3-4. Breakthrough curves (BTCs) with error bars representing standard error/deviation from triplicate transport experiments with <i>E. coli</i> suspended in nutrient solution (red squares) and in synthetic stormwater (blue diamonds).	45
Figure 4-1. Procedure of two-phase Monte Carlo analysis.....	59
Figure 4-2. Schematic diagram of stormwater infiltration and bacterial transport and deposition in the subsurface.....	62
Figure 4-3. The schematic of the modeling approach of HP1, reproduced from Jacques and Šimůnek (2005).....	63
Figure 4-4. Schematic of the column setup for water flow and bacterial transport experiments	72
Figure 4-5. Predicted attachment rate using combined rate equations and corrected attachment rate versus the experimentally determined attachment rate from Elimelech, Magaiet <i>et al.</i> (2000). The background ionic strength is 1mM.	74
Figure 4-6. Predicted bacterial attachment rate using combined rate equations and corrected attachment rate versus experimentally determined attachment rate from Redman, Walker <i>et al.</i> (2004). The ionic strength varied from 1 mM to 100 mM.	74

Figure 4-7. Profiles of pH, ionic strength and bacterial attachment rate at the SWI 6 inches from the top of the column under two transport scenarios: infiltration of bacteria and synthetic stormwater (SSW) into columns equilibrated with artificial groundwater (SSW_AGW, blue diamonds), and infiltration of bacteria and artificial groundwater (AGW) into columns equilibrated with AGW (AGW_AGW, red squares).	76
Figure 4-8. The variation of bacterial attachment rate due to physical variables (physical simulations) and chemical variables (chemical iterations within each physical simulation). (a) Boxplot of bacterial attachment rate at the SWI under different physical simulations; chemical parameters are varied within each simulation in 500 iterations; (b) distribution of CDFs of attachment rate resulting from 500 chemical iterations within 500 physical simulations; each CDF represents the distribution of attachment rate within each physical simulation resulting from variation of chemical variables; the distribution of 500 CDFs represents the variability of attachment rate due to physical variables. (c) 5 th , 50 th and 95 th percentile of the distribution of simulated CDFs of attachment rate.	79
Figure 4-9. Observed (red square vs blue diamond) and modeled (red line vs blue line) bacterial breakthrough curves under constant solution chemistry (AGW_AGW, R squared = 0.951) and variable solution chemistry (SSW_AGW, R squared = 0.986). Each observation point represents the average of triplicate experiments with error bars representing standard error.	81
Figure 5-1. Schematic of Nashville bioretention area and Colfax bioretention area.....	90
Figure 5-2. Site setup of Nashville basin (A-E) and Colfax bioretention area (F). (A) overview of Nashville bioretention area; (B) the flume and the still pond; (C) the influent housing; (D) the weighing lysimeter; (E) the effluent housing; (F) overview of Colfax bioretention area with the weighing lysimeter and the effluent housing.	90
Figure 5-3. The particle size distribution of soil mix from Nashville bioretention area ..	95
Figure 5-4. Precipitation and bacterial concentration in water samples collected at the Nashville bioretention area for the storm event on 20 th , July 2012: (1) precipitation; (2) <i>E.coli</i> concentrations in the lysimeter influent and effluent.	98
Figure 5-5. Precipitation and bacterial concentration in the water samples collected at the Nashville bioretention area for the storm event on 15 th , August, 2012: (1) precipitation; (2) <i>E. coli</i> concentrations in the lysimeter influent and effluent.	99
Figure 5-6. Precipitation and bacterial concentration in water samples collected at the Nashville bioretention area for the storm event on 18 th , September, 2012: (1) precipitation; (2) <i>E. coli</i> concentrations in the lysimeter influent and effluent.....	100
Figure 5-7. Chemical properties of water samples collected at the Nashville bioretention area for the storm event on 20 th , July, 2012: (1) total nitrogen; (2) total phosphorous; (3) turbidity in both influent and effluent.	103

Figure 5-8. Chemical properties of water samples collected at the Nashville bioretention area for the storm event on 15th, August, 2012: (1) total nitrogen; (2) total phosphorous; (3) turbidity in both influent and effluent. 104

Figure 5-9. Chemical properties of water samples collected at the Nashville bioretention area for the storm event on 18th, September, 2012: (1) total nitrogen; (2) total phosphorous; (3) turbidity in both influent and effluent 105

Figure 5-10. Chemical properties of water samples collected at the Colfax bioretention area for the storm event on 15th, August, 2012 and 18th, September, 2012: (1) total nitrogen; (2) total phosphorous; (3) turbidity. 106

Figure 5-11. The monitored soil water content at five discrete depths (5 cm, 10 cm, 20 cm, 30 cm and 50 cm) right before the storm occurred on August 15th, 2012. A linear trend line was established and used to estimate soil water content at other soil depths. 111

Figure 5-12. The observed (D, circle) and fitted (N, solid line) volumetric water content at different depths during the storm event on August 15th, 2012. Number 1, 2, 3 and 4 represent depths of 5 cm, 10 cm, 20 cm and 30 cm. 112

Figure 5-13. The observed (diamond) bacterial breakthrough data and modeled (square) bacterial breakthrough data at Nashville bioretention area for the storm event on August 15th, 2012. 114

Figure 5-14. The observed (diamond) and modeled (square) cumulative bacterial counts in effluent samples at Nashville bioretention area for the storm event on August 15th, 2012..... 114

Figure 5-15. The water volume of influent and effluent during the storm event on August 15th, 2012 117

Figure 5-16. The changes of volumetric water content (VWC) at different depths corresponding to the precipitation on August 15th, 2012 and September 18th, 2012..... 119

Figure 5-17. The changes of lysimeter mass over time during the storm events on August 15th and September 18th, 2012. 120

ABSTRACT

Investigating the effects of variable water chemistry on bacterial transport during stormwater infiltration

Haibo Zhang

Pathogenic microorganisms and heavy metals have frequently been detected in urban stormwater runoff. Pathogens transport to the groundwater table with the infiltrating water and cause groundwater contamination. A variety of physical, chemical and biological factors have been studied for their effects on bacterial transport. However, the effect of heavy metals has largely been ignored, despite the elevated concentrations common in stormwater runoff. This work examines changes in bacterial and soil surfaces using scanning electron microscopy and energy dispersive X-ray spectroscopy after exposure to synthetic stormwater amended with heavy metals. Sets of batch bacterial sorption experiments were conducted under different conditions by varying heavy metal concentrations in synthetic stormwater and soil exposure history. The results indicate that the presence of heavy metals increases bacterial attachment to soil surfaces.

Modeling bacterial transport during stormwater infiltration is challenging due to the variability and complexity of the physical, chemical and biological interactions in the soil-water-bacteria system. This work quantified changes in bacterial attachment under variable solution chemistry using a newly combined rate equation, which varies temporally and spatially with changes in solution chemistry. The relative importance of physiochemical variation on the estimation of bacterial attachment was quantitatively described using two-phase Monte Carlo analysis. A semi-reactive microbial transport

model was further developed in HP1 (HYDRUS1D-PHREEQC) with the incorporation of the newly combined rate equation. The model matched observed bacterial breakthrough curves in laboratory column experiments well. This method represents one step towards a more realistic model of bacterial transport in complex microbial-water-soil systems.

The developed model was further applied to the investigation of bacterial removal in field bioretention systems. The influent and effluent water samples from bioretention systems in New York City were sampled and analyzed over the summer of 2012 for fecal indicator *Escherichia coli*. Reduction of the effluent bacterial concentrations was observed and the removal efficiency was up to 66%. The antecedent dry period was found to affect bacterial removal. Shorter antecedent dry period results in higher soil moisture which is favorable for bacteria in soil to persist. The semi-reactive microbial transport model was applied and the modeled bacterial removal efficiency agrees well with observed values with a slight overestimation. This is primarily due to the presence of preferential flow paths in the field bioretention systems, which are not considered in the model.

CHAPTER 1. INTRODUCTION

1.1 Motivation and Significance of Research

Transport of pathogenic microorganisms into subsurface environments has drawn considerable attention in the last two decades due to the outbreak of waterborne diseases associated with the microbial contamination of groundwater (Blackburn, Craun et al. 2004). Urban stormwater runoff has been identified as one of the primary sources of water pollution to groundwater due to its high content of pollutants. Large volumes of stormwater runoff are generated due to the increase of impervious surfaces along with urbanization. The stormwater runoff often carries pollutants as it infiltrates through surfaces, including total suspended solids, nutrients, heavy metals, organics as well as pathogenic microorganisms (Pitt, Clark et al. 1999; Davies and Bavor 2000; Prestes, Anjos et al. 2006; Brownell, Harwood et al. 2007; Helmreich, Hilliges et al. 2010)..

Understanding microbial transport behavior in the subsurface is essential to prevent aquifer contamination from pathogenic microorganisms. Large research efforts have been devoted to examining the factors that influence bacterial attachment/retention in porous media, including solution chemistry, porous media properties and bacterial properties. However, limited research is available on how stormwater composition may affect bacterial transport, even though elevated concentrations of heavy metals have been frequently reported in the stormwater runoff. Research questions in this work include: Do heavy metals in solution create more reactive sites for bacteria to attach to soil surfaces, and/or alter the charge of bacterial cell surfaces? To what extent do heavy metals affect

bacterial attachment and transport? Is there a correlation between bacterial attachment rate and dissolved heavy metals concentration?

Describing and modeling bacterial transport during infiltration of stormwater runoff is another challenge due to the variability and complexity of the physical, chemical and biological interactions in the soil-water-bacteria system. Porous media are naturally heterogeneous in terms of texture, structure, surface properties and composition. Solution chemistry varies spatially and temporally due to mixing of two water sources, stormwater runoff (composition depends on land use type and human activities) and groundwater (composition relies on the geological nature of the soil). Bacteria also present different surface properties under varying solution chemistries. Research questions in this work include: Do changes in solution chemistry significantly affect bacterial attachment rates during stormwater infiltration? Can this transport be modeled using a semi-reactive microbial transport model to capture changes in attachment rate due to changes in solution chemistry? What is the relative importance of the physical and chemical parameters on bacterial attachment?

Understanding the factors affecting bacterial attachment and further modeling of bacterial transport during stormwater infiltration provides supporting information for the design and construction of best management practices (BMPs), which have been widely constructed in urban areas to mitigate stormwater pollution. The BMPs include bioretention systems, detention basins, retention ponds, stormwater wetlands, vegetated strips. Bioretention systems are consistently recommended by the EPA to treat stormwater runoff and generally consist of water storage space, vegetation, mulch, bioretention soil mix, and gravel layer (from top to bottom). They can efficiently reduce

runoff volume and peak flow rate, promote infiltration and recharge groundwater, and reduce pollutant loads. However, large research efforts have been focused on the ability of those BMPs to remove physical and chemical contaminants, such as total suspended solids, nutrients and metals, while comparatively little effort has been placed on the effectiveness of microorganism removal from stormwater runoff. Peer reviewed literature on microorganism removal by bioretention systems is very limited, with most studies conducted in the laboratory scale and very few in the field. The laboratory studies are relatively easy to carry out with high degree of control over the experimental conditions although those studies fail to capture the heterogeneities in the field, such as the soil structure and composition and microbial activity. Research questions in this work include: How effective are the field bioretention systems at removing microbial pollutants? Can bacterial transport in field bioretention system be modeled using a semi-reactive microbial transport model?

1.2 Objectives

In view of the research needs stated above, three main objectives have been identified and specific tasks were developed as follows:

- 1) Investigate the effect of stormwater composition on bacterial attachment.
 - a. quantify changes in bacterial surface charge and soil elemental surface coverage following exposure to synthetic stormwater amended with heavy metals;
 - b. quantify changes in bacterial attachment onto soil samples due to the presence of heavy metals in synthetic stormwater.

- 2) Evaluate the effects of variable water chemistry on bacterial transport during infiltration.
 - a. develop a combined rate equation to predict bacterial attachment at the soil-water interface in response to changes in solution chemistry, and quantitatively evaluate the relative importance of physical and chemical parameters on bacterial attachment;
 - b. develop a semi-reactive microbial transport model incorporating the effects of variable water chemistry on bacterial attachment;
 - c. apply the model to predict bacterial transport under heterogeneous water chemistries.
- 3) Evaluate and model microbial pollutant removal in field bioretention systems using a semi-reactive microbial transport model
 - a. evaluate the performance of field bioretention systems in removing microbial pollutants;
 - b. model bacterial transport through a bioretention system using a semi-reactive microbial transport model.

1.3 Dissertation Structure

The remainder of this dissertation is presented in five additional chapters. Chapter 2 provides general background information to help understand the following research chapters. Chapter 3 examines the effects of stormwater solution chemistry on bacterial adsorption and transport behavior. Soil and bacterial surfaces were examined following exposure to synthetic stormwater and non-polluted nutrient media in order to quantify differences in bacterial attachment behavior. Chapter 4 describes the development of a

semi-reactive microbial transport model to predict bacterial transport under heterogeneous water chemistries within HP1 and the validation of this model using bacterial transport data from lab-scale column transport experiments. Chapter 5 presents field work measuring microbial pollutant removal in bioretention areas in New York City and includes modeling of bacterial transport data collected from the bioretention areas over the summer of 2012 using the semi-reactive microbial transport model. Finally, in Chapter 6, conclusions are presented along with recommendations for future work.

CHAPTER 2. BACKGROUND

2.1 Introduction

In this chapter, we present general background information regarding microbial contaminants in urban stormwater runoff, factors controlling microbial deposition and transport in porous media, modeling methods being used to describe microbial transport in the subsurface and finally the best management practices (BMPs) used to control stormwater runoff pollution.

2.2 Stormwater Runoff Pollutants

Prior to urbanization, groundwater was recharged from infiltration of relatively uncontaminated precipitation through permeable surfaces. With urbanization, permeable surfaces were replaced with impervious surfaces, which reduce natural groundwater recharge while greatly increasing the peak flow and the volume of stormwater runoff. In addition, the stormwater runoff available for recharge generally carries a significant load of pollutants, which can be detrimental to the quality of the groundwater and/or receiving water body. Pollutant concentrations in stormwater runoff are highly variable due to different types of land use, precipitation intensity, pollutant sources and other physiographic conditions. Typical pollutants in stormwater runoff are generally categorized as:

- Total Suspended Solids (TSS)
- Nutrients
- Pesticides, and other organic carbons

- Heavy metals
- Pathogenic microorganisms

TSS is primarily from erosion of soil surfaces and dust deposits on impervious surfaces. Nutrients in runoff are from plant fertilizers, detergents and animal waste. Pesticides in stormwater runoff are a result of their application to control weeds and insects, and are washed off during wet weather conditions. Contamination of runoff, and underlying groundwater, with pesticides such as diazinon, malathion, dacthal, dioxathion, chlordane, was reported in Florida, Arizona and California (Wilson, Osborn et al. 1990; Greene 1992). Other organic compounds are primarily from use of petroleum products (Pitt, Clark et al. 1999).

Heavy metals are found in urban runoff originating from a variety of sources associated with transportation (Yousef, Hvitved-Jacobsen et al. 1990; Brown and Peake 2006). The concentrations of heavy metals in urban stormwater runoff, including copper (Cu), lead (Pb), zinc (Zn), cadmium (Cd) and nickel (Ni), vary in order of magnitude. Lead, zinc and copper are abundant in stormwater runoff, and contribute to about 90% of the dissolved heavy metals (Harper 1985). Observed concentration ranges of Cu (0.00006- 1.41 mg/L), Pb (0.00057-26.0 mg/L) and Zn (0.0007-22 mg/L) have been summarized in a study by Walker et al. (Walker 1999). Several other studies on stormwater runoff have also reported concentrations of heavy metals within these ranges (Yousef 1984; May and Sivakumar 2009; Helmreich, Hilliges et al. 2010; Zgheib 2011).

Pathogenic microorganisms in stormwater runoff are most likely from feces of domestic animals and wildlife or human beings. The presence of pathogenic

microorganisms in stormwater runoff has been frequently reported (O'Shea and Field 1992; Davies and Bavor 2000; Jiang and Chu 2004; Arnone, Borst et al. 2005; Selvakumar and Borst 2006), including reports of *Salmonella* spp., *Pseudomonas aeruginosa*, *Staphylococcus aureus*, *Bacillus* spp., and *Clostridium perfringens*, viruses such as rotavirus, adenovirus, hepatitis A and enterovirus, and protozoa such as *Cryptosporidium* and *Giardia*.

The enumeration of bacterial, viral and parasitic pathogens in stormwater runoff is prohibitively expensive and time consuming. In contrast, fecal indicator organisms have been measured extensively due to relative ease of enumeration. *Escherichia coli* (*E. coli*) is a commonly used fecal indicator bacterium (others include total coliform, fecal coliform, fecal *Streptococci* and *Enterococcus*). Bacterial indicators are quantified to test if pathogenic microorganisms may be present in surface water. The criterion for *E. coli* is that the geometric mean concentration of *E. coli* over a 30-day period should not exceed 126 CFU/100ml for primary contact recreation as established by the U.S. EPA (USEPA 1986). *E. coli* concentrations in stormwater runoff have been reported with a wide range which varies due to land use and seasonal effects (Selvakumar and Borst 2004; Selvakumar and Borst 2006). However, the majority of stormwater runoff has *E. coli* concentrations much higher than the primary contact recreational criterion. The geometric mean concentration of *E. coli* in stormwater runoff ranges from 241 to 2400 CFU/100ml at six sites in Charlotte, NC while 111 to 1135 CFU/100ml at 4 sites in Wilmington, NC (Hathaway, Hunt et al. 2009). The median concentration of *E. coli* was reported with a range of 150 to 3990 CFU/100ml in International Stormwater Best

Management Practices (BMP) Database (Geosyntec Consultants and Wright Water Engineers 2012).

2.3 Potential Microbial Contamination to Groundwater

Groundwater is used as an important water supply source worldwide. According to the National Ground Water Association, approximate 44 percent of the U.S. population relies on groundwater for its drinking water supply from either a public source or private well (National Ground Water Association 2010). Transport of pathogenic microorganism into subsurface environments has drawn considerable attention in the last few decades due to the outbreak of waterborne diseases associated with the microbial contamination of groundwater (Blackburn, Craun et al. 2004). In addition to contamination resulting from the application of animal waste or leakage of human septic waste, stormwater runoff is also a pollution source contributing to groundwater contamination in urban areas. Pathogens present in stormwater runoff may transport to the groundwater table with the infiltrating water and cause contamination of groundwater, especially when the groundwater table is shallow and aquifer composition is mainly sandy soil mix. Viruses have been detected in groundwater up to 35 ft below a stormwater recharge basin located on Long Island (Vaughn, Landry et al. 1978).

2.4 Factors Affecting Microbial Deposition and Transport

Understanding the deposition of microorganisms in subsurface environments is critical to protect underlying groundwater from harmful microorganisms that may be present in the infiltrating water. Microbial deposition is controlled by the interactions between microorganisms and collector surfaces. The comprehensive theory of these interactions is the Derjaguin-Landau-Verwey-Overbeek (DLVO) theory which includes

electrostatic interactions and van der Waals forces (Hogg, Healy et al. 1966; Gregory 1981), shown in **Figure 2-1**. Typical total interaction energy profiles contain deep primary attractive wells at very small separation distances, an energy barrier and a smaller secondary attractive region at larger separation distances. Deposition in the primary well is considered to be irreversible due to the very large energy barrier, while deposition on secondary minima is reversible under constant chemical conditions. A great number of studies have been carried out to investigate the chemical, physical and biological factors influencing microorganism deposition and transport.

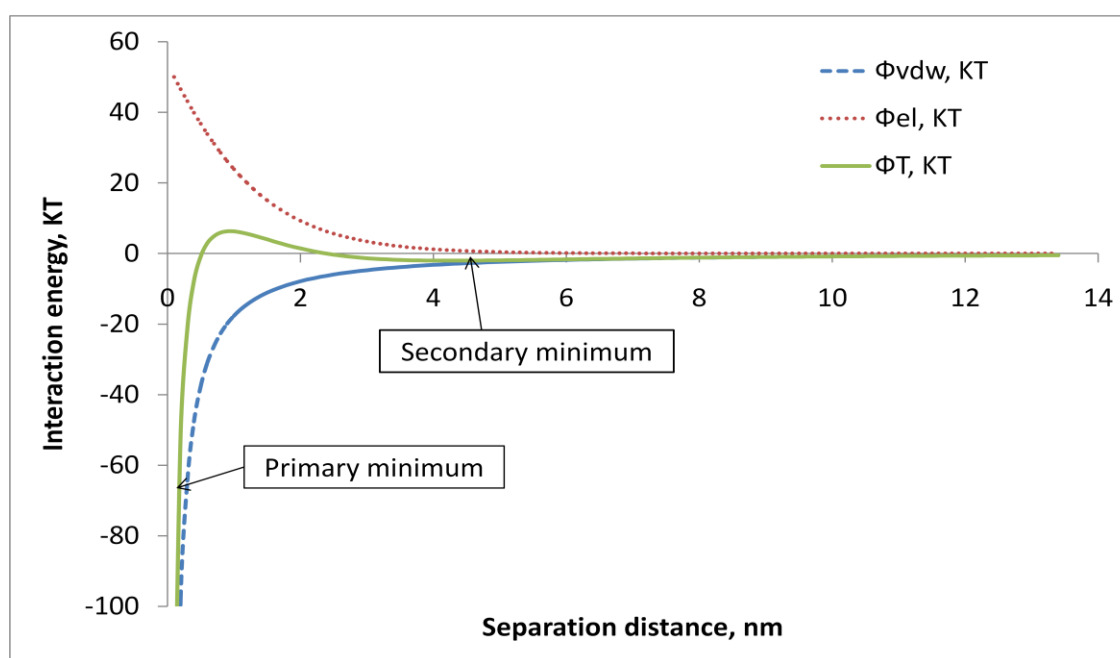


Figure 2-1. Illustration of DLVO theory including total interaction energy (Φ_T), the electrostatic interaction energy (Φ_{el}) and the van der Waals forces (Φ_{vdw}).

2.4.1 Chemical factors

The importance of solution chemistry in determining bacterial deposition has been well studied. An increase in ionic strength results in a notable increase in bacterial deposition (Fontes, Mills et al. 1991; Bolster, Mills et al. 2001; Schinner, Letzner et al. 2010), despite the presence of an energy barrier as described in the DLVO theory (Redman, Walker et al. 2004), with or without the presence of humic acid (Franchi and O'Melia 2003). Conversely, an increase in solution pH leads to a decrease in bacterial deposition (Yee, Fein et al. 2000; Abudalo, Bogatsu et al. 2005; Kim, Bradford et al. 2009). The presence of natural organic matter may also reduce bacterial deposition due to additional repulsive interaction energy (Johnson and Logan 1996; Franchi and O'Melia 2003; Morales, Zhang et al. 2011). Solution composition affects bacterial deposition by altering the surface charge of both the bacteria and the collectors. Bacterial surface charge is altered in the presence of heavy metal ions (Collins and Stotzky 1992). In a study of Yukselen, Y. and A. Kaya (2003), the zeta potential of kaolinite turned less negative with an increase in concentration of divalent ions, Ca^{2+} , Mg^{2+} , Cu^{2+} and Pb^{2+} etc.

Solution chemistry has been shown to have great influence on bacterial deposition. However, bacteria deposition was previously not examined within the stormwater runoff, which contains high levels of dissolved heavy metals.

2.4.2 Physical factors

Physical factors, including flow velocity, collector shape and size, collector surface coating all play different roles on bacterial deposition. Bacterial transport is facilitated as flow velocity increases (Kim, Boone et al. 2009; Lian, Liu et al. 2011). Bacterial mass

recovery is decreased, or bacteria penetrate shorter distances when transporting through fine-grain sand compared to coarse-grain sand (Fontes, Mills et al. 1991; Gargiulo, Bradford et al. 2007). It has been observed in many studies that the presence of Al- or Fe-coated soil surfaces enhances bacterial deposition/retention (Bolster, Mills et al. 2001; Chu, Jin et al. 2003; David, Jeremy et al. 2004; Abudalo, Bogatsu et al. 2005). There is a nonlinear dependency of bacterial mass removal on the percentage of coated surfaces (Kim, Park et al. 2008).

2.4.3 Biological factors

Biological factors also have influences on microbial deposition, including the types of microorganisms, their size and shape, cell surface properties, growth phase and cell motility. Viral, bacterial, and parasitic microorganisms differ markedly in their cell size and shape. Their sizes range from tens of nanometers (nm) to several microns (μm). Different microorganisms display various shapes, such as rods, spheres, simple helical and other complex forms. The retention of microorganisms has been found to be statistically related to cell size and shape (Fontes, Mills et al. 1991; Gannon, Manilal et al. 1991; Weiss, Mills et al. 1995), with bacteria smaller than $1.0 \mu\text{m}$ transporting in high percentages through soil (Gannon, Manilal et al. 1991). Different microorganisms certainly have distinct surface properties in terms of functional groups, surface polymers, surface charges and surface lipopolysaccharides, which may also affect their deposition (Johnson, Martin et al. 1996; Kuznar and Elimelech 2004; Walker 2004; Hyunjung, Tazehkand et al. 2006; Jacobs, Lafolie et al. 2007; Kim, Bradford et al. 2009). Bacteria in the starvation phase can transport further than non-starved cells (Cunningham, Sharp et al. 2007). Cell motility affects attachment under low fluid velocity, but has no effect when

fluid velocity is high (Camesano and Logan 1998; McClaine and Ford 2002; Becker, Collins et al. 2004).

Even though a great deal of research effort has been spent determining the effects of each controlling factor on bacterial deposition, they have often been studied in isolated conditions. Bacterial transport under heterogeneous conditions are commonly seen when surface water mix with groundwater and infiltrates into heterogeneous media. Therefore, it is necessary to evaluate the collective variability of both physical and chemical parameters on the estimation of bacterial deposition.

2.5 Microbial Transport Modeling

Despite the fundamental understanding of microbial deposition, predicting microbial transport in variable environments remains challenging, due to the variety and complexity of the physical, chemical and biological interactions among the soil-water-bacteria system.

2.5.1 The governing solute transport equation

The governing solute transport equation is the advection dispersion equation which generally includes three terms: advection, dispersion and sinks/sources. Solute transport is driven by advection of water movement (advection) and influenced by molecular diffusion and mechanical dispersion (dispersion). The sinks/sources are used to describe physicochemical and biological processes during transport other advection and dispersion and can be modeled in different ways. The one-dimensional advection-dispersion equation is given below:

$$\frac{\partial C}{\partial t} = -v \frac{\partial C}{\partial x} + D_L \frac{\partial^2 C}{\partial x^2} - \text{sinks/sources} \quad (2-1)$$

Where C is the bacterial concentration in aqueous phase; v is the flow velocity; x is longitudinal distance; D_L is the dispersion coefficient. A one-dimensional solute transport scenario is considered in this study because the software package HP1 is currently available in one-dimension only.

When modeling bacterial transport in the subsurface, physicochemical processes to be considered include advection, diffusion, dispersion, exclusion, straining, and physical filtration. The biological processes include bacterial growth/decay, chemotaxis, predation and survival. The advection-dispersion equation has been extended into various forms to account for processes taking place during bacterial transport in the subsurface. In a study by Schäfer et al. (1998), bacterial attachment/detachment to the soil-water interface and attachment to the air-water interface was considered during bacterial transport through the vadose zone, where changes in available surface areas are investigated (Schäfer, Ustohal et al. 1998). In a study by Kim et al. (2008), reversible/irreversible attachment to the soil-water interface and attachment to the air-water interface were considered where three different air water interface area models are evaluated for transport in the vadose zone (Kim, Kim et al. 2008). Bradford et al. (2003) studied the attachment, straining and exclusion for colloid transport in porous media under saturated condition (Bradford, Simunek et al. 2003). Gargiulo et al. (2007) included the attachment and straining when investigating the role of matrix grain sizes and bacterial surface proteins (Gargiulo, Bradford et al. 2007).

Modeling bacterial transport during stormwater infiltration is the goal of this work and those studies described above form the basis of the model development. The

processes to be considered primarily includes attachment/detachment at the soil-water interface, attachment to the air-water interface, straining and bacterial inactivation.

2.5.2 Reactive transport modeling

The reactive transport model represents a collection of coupled physical, chemical and biological processes to describe a coupled dynamic system. Microbial transport in the subsurface is a host of complex and interacting processes, which consist of the physiochemical processes (advection, dispersion, straining, physical filtration and adsorption) and the biological processes (bacterial growth and decay). One aspect of a reactive system that is most important for modeling fate and transport in porous media is the range of the reaction rates. The reaction rates can range from the very slow to instantaneous. Instantaneous reactions involve equilibrium relationships between interacting chemicals and are termed equilibrium reactions, while reactions that involve a rate that is on the same time scale as transport are termed non-equilibrium, or kinetic reactions. Most reactive transport models incorporate major physical processes, including advection, diffusion, dispersion, straining and physical filtration, and these processes have been the focus of many experimental and modeling studies on colloid and microbial attachment and transport. Initially, bacterial transport modeling adopted the equilibrium adsorption approach (Jaffe and Taylor 1990; Reddy and Ford 1996). Incorporating first-order kinetic attachment and detachment rates of bacteria was then suggested, applied, and validated in bacterial transport experiments (Hornberger, Mills et al. 1992; Clement, Peyton et al. 1997). A two-site kinetic model was later considered in modeling bacterial movement in porous media (Harvey and Garabedian 1991; McCaulou, Bales et al. 1994), where one site is controlled by equilibrium adsorption and another controlled by first-

order kinetics. Adsorption to two kinetic sites was applied to describe viral transport in column experiments (Hassanizadeh and Schijven 2000) and field studies (Schijven and Šimůnek 2002), where different sets of attachment rates and detachment rates were used to describe the two sorption sites.

Changes in solution chemistry commonly take place during the infiltration of stormwater runoff, which may potentially affect bacterial deposition and transport through the subsurface. Developing a reactive transport model with attachment rates varying in response to the changes of solution chemistry is desirable to describe bacterial transport under such situations. There are only few studies available to investigate particle transport under transient solution ionic strength in saturated porous media. Tosco et al. (2009) investigated ionic strength dependent deposition and release of microparticles in saturated porous media, where attachment/detachment are estimated via two empirical functions tied with salt concentration (Tosco, Tiraferri et al. 2009). Lenhart and Saiers (2003) modeled colloid release and transport under transient chemical conditions by including a series of compartments representing immobile colloids, each of which exhibits a unique colloid-release with respect to changes in pore water solute concentrations (Lenhart and Saiers 2003). Bradford et al. (2012) modified a sophisticated dual-permeability transport model to model colloid transport and release under transient solution ionic strength, where colloid immobilization was determined from balance of applied hydrodynamic and resisting adhesive torques (Bradford, Torkzaban et al. 2012). While the solution ionic strength on bacterial deposition and release has been shown to be an important factor and incorporated into the model, the solution pH and solution composition were not taken into account. It is also important to know variability of both

chemical and physical parameters on bacteria transport due to heterogeneities of water chemistry and porous media during stormwater infiltration.

2.5.3 Laboratory method

Most research on bacterial transport has been carried out at the lab scale, in column transport experiments. The laboratory experiments have high degree of control over the experimental conditions and can be relatively easy to conduct and repeat. The breakthrough curves (BTCs) generated from such column transport experiments provide useful information to help identify the physicochemical processes involved during bacterial transport. The parameters obtained can be used for comparison of different physiochemical characteristics of bacteria, porous media or solution chemistry that bacteria transport within. Some input parameters to transport models can be independently determined by experimental measurements. Other parameters are obtained via inversely fitting the observed breakthrough data points with the solute transport model, such as dispersion coefficient, attachment/detachment rate and other coefficients depending on the processes included in the transport model.

Laboratory column transport experiments do provide valuable information on bacterial movement through the soil. However, the applicability of results from laboratory column experiments to field situations is questionable, mainly due to the lack of consideration of heterogeneous conditions present in the field, such as the structure and composition of soil and microbial activity.

2.6 Stormwater Best Management Practices (BMPs)

To mitigate increases in storm-water pollution, the U.S. Environmental Protection Agency's National Pollutant Discharge Elimination System (NPDES) storm-water

permitting program requires many communities to use storm-water best management practices (BMPs). BMPs include a variety of stormwater runoff treatment controls used to reduce the volume, velocity, and pollutant loads of stormwater runoff from a catchment. The removal of pollutants relies on sedimentation, filtration and adsorption through soil (Olivieri 2007). Examples of stormwater BMPs are detention basins, retention ponds, infiltration basins & trenches, bioretention systems, stormwater wetlands, vegetated swales and sand filters.

2.6.1 Bioretention systems

A bioretention system generally consists of a water storage space, vegetation, mulch, bioretention soil mix, and a gravel layer (from top to bottom). A schematic diagram of a typical bioretention system is shown in **Figure 2-2**. The stormwater runoff filters through the vegetation and soil within the bioretention area. This filtered runoff is either collected in an underdrain system or is allowed to infiltrate into the subsurface.

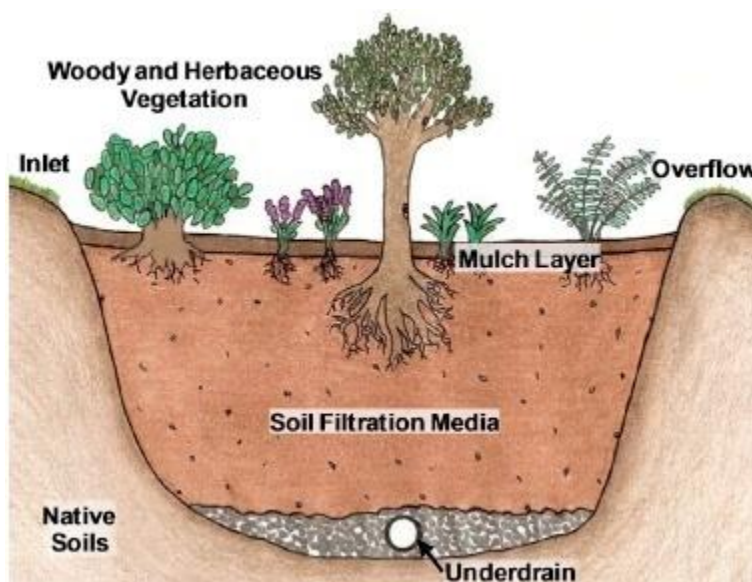


Figure 2-2. Schematic of a typical bioretention system (Roy-Poirier, Champagne et al. 2010)

The removal of physical and chemical contaminants by bioretention systems has been extensively studied in both laboratory and field studies, including total suspended solids, nutrients, heavy metals and oil and grease (Davis, Shokouhian et al. 2001; Davis 2003; Glass and Bissouma 2005; Hsieh and Davis 2005; Davis 2006; Hong 2006; Hunt, Jarrett et al. 2006; Davis 2007; Muthanna, Viklander et al. 2007; Rusciano and Obropta 2007). The application of stormwater BMPs to control pathogen transport is studied to a much lesser extent. **Table 2-1** summarizes the removal efficiencies for various pollutants in bioretention systems in both laboratory and field studies.

A limited amount of peer-reviewed literature is available on bacterial removal in bioretention systems. The effectiveness of the field bioretention systems on microbial pollutant removal is as of yet still unknown.

Table 2-1 (continued).

Study	Types of study	Fecal coliform	<i>E. Coli</i>	<i>Enterococci</i>	Oil and grease
Davis, et al. (2001)	Lab	-	-	-	-
Davis, et al. (2003)	Lab	-	-	-	-
Hsieh and Davis (2005)	Lab	-	-	-	>96
Glass and Bissouma (2005)	Field	-	-	-	-
Davis, et al. (2006)	Field	-	-	-	-
Hong, et al. (2006)	Lab	-	-	-	80-95
Hunt, et al. (2006)	Field	-	-	-	-
Davis (2007)	Field	-	-	-	-
Muthanna, et al. (2007)	Field	-	-	-	-
Rusciano and Obropta (2007)	lab	54.5-99.8	-	-	-
Hunt, et al. (2008)	Field	69	71	-	-
Hathaway, et al. (2009)	Field	89	92, 60, negative removal	86, negative removal	-
Chapman and Horner (2010)	Field	-	-	-	92-96
Zhang, et. al (2010)	Lab	-	82	-	-
Zhang, et. al (2011)	Lab	-	72-97	-	-

2.6.2 Bacterial removal in bioretention systems

Little literature is available to quantify bacterial removal efficiency in bioretention systems, which is likely due to the difficulty of collecting effluent water samples infiltrating into the underlying soil. From the very few studies on bacterial removal (Rusciano and Obropta 2007; Hunt, Smith et al. 2008; Hathaway, Hunt et al. 2009; Chapman and Horner 2010; Zhang, Seagren et al. 2010; Zhang, Seagren et al. 2011), highly variable removal efficiencies were observed. The removal efficiency can be as high as 99.8% for fecal coliform, 97% for *E. coli*, and 86% for *Enterococci*. However, negative bacterial removal was also observed in field studies conducted at North Carolina (Hathaway, Hunt et al. 2009). This bioretention unit did not reduce bacterial concentration, rather acted like a source of bacteria. The poor performance was caused by high moisture in the unit resulting from large drainage area and shallow soil (30cm), which provide a favorable environment for indicator bacteria to persist. The bacterial removal efficiency was found to be independent of temperature, although the inflow bacterial concentration is related with the increase of daily temperature (Zhang, Seagren et al. 2012). The highly variable removal efficiency data shown indicate that a variety of conditions affect the behavior of microorganisms, their removal and transport, and thus the performance of bioretention systems. Among these factors are microorganism type, properties of soil, wet weather condition, temperature, light intensity, plant type, filter design, and maintenance.

The roles of those factors on bacterial removal in bioretention systems are not clear, because of the limited number of field studies available. A better understanding of the

factors affecting bacterial removal could provide useful information on the design of bioretention system.

2.7 Knowledge Gap

Solution chemistry has been demonstrated to play an important role in bacterial deposition, such as pH, ionic strength and solution composition. However, bacteria deposition has not been examined in the stormwater runoff itself, which often contains high levels of dissolved heavy metals. A better understanding of the effects of heavy metals on bacterial deposition provides more insights on bacterial transport behavior in the subsurface during the infiltration of stormwater runoff.

The effects of the chemical, physical and biological factors on bacterial deposition have been investigated extensively. However, the effect of each of these factors on bacterial deposition has often been assumed to be static and studied in an isolated condition. It is important to evaluate the collective variability of both physical and chemical parameters when modeling bacterial transport in heterogeneous conditions, as is common when surface water mixes with groundwater and infiltrates into heterogeneous media.

Few models address bacterial transport scenarios in which the bacterial deposition rate changes in response to changes in physicochemical factors. Developing a reactive transport model in a user friendly interface that account for the variation of physiochemical factors is desirable, which could be conveniently applied in predicting bacterial transport under heterogeneous water chemistry and porous media.

Given the frequent detection of bacteria in stormwater runoff, it is increasingly important to consider the removal of bacterial, as well as physical and chemical pollutants when to assess the effectiveness and sustainability of bioretention systems operating under heterogeneous field conditions. It is also of great interest to know if the reactive transport model is applicable for bioretention systems under heterogeneous conditions.

CHAPTER 3. THE EFFECTS OF HEAVY METAL ON BACTERIAL TRANSPORT IN THE SUBSURFACE

Abstract

The presence of both heavy metals and bacteria is frequently reported in urban stormwater runoff. Adsorption and complexation of metals onto bacteria and soil takes place as stormwater runoff infiltrates into the subsurface, potentially changing both bacterial and mineral surfaces, and altering the attachment of bacteria onto soil surfaces. Scanning electron microscopy and energy dispersive X-ray spectroscopy analyses were performed on soil samples equilibrated with synthetic stormwater amended with copper, lead and zinc to determine changes in the elemental content of soil. Sets of batch sorption experiments of *Escherichia coli* (*E. coli*) onto soil were conducted under different conditions by varying solution composition and soil exposure history. *E. coli* attachment increases in synthetic stormwater with elevated heavy metals concentrations ($K_d = 0.0229 \text{ mL/mg}$) as opposed to nutrient buffer ($K_d = 0.0100 \text{ mL/mg}$) for the same untreated soil. For *E. coli* suspended in nutrient buffer, K_d is higher when equilibrated with metals-treated soil ($K_d = 0.0119 \text{ mL/mg}$) in comparison with untreated soil ($K_d = 0.0100 \text{ mL/mg}$). Results indicate that the presence of heavy metals in solution increases bacterial attachment to soil surfaces.

Keyword: synthetic stormwater, heavy metals, bacterial transport, K_d value, attachment efficiency

3.1 Introduction

Urban stormwater is an underutilized but potentially significant source of water, and as such is being increasingly exploited as a source for groundwater recharge. Large volumes of urban stormwater runoff are collected in infiltration basins and allowed to percolate into the subsurface, recharging the underlying groundwater. However, stormwater runoff carries various pollutants, which can be detrimental to the quality of the water. Heavy metals are found in urban runoff originating from a variety of sources associated with transportation (Yousef, Hvitved-Jacobsen et al. 1990; Brown and Peake 2006). In addition to metals pollution, the presence of pathogenic microorganisms in stormwater has frequently been reported (O'Shea and Field 1992; Davies and Bavor 2000; Jiang and Chu 2004; Arnone, Borst et al. 2005; Selvakumar and Borst 2006).

Bacterial cell walls contain a variety of surface organic functional groups which display electrostatic, chemical, and hydrophobic affinities for aqueous metals, dissolved organic molecules, and mineral surfaces (Fein 1997; Fein 2000). Metal adsorption onto bacteria is influenced by bacterial surface functional groups and metal speciation and chemistry in the aqueous phase. The carboxyl groups, phosphate sites, and amine groups contribute to the uptake of metals (Akthar, Sastry et al. 1996; Fein 1997). Metal adsorption experiments conducted by Fein et al. show pH-dependent adsorption of Cd, Pb, Cu and Al onto *Bacillus subtilis* (Fein 1997). The adsorption of metals onto bacterial could potentially affect bacterial attachment.

Studies of bacterial sorption and/or removal (Abudalo, Bogatsu et al. 2005; Kim, Park et al. 2008; Schinner, Letzner et al. 2010) fail to consider the effects of heavy metals, despite elevated concentration of heavy metals in stormwater runoff. Experiments in this study were designed to mimic the processes that dominate microbial transport during

infiltration of urban stormwater runoff into the subsurface when the dominant stormwater pollutants are heavy metals and microorganisms. Results may be used to inform more realistic models of pollutant transport during stormwater infiltration. Metals and bacteria equilibrate in ponded water prior to infiltration and adsorption and complexation of metals onto bacteria and soil occurs as stormwater runoff infiltrates into the subsurface, potentially changing both bacterial and mineral surfaces, and altering the attachment of bacteria onto soil mineral surfaces.

In this chapter, we quantify (1) changes in bacterial surface charge and soil elemental surface coverage following exposure to synthetic stormwater amended with heavy metals; and (2) changes in bacterial attachment onto soil samples due to the presence of synthetic stormwater. Individual interactions between bacteria and metals, as well as bacterial transport in solutions with elevated metals concentrations are examined. The heavy metals of concern in this study are copper, lead and zinc, which comprise 90 percent of dissolved heavy metals in highway stormwater runoff (Harper 1985).

3.2 Materials and Methods

3.2.1 Soil characteristics

Soil samples were collected from the top eight inches of a newly constructed bioretention basin in Philadelphia, PA. Soil moisture content was measured in duplicate samples by drying the soil sample at 105 °C until the soil weight remained constant. Organic matter (OM) was determined in duplicate samples by comparing the difference between original sample weight and dry sample weight following 400 °C heat for four hours. The soil particle size distribution was determined via sieve analysis. The mean grain size and coefficient of uniformity were determined. Select soil samples were treated

by equilibrating a portion of the soil with a synthetic stormwater solution described in **Table 3-1** at a mass ratio of 1:50, and then drying in air. Scanning electron microscopy (SEM) (Zeiss Supra 50VP) and energy dispersive X-ray spectroscopy (EDS) (Oxford INCA EDS) analyses were conducted on native soil samples and treated (equilibrated with synthetic stormwater solution) soil samples to compare the average elemental content of soil samples. As per instructions in the Cressington carbon coater 208C user manual, soil samples were loaded onto the instrument stub and then exposed to carbon rod evaporation for 20 seconds to prevent charging of the surfaces. X-ray mapping of the specimens determined the elemental composition of soil samples and specific elemental distributions on soil particles.

3.2.2 Solution chemistry

Synthetic stormwater was prepared according to **Table 3-1**, modifying a previously described recipe (Davis, Shokouhian et al. 2001), by increasing the concentration of heavy metals while keeping the remaining components unchanged. The ionic strength of the synthetic stormwater was 6.8 mM and the pH was adjusted to 6. Saturation indices were determined using the PHREEQC (D.L. Parkhurst 1999), confirming no expected precipitation. A nutrient buffer solution was prepared using the same recipe, but replacing cupric sulfate (CuSO_4), lead chloride (PbCl_2) and zinc chloride (ZnCl_2) with sodium nitrate (NaNO_3) to ensure an equivalent ionic strength. The nutrient solution was buffered to a pH of 6.

3.2.3 Bacterial growth and quantification

Escherichia coli (*E. coli*) K12 was selected for this study due to its wide use as an indicator for bacterial contamination. *E. coli* was cultured in 75 mL Luria-Bertani (LB)

medium for 12 hours at 35 °C. Cell cultures were centrifuged at 7100 rpm for five minutes and rinsed with deionized water (DI water). The resulting cell pellet was resuspended in either nutrient solution or synthetic stormwater as prescribed for batch or column transport experiments. Cell concentration was determined by measuring optical density at 400 nm. A ten-point calibration curve ($R^2 = 0.98$) relating optical density to cell concentration (cells/mL) was constructed using acridine orange direct counts (AODC). The wavelength of 400 nm was chosen for quantifying optical density to resolve low bacterial concentrations (Yee and Fein 2002).

3.2.4 Live-dead bacterial viability assay

A bacterial viability assay was performed to test the toxicity of heavy metals to bacteria. The viability of *E. coli* cells following a 3-hour equilibration with synthetic stormwater was measured using the Live/Dead BacLight™ Bacterial Viability Kit (Invitrogen). Live cells with intact membranes fluoresce green, whereas dead or dying cells with damaged membranes fluoresce red when viewed using microscopy and suitable optical filter sets. Briefly, equal volumes of SYTO 9 dye and propidium iodide were added to a microcentrifuge tube and vortexed for 30 seconds. Three microliter (μL) of the dye mixture was pipetted into 1 mL of bacterial suspension, vortexed and incubated in the dark for 15 minutes. Finally 5 μL of the stained bacterial suspension was loaded onto a microscope slide and covered with a square coverslip. The live and dead cells were enumerated via microscopy.

3.2.5 Zeta potential measurement

The zeta potential of *E. coli* cells suspended in both nutrient solution and synthetic stormwater was determined following a 3-hr equilibration period using a zeta-meter

system 3.0+ (Zeta meter, Inc.). Bacterial concentrations were approximately 2×10^8 cells/mL. Bacterial migration was manually tracked and zeta potential was automatically calculated as millivoltage.

3.2.6 Metal-bacteria batch adsorption experiments

Batch adsorption experiments to determine the attachment of metal ions to bacterial cell surfaces were performed in duplicate. Washed and suspended *E. coli* cells were distributed into centrifuge tubes in 15 mL aliquots and centrifuged. Cell pellets were then resuspended in synthetic stormwater with varying metals concentrations. Average initial cell concentrations were $1.8 \times 10^9 \pm 1.5 \times 10^7$ cells/mL. A series of synthetic stormwater solutions were prepared by adding 0.1, 0.2, 0.4, 0.6 and 1 times the metals concentrations listed in **Table 3-1**, along with additional NaNO_3 to achieve the same ionic strength as the main synthetic stormwater solution (**Table 3-1**). Initial cell concentrations were determined by measuring optical density at 400nm. Centrifuge tubes with metal-bacteria suspensions were rotated for 3 hrs to ensure equilibrium although equilibrium could be achieved within an hour (Fein 1997). Once equilibrium was achieved, the suspension was filtered through a 0.45 μm pore size membrane filter. The filtrate was collected and acidified for quantification of aqueous-phase metals via atomic adsorption spectroscopy (AA 240 FS, Varian). Briefly, lamps specific for copper, lead and zinc were installed, optimized and calibrated. For each metal, a five-point calibration curve was constructed with known standards and used to measure concentrations of digested samples. To recover metals absorbed onto the bacteria, the membrane filter was resuspended in deionized water and the suspension was digested with acid for quantification of metal concentrations. The loss of metals during filtration and acid digestion was calculated

through mass balance. Duplicate experiments were conducted for each set of batch adsorption experiments. Adsorption data were fitted with theoretical linear, Langmuir and, Freundlich isotherms.

Table 3-1. Synthetic stormwater and nutrient solution composition

Pollutants	Chemical	Concentration (mg/L)		
		Synthetic stormwater	Nutrient solution	Element
Phosphorus	Dibasic sodium phosphate (Na_2HPO_4)	0.6	0.6	as P
Nitrate	Sodium nitrate (NaNO_3)	2	49.2	as N
Dissolved solid	Calcium Chloride (CaCl_2)	120	120	
Total copper	Cupric sulfate (CuSO_4)	8	-	as Cu
Total lead	Lead chloride (PbCl_2)	8	-	as Pb
Total zinc	Zinc chloride (ZnCl_2)	60	-	as Zn
pH		6	6	

The recipe for synthetic stormwater was adapted from Davis et al (Davis, Shokouhian et al. 2001). In batch experiments, 0.1, 0.2, 0.4, 0.6 and 1 times metal concentration were used to construct isotherms.

3.2.7 Bacteria-soil batch adsorption experiments

Four sets of bacteria-soil batch adsorption experiments were conducted: bacteria suspended in nutrient solution mixed with untreated (native) soil (BNS-U), bacteria suspended in nutrient solution mixed with treated (ie. pre-equilibrated with synthetic stormwater) soil (BNS-T), bacteria suspended in synthetic stormwater mixed with

untreated soil (BSS-U), and bacteria suspended in synthetic stormwater mixed with treated soil (BSS-T). Test tubes were cleaned with 10% nitric acid, followed by DI water. Washed *E. coli* cells were resuspended in either nutrient buffer or synthetic stormwater. To construct adsorption isotherms, 10 mL aliquots of bacteria suspended in either nutrient solution or synthetic stormwater were distributed into 15 mL test tubes containing various amounts of treated or untreated soil. Initial cell concentrations were approximately $2.46 \times 10^9 \pm 2.58 \times 10^8$ cells/mL. Test tubes were placed on a rotating mixer for 3hrs to ensure equilibrium, which was verified by confirming that aqueous cell concentrations were constant over time. After equilibrium was established, unattached bacteria were separated from soil-attached bacteria by injecting 3 mL of 60% w/w sucrose solution into the bottom of the test tubes (Yee and Fein 2002) and centrifuging. Unattached bacteria remained above the sucrose layer while bacteria attached to the soil settled below that layer due to density differences. Unattached bacteria in the supernatant were pipetted out for enumeration. The number of sorbed bacteria was calculated by subtraction. Adsorption data were fit with theoretical linear, Langmuir and, Freundlich isotherms.

3.2.8 Column transport experiments

Field collected soil samples were sieved (metric sizes 425, 300, 250 and 150 μm), re-mixed according to the measured grain size distribution of the soil and then dry-packed into Omnifit columns with an inner diameter of 1.5 cm and height of 10cm. In order to observe the effect of heavy metals on bacterial transport, two sets of column experiments were conducted: one with bacteria suspended in synthetic stormwater and another with bacteria suspended in nutrient solution. Bacteria were resuspended in and

mixed with either synthetic stormwater or nutrient solution for 1 hr. Prior to each transport experiment, columns were flushed with DI water and then equilibrated with 20 mL (3.3 pore volumes) of nutrient solution at a flow rate of 0.1 mL/min. After equilibration, 10 mL (1.7 pore volumes) of bacteria suspended in either synthetic stormwater or nutrient solution was passed through the column followed by 20 mL (3.3 pore volumes) of bacteria-free nutrient solution at a flow rate 0.5 mL/min. Effluent samples were collected every two minutes using an automatic fraction collector (ISCO Retriever 500, USA). The absorbance of effluent samples at 400 nm wavelength was measured, as was the pH of each sample. Triplicate experiments were run for bacteria in synthetic stormwater and nutrient solution, with a new packed column for each experiment. Porosity was calculated for each column used, with an average porosity of 0.345 ± 0.013 for all six columns.

Bacterial mass recovery (MR) was calculated using (Kim, Park et al. 2008; Schinner, Letzner et al. 2010):

$$MR = \frac{\int_0^{\infty} C dt}{C_0 t_0} \quad (3-1)$$

Where C_0 is the initial bacteria concentration and t_0 is the injection time.

Bacterial attachment efficiency was computed using the following equation:

$$\alpha = -\frac{2d_c}{3(1-n)L\eta} \ln(MR) \quad (3-2)$$

Where d_c is collector grain size, n is the porosity of the soil column, L is the length of the soil column and η is single collector contact efficiency obtained from the TE equation developed by Tufenkji and Elimelech (Tufenkji and Elimelech 2004).

$$\eta = 2.4A_s^{1/3}N_R^{-0.081}N_{Pe}^{-0.715}N_{vdW}^{0.052} + 0.55A_sN_R^{1.675}N_A^{0.125} + 0.22N_R^{-0.24}N_G^{1.11}N_{vdW}^{0.053} \quad (3-3)$$

Where A_s is a porosity dependent parameter; N_R is aspect ratio; N_{Pe} is the Peclet number; N_{vdW} is the van der Waals number; N_A is the attraction number; and N_G is the new gravity number.

The parameters used to calculate single collector contact efficiency and attachment efficiency are summarized in **Table 3-2**.

Table 3-2. Summary of parameters used to calculate single collector contact efficiency and attachment efficiency of *E. coli* in soil

Parameters	Values	
Particle diameter, d_p	0.838	μm
Porosity, f	0.345	-
Collector (grain) diameter, d_c	225.098	μm
Fluid approach velocity, U	4.72×10^{-5}	m s^{-1}
Hamaker constant, A	6.5×10^{-20}	J
Particle density, ρ_p^*	1.105	g cm^{-3}
Fluid absolute temperature, T	298	K
Bulk diffusion coefficient, D_∞^{**}	5.85×10^{-9}	$\text{cm}^2 \text{s}^{-1}$
Fluid viscosity, μ	0.0089	$\text{g cm}^{-1} \text{s}^{-1}$
Boltzmann constant, k	1.38×10^{-23}	J K^{-1}
Fluid density, ρ_f	0.988	g cm^{-3}
Gravitational acceleration, g	9.8	m s^{-2}
Column length, L	10	Cm

*Particle(*E. coli*) density was adopted from study of Martinez-Salas et al. (Martinez-Salas, Martin et al. 1981). **Bulk diffusion coefficient D_∞ was calculated via equation $D_\infty = kT/(3\pi\mu d_p)$ (Tufenkji and Elimelech 2004).

3.3 Results

3.3.1 Soil elemental coverage

Duplicate soil samples were collected from the field and analyzed for organic matter content ($3.4 \pm 0.11\%$) and moisture content ($20.1 \pm 0.14\%$). The mean grain (d_{50}) size was determined using the cumulative weight fraction, as defined by the grain diameter

where 50% of the total particles are finer. The mean grain size was 225 μm , and the coefficient of uniformity (d_{60}/d_{10}) was 5.9, indicating a highly non-uniform distribution. Soil samples equilibrated with synthetic stormwater were analyzed to determine the extent to which heavy metals from the synthetic stormwater attached to soil particles. Five replicate samples of soil treated with synthetic stormwater were observed to have $2.24 \times 10^{-3} \pm 7.73 \times 10^{-4}$ mg zinc per mg soil, $3.89 \times 10^{-4} \pm 1.93 \times 10^{-5}$ mg copper per mg soil and $4.14 \times 10^{-4} \pm 5.14 \times 10^{-5}$ mg lead per mg soil, as determined by subtracting the final metals concentration in the aqueous phase from the initial input.

Figure 3-1 (A) displays the SEM image of a soil sample, where the black portion represents the carbon coating. Energy dispersive X-ray spectroscopy (EDS) analysis confirmed the presence of copper and zinc in soil samples. As shown in **Figure 3-1** (B) and (C), the common elements of soil with/without treatment are carbon, silicon, oxygen, aluminum and iron, indicating the soil composition of quartz, some aluminum and iron oxides. Zinc, copper and lead were only detected in soil samples following equilibration with synthetic stormwater. The high fraction of carbon is from the carbon coating procedure to prevent surface charging. The elemental distribution was obtained by analyzing X-ray intensity distributions over a selected region of the sample.

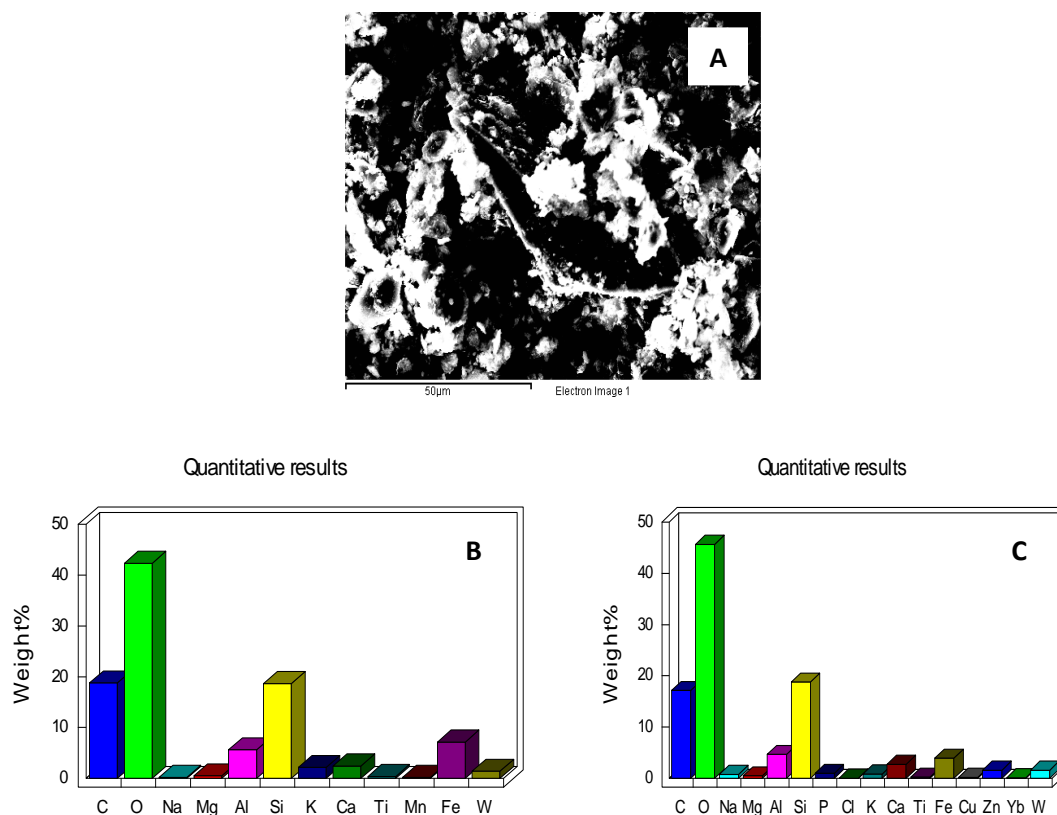


Figure 3-1. SEM images of soil equilibrated with synthetic stormwater (A); quantitative histogram for all elements present on soil surfaces before (B) and after (C) equilibrated with synthetic stormwater. The presence of carbon is from carbon coating during sample preparation to prevent surface charging up.

3.3. 2 Bacterial characteristics

Heavy metals may be toxic to microorganisms at high concentrations. The copper, zinc and lead concentrations in synthetic stormwater were 0.126 mM, 0.918 mM and 0.039 mM, respectively, all of which were lower than the minimum inhibitory concentrations (MICs) of these heavy metals for *E. coli*, as determined on agar media at

different acidities by Mergeay et al. (Mergeay 1985). The MICs of copper, lead and zinc are 1mM, 1mM and 5 mM, respectively. Results from the live/dead viability assay indicate that 81% of *E. coli* cells were viable following a 3-hour equilibration with synthetic stormwater, as compared to 97% viable cells following equilibration with nutrient solution.

Zeta potential was used to measure the effect of synthetic stormwater solutions on the surface charge of bacterial cells. Over 30 measurements were taken for bacteria suspended both in synthetic stormwater and in nutrient solution. *E. coli* equilibrated with synthetic stormwater exhibit an average zeta potential of -17.0 ± 5.96 mv compared to -21.6 ± 5.45 mv for *E. coli* equilibrated with nutrient solution. Comparing the measured zeta potential of bacteria in nutrient solution and synthetic stormwater, the p-value was calculated to be smaller than 0.001, indicating a significant difference in the surface charge of bacteria equilibrated with nutrient solution compared with those suspended in synthetic stormwater.

3.3.3 Metal adsorption to bacteria

In metal-bacteria batch experiments, saturation of the bacterial surface sites was not observed within the experimental metals concentration range (Cu: 0~8 mg/L, Pb: 0~8 mg/L and Zn: 0~60 mg/L). Adsorption data were fitted with theoretical linear, Langmuir and, Freundlich isotherms. Linear isotherms provided the best fit for all adsorption data.

$$C_s = K_d \times C \quad (3-4)$$

where

C_s = concentration in solid phase

C = concentration in fluid phase

K_d = equilibrium distribution coefficient

Figure 3-2 displays the adsorption isotherm plots of copper, zinc and lead onto bacteria in synthetic stormwater. The equilibrium coefficient K_d for copper, zinc and lead in synthetic stormwater are 0.235 L/10⁹ cells ($R^2 = 0.83$), 0.616L/10⁹ cells ($R^2 = 0.97$) and 4.34 L/10⁹ cells ($R^2 = 0.88$), respectively.

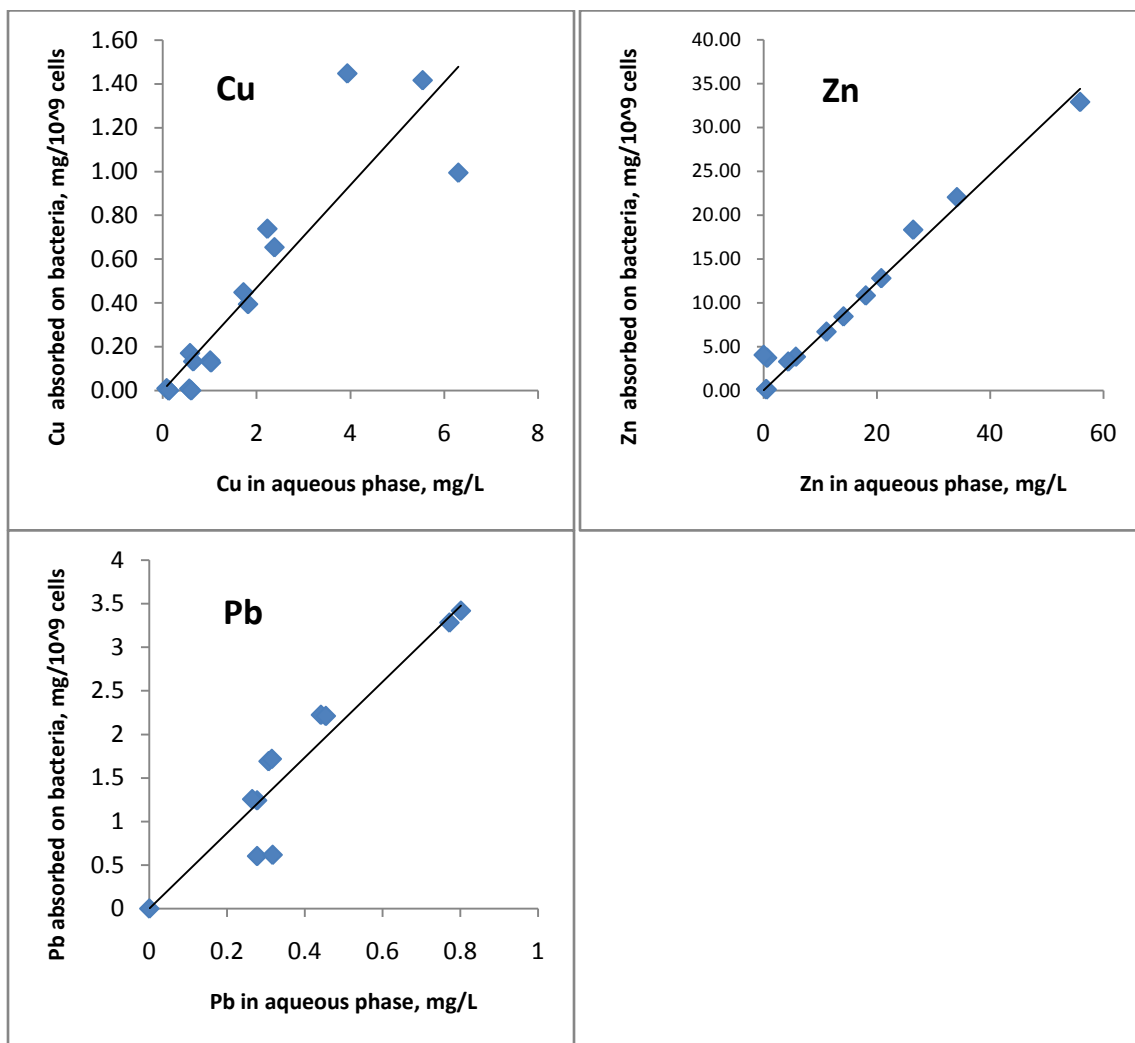


Figure 3-2. Adsorption of copper, zinc and lead to *E. coli* K12 cells in synthetic stormwater. Solid lines represent linear isotherms fitted with $K_d = 0.235 \text{ L}/10^9 \text{ cells}$ ($R^2 = 0.83$) for copper, $K_d = 0.616 \text{ L}/10^9 \text{ cells}$ ($R^2 = 0.97$) for zinc and $K_d = 4.34 \text{ L}/10^9 \text{ cells}$ ($R^2 = 0.88$) for lead.

3.3.4 Bacterial adsorption to soil

Different soil exposure histories and solution chemistries were tested to investigate bacterial adsorption to soil. Adsorption data of bacterial to soil was best fit with theoretical linear isotherms. **Figure 3-3** shows a comparison of the adsorption isotherm plots of two bacterial suspensions onto treated and untreated soil samples.

For bacteria suspended in synthetic stormwater, the equilibrium distribution coefficient value was higher when equilibrated with treated soil (BSS-T, $K_d = 0.0338$ mL/mg, $R^2 = 0.86$) in comparison with untreated soil (BSS-U, $K_d = 0.0229$ mL/mg, $R^2 = 0.89$). This same effect was observed in nutrient solution with treated soil (BNS-T, $K_d = 0.0119$ mL/mg, $R^2 = 0.83$) and untreated soil (BNS-U, $K_d = 0.0100$ mL/mg, $R^2 = 0.91$). With the same soil treatment, a higher equilibrium distribution coefficient value was observed onto treated soil for bacteria suspended in synthetic stormwater (BSS-T, $K_d = 0.0338$ mL/mg, $R^2 = 0.86$) compared with those suspended in nutrient solution (BNS-T, $K_d = 0.0199$ mL/mg, $R^2 = 0.83$). Similarly with untreated soil, the equilibrium coefficient for bacteria suspended in synthetic stormwater containing heavy metals (BSS-U, $K_d = 0.0229$ mL/mg, $R^2 = 0.89$) was higher than that describing bacteria suspended in nutrient solution (BNS-U, $K_d = 0.0100$ mL/mg, $R^2 = 0.91$).

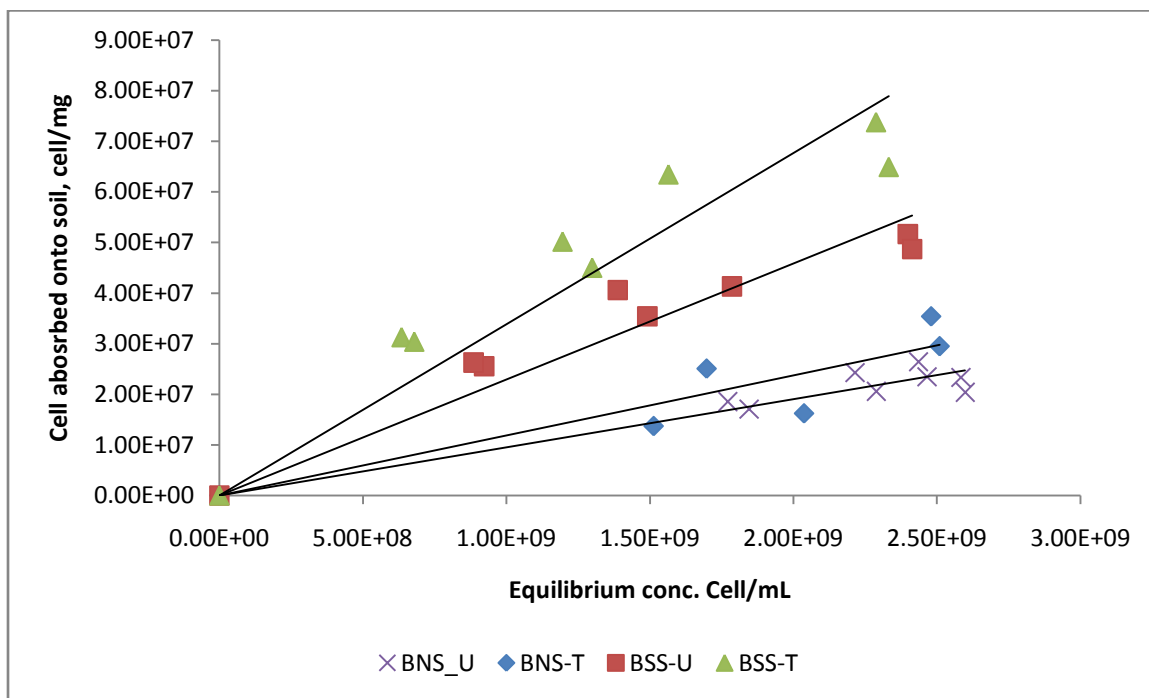


Figure 3-3. Isotherms of bacteria-soil batch adsorption experiments. Solid lines show linear isotherms fitted with $K_d = 0.0100$ mL/mg, $R^2 = 0.91$ (BNS-U), $K_d = 0.0119$ mL/mg, $R^2 = 0.83$ (BNS-T), $K_d = 0.0229$ mL/mg, $R^2 = 0.89$ (BSS-U), and $K_d = 0.0338$ mL/mg, $R^2 = 0.86$ (BSS-T).

3.3.5 Column transport experiments

Results from bacterial breakthrough curves (BTCs) using different solution compositions (nutrient solution vs synthetic stormwater) with identical ionic strength and pH are presented in **Figure 3-4**. The average bacterial concentration of the injectate was $2.42 \times 10^9 \pm 3.29 \times 10^7$ cells/mL. Normalized cell concentration, C/C_0 , collected at the column effluent is plotted as a function of time. Curves represent the average of triplicate experiments run in separate columns with associated error bars representing standard

deviation. A high degree of variance is seen in the curves due to the heterogeneity of the soil, however significant differences between the two BTCs are apparent. The peak normalized concentration is 0.44 for bacteria suspended in nutrient solution and 0.17 for bacteria suspended in synthetic stormwater. Bacterial mass recovery was calculated following equation (3-1). 12.4% of bacteria were recovered from experiments using synthetic stormwater while 35.9% of bacteria were recovered from experiments in nutrient solution.

Bacterial attachment efficiency was calculated to qualitatively compare bacterial adsorption behavior under different solution compositions. As mentioned previously, the soil is highly non-uniform and the mean particle d_{50} is not the dominant size among all size ranges. The single collector contact efficiency η was calculated using equation (3-3) using the mean particle d_{50} . Therefore, the attachment efficiency calculated should be considered with caution. Bacterial attachment efficiency in synthetic stormwater was found to be 0.274, twice as high as that in nutrient solution ($\alpha=0.134$). The ratio of bacterial diameter : collector diameter is 3.7×10^{-3} , indicating minimal bacterial straining during transport. The pH values of bacterial suspensions were within the range of 6.6 and 6.7 after passing through the soil column. Since the pH value remained relatively stable during column transport experiments, pH was not believed to contribute to the change in bacterial attachment efficiency. The presence of metals in synthetic stormwater leads to an increase in bacterial attachment efficiency.

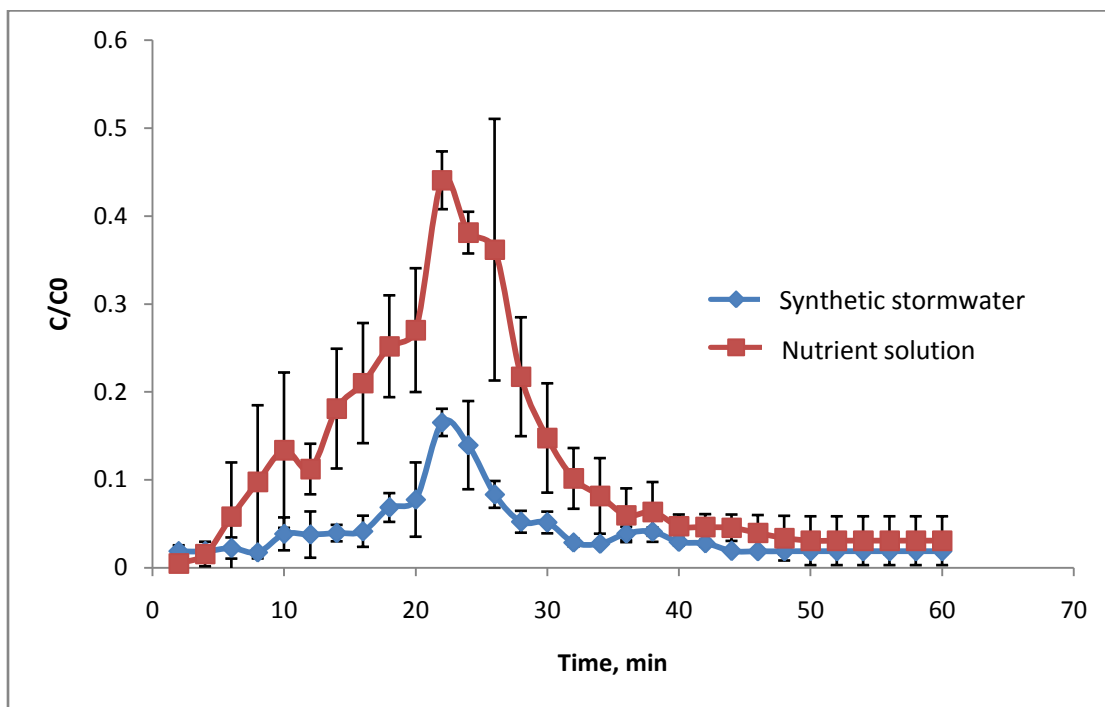


Figure 3-4. Breakthrough curves (BTCs) with error bars representing standard error/deviation from triplicate transport experiments with *E. coli* suspended in nutrient solution (red squares) and in synthetic stormwater (blue diamonds).

3.4 Discussion

Both heavy metals and bacterial pollutants are present in urban stormwater runoff, which is often collected in ponding infiltration basins, allowing for equilibration of heavy metals and bacteria prior to infiltration through the subsurface. Experiments presented in this paper indicate that adsorption of metal ions onto bacterial surfaces while ponded water equilibrates prior to infiltration significantly decreases the negative surface charge of bacterial cells, increasing their potential for attachment during subsurface transport. An examination of soil exposed to synthetic stormwater enhanced with heavy metals

confirms the accumulation of metals in soil samples via SEM and EDS analyses. These results imply that metal complexes may be formed on soil particle surfaces from successive infiltration events of stormwater containing elevated concentrations of heavy metals.

Accumulation of metals onto soil particle surfaces tends to create favorable conditions for bacterial attachment. Higher equilibrium distribution coefficients (K_d) were observed in batch bacterial adsorption experiments performed with soil treated with synthetic stormwater, as opposed to untreated soil. As indicated previously, soil treated with synthetic stormwater accumulates zinc, copper and lead, contributing to the increase in bacterial attachment.

The increase in bacterial attachment to soil in the presence of heavy metals may also be due to changes in cell surfaces. Comparison of K_d values obtained from batch experiments in treated soil in which bacteria were suspended either in nutrient solution or in synthetic stormwater suggests that bacterial attachment increases in synthetic stormwater, as evidenced by a higher equilibrium attachment coefficient (K_d) for the same soil. As confirmed in metal-bacteria batch adsorption experiments, metals are readily adsorbed onto bacterial surfaces. A comparison of net cell surface charge determined using zeta potential measurement indicates that the adsorption of heavy metals onto bacterial surfaces significantly decreases their negative surface charge, thereby further increasing bacterial attachment to soil surfaces. Although beyond the scope of this work, it would be possible to explore the potential competitive adsorption between aqueous metal species and bacteria/heavy metal complexes onto soil surfaces.

Column transport experiments were performed both to confirm results from bacterial soil batch experiments, and also to further quantitatively calculate the influence of heavy metals on bacterial attachment efficiency. Consistency between batch experiments and column experiments was observed with higher equilibrium coefficients K_d in batch experiments conducted with synthetic stormwater, corresponding to lower bacterial mass recovery in column transport experiments conducted with synthetic stormwater.

Adsorption of metals onto bacteria and soil takes place as stormwater runoff infiltrates into the subsurface. Changes in both bacterial surfaces and soil elemental content have been observed, and may alter the attachment of bacteria to soil surfaces. Higher bacterial attachment efficiency was observed for bacteria suspended in synthetic stormwater compared with bacteria suspended in nutrient buffer during transport through soil columns, likely due to the presence of heavy metals in the synthetic stormwater. A plausible explanation for the enhanced adsorption of bacteria in synthetic stormwater is the reduction of repulsive forces between bacterial and soil surfaces. High concentrations of multivalent cations may suppress the thickness of the diffuse double layer more effectively than monovalent cations. As observed in other studies, high concentrations of divalent cations significantly increase the attachment of viruses onto mineral surfaces (Moore 1982; Lipson and Stotzky 1983). Adsorption of negatively charged cells onto negatively charged soil surface requires cells to overcome repulsive forces between the soil and the bacterial cell surface. The addition of multivalent cations (heavy metals in this study) reduces the negative charge of bacterial surfaces as seen from zeta potential measurement, which may reduce repulsive forces between bacteria and soil surfaces. Also the high concentrations of multivalent cations compresses the double layer such that

physical forces such as Van der Waals forces and hydrogen bonding may become dominant (Lipson and Stotzky 1983). It is unclear from these experiments whether the attachment of bacteria due to the reduced double layer is primary and secondary in nature, therefore the potential release of bacteria from soil surfaces should be considered when solution chemistry changes.

In terms of protecting underlying ground water during stormwater infiltration, the presence of heavy metals seems to decrease the transport capacity of viable bacteria, primarily by increasing bacterial attachment to soil surfaces. As bacterial cell surfaces become less negatively charged due to the adsorption of heavy metals, bacterial attachment increases. There are many competing factors controlling the attachment of bacteria, including complex combinations of cell surface charge heterogeneity and LPS composition (Walker 2004). Results from this work indicate that heavy metals in solution significantly alter this surface charge.

CHAPTER 4. EVALUATING THE EFFECTS OF VARIABLE WATER CHEMISTRY ON BACTERIAL TRANSPORT DURING INFILTRATION

Abstract

Bacterial infiltration through the subsurface has been studied experimentally under different conditions of interest and is dependent on a variety of physical, chemical and biological factors. However, most bacterial transport studies fail to adequately represent the complex processes occurring in natural systems. Bacteria are frequently detected in stormwater runoff, and may present risk of microbial contamination during stormwater recharge into groundwater. Mixing of stormwater runoff with groundwater during infiltration results in changes in local solution chemistry, which may lead to changes in both bacterial and collector surface properties and subsequent bacterial attachment rates. This study focuses on quantifying changes in bacterial transport behavior under variable solution chemistry, and on comparing the influences of chemical variability and physical variability on bacterial attachment rates. Bacterial attachment rate at the soil-water interface was predicted analytically using combined rate equations, which vary temporally and spatially with respect to changes in solution chemistry. Two-phase Monte Carlo analysis was conducted and an overall input-output correlation coefficient was calculated to quantitatively describe the importance of physiochemical variation on the estimates of attachment rate. Among physical variables, soil particle size has the highest correlation coefficient, followed by porosity of the soil media, bacterial size and flow velocity. Among chemical variables, ionic strength has the highest correlation coefficient.

A semi-reactive microbial transport model was developed within HP1 (HYDRUS1D-PHREEQC) and applied to column transport experiments with constant and variable solution chemistries. Bacterial attachment rate varied from $9.10 \times 10^{-3} \text{ min}^{-1}$ to $3.71 \times 10^{-3} \text{ min}^{-1}$ due to mixing of synthetic stormwater (SSW) with artificial groundwater (AGW), while bacterial attachment remained constant at $9.10 \times 10^{-3} \text{ min}^{-1}$ in a constant solution chemistry (AGW only). The model matched observed bacterial breakthrough curves well. Although limitations exist in the application of a semi-reactive microbial transport model, this method represents one step towards a more realistic model of bacterial transport in complex microbial-water-soil systems.

Key words: bacterial attachment rate, solution chemistry, microbial transport model, HP1.

4.1 Introduction

Understanding the transport and deposition of microorganisms in subsurface environments is critical to protect underlying groundwater from harmful microorganisms that may be present in infiltrating surface water. A great amount of research efforts have been devoted to investigating the chemical, physical and biological factors influencing microorganism transport and deposition. Those studies have been reviewed and summarized in Chapter 2. The importance of solution chemistry in determining bacterial deposition has been well studied. An increase in ionic strength results in a notable increase in bacterial deposition (Fontes, Mills et al. 1991; Bolster, Mills et al. 2001; Schinner, Letzner et al. 2010) while an increase in solution pH leads to a decrease in bacterial deposition (Yee, Fein et al. 2000; Abudalo, Bogatsu et al. 2005; Kim, Bradford et al. 2009). The presence of organic matter (Johnson and Logan 1996; Franchi and O'Melia 2003; Morales, Zhang et al. 2011), heavy metals ions (Collins and Stotzky 1992) and other multivalent ions (Yukselen and Kaya 2003) in solution could alter the surface charge of bacteria or soil surfaces, and therefore affect bacterial deposition.

The effect of each of these factors on bacterial attachment has often been assumed to be static. However, solution chemistry changes, especially when different water sources mix. Infiltration of urban stormwater runoff into the subsurface has been widely applied as a best management practice in urban stormwater management to control large volumes of runoff and to remove pollutants. Stormwater runoff differs from groundwater in terms of solution chemistry. Urban stormwater runoff typically contains suspended solids, nutrients, organic carbons (Rasmussen 1998; Pitt, Clark et al. 1999) and heavy metals (Yousef, Hvitved-Jacobsen et al. 1990; Pitt, Clark et al. 1999; Prestes, Anjos et al. 2006;

Helmreich, Hilliges et al. 2010) as well as microorganisms (Schillinger and Gannon 1985; Davies and Bavor 2000; Prestes, Anjos et al. 2006; Selvakumar and Borst 2006; Brownell, Harwood et al. 2007).

The solution chemistry of groundwater depends on the geological nature of the soil. As stormwater runoff infiltrates into the subsurface, the two water sources mix, causing a subsequent change in solution chemistry, which may in turn alter the surface properties of both bacteria and soil. Theoretical studies by Chrysikopoulos et al. have shown that spatially variable solute sorption leads to reduced solute migration and enhanced spreading (Chrysikopoulos, Kitanidis et al. 1990; Chrysikopoulos, Kitanidis et al. 1992), suggesting that spatially variable bacterial attachment may significantly influence bacterial transport. Therefore determining the effects of spatially- and temporally-variable water chemistry on bacterial deposition is critical in order to accurately predict bacterial transport in the subsurface.

Previous studies have investigated isolated effects of transient solution chemistry on particle transport in saturated porous media. Tosco et al. (Tosco, Tiraferri et al. 2009) estimated the ionic strength dependent deposition and release of microparticles in saturated porous media using two empirical functions tied to the salt concentration. Lenhart and Sayers (Lenhart and Sayers 2003) modeled colloidal release and transport under transient chemical conditions by including a series of compartments representing immobile colloids, each of which exhibits a unique colloid-release with respect to changes in pore-water solute concentrations. Bradford et.al (Bradford, Torkzaban et al. 2012) modified a sophisticated dual-permeability transport model to predict colloidal transport and release under transient solution ionic strength, where colloid

immobilization was determined by considering applied hydrodynamic and resisting adhesive torques. While ionic strength is clearly an important chemical variable affecting bacterial attachment and transport, it is important to evaluate the collective variability of both physical and chemical parameters when predicting bacterial transport in heterogeneous media. This study aims to (1) develop a rate equation to predict bacterial attachment at the soil-water interface in response to changes in solution chemistry, and to statistically evaluate the relative importance of both physical and chemical parameters on bacterial attachment rate using Monte Carlo analysis; (2) develop a semi-reactive microbial transport model incorporating the effects of variable water chemistry on bacterial attachment using HP1 (HYDRUS1D (Šimůnek, Šejna et al. 2008) and PHREEQC (D.L. Parkhurst 1999)); and (3) apply the model to predict bacterial transport in experiments with mixing water sources.

4.2 Material and Methods

4.2.1 Development of rate equation to predict attachment at the soil-water interface (SWI)

Bacterial attachment at the soil-water interface (SWI) is predicted by combining semi-empirical and theoretical approaches as described in equations (4-1) - (4-15) to account for the effect of changes in solution chemistry on bacterial attachment. The attachment rate is predicted using a semi-empirical approach which has been widely used in transport studies (Harvey and Garabedian 1991; Logan, Jewett et al. 1995; Redman, Walker et al. 2004; Tufenkji and Elimelech 2004; Tufenkji 2006; Brown 2007):

$$k_{SWI} = \frac{3(1-\theta)}{2d_c} \eta \alpha v \quad (4-1)$$

where θ is the water content, d_c is collector diameter, η is single collector contact efficiency which has a closed-form equation (4-2) to calculate its value; v is the interstitial fluid velocity; α is the attachment efficiency which could be obtained via theoretical prediction, as shown from equations (4-3)-(4-15).

$$\eta = 2.4A_s^{1/3}N_R^{-0.081}N_{Pe}^{-0.715}N_{vdW}^{0.052} + 0.55A_sN_R^{1.675}N_A^{0.125} + 0.22N_R^{-0.24}N_G^{1.11}N_{vdW}^{0.053} \quad (4-2)$$

Where A_s is a porosity dependent parameter; N_R is aspect ratio; N_{Pe} is Peclet number; N_{vdW} is van der Waals number; N_A is the attraction number; and N_G is the new gravity number.

The value of the single collector contact efficiency (η) is obtained via the equations shown below:

$$\eta = 2.4A_s^{1/3}N_R^{-0.081}N_{Pe}^{-0.715}N_{vdW}^{0.052} + 0.55A_sN_R^{1.675}N_A^{0.125} + 0.22N_R^{-0.24}N_G^{1.11}N_{vdW}^{0.053} \quad (4-3)$$

$$As = \frac{2(1-\gamma^5)}{2-3\gamma+3\gamma^5-2\gamma^6} \quad (4-4)$$

$$N_R = \frac{d_p}{d_c} \quad (4-5)$$

$$N_{Pe} = \frac{Ud_c}{D_\infty} \quad (4-6)$$

$$N_{vdW} = \frac{A}{k_B T} \quad (4-7)$$

$$N_A = \frac{A}{12\pi\mu a_p^2 U} \quad (4-8)$$

$$N_G = \frac{2 a_p^2 (\rho_p - \rho_f) g}{9 \mu U} \quad (4-9)$$

Where A_s is a porosity dependent parameter and $\gamma = (1 - n)^{1/3}$; N_R is aspect ratio; N_{pe} is the Peclet number; N_{vdW} is the van der Waals number; N_A is the attraction number; and N_G is the new gravity number; n is porosity; d_p is particle diameter; d_c is collector diameter; U is fluid approach velocity; k_B is Boltzmann constant; T is temperature; a_p is particle radius; μ is fluid viscosity; ρ_p is particle density; ρ_f is fluid density; g is gravitational acceleration; and $D_\infty = \frac{k_B T}{6\pi\mu a_p}$.

Bacterial attachment at the SWI is categorized both under favorable conditions where the attachment efficiency (α_f) is 1, and under unfavorable conditions where the attachment efficiency (α_u) is much less than 1 (Elimelech, Nagai et al. 2000; Abudalo, Bogatsu et al. 2005). The overall attachment efficiency α is

$$\alpha = \alpha_u(1 - f) + \alpha_f f \quad (4-10)$$

where α_u is the attachment efficiency under unfavorable conditions; f is the fraction of mineral surface; $\alpha_f (\approx 1)$ is the attachment efficiency under favorable condition.

Theoretical mathematical models/approaches have been developed to predict the attachment efficiency, using the interaction force boundary layer (IFBL) model and the Maxwell approach. The IFBL model assumes that particle deposition onto a collector is at the primary energy minimum while the Maxwell model is based on particle deposition at secondary minima. The Maxwell model has been demonstrated to better predict attachment than the IFBL model (Hahn and O'Melia 2003; Shen, Li et al. 2007). As studied by Shen, Li et al (2007), the Maxwell approach can provide even more accurate

predictions of attachment efficiency if both primary and secondary minima are considered. In this study, the Maxwell approach is used to predict attachment efficiency under unfavorable conditions considering deposition at both primary- and secondary-minima:

$$\alpha_u = \alpha_{pri} + \alpha_{sec} = 1 - \int_{\sqrt{\Delta\phi_{sec}}}^{\sqrt{\Delta\phi}} \frac{4}{\pi^{1/2}} x^2 \exp(-x^2) dx \quad (4-11)$$

where $\Delta\phi$ is the sum of ϕ_{sec} and ϕ_{max} ; ϕ_{max} is maximum energy barriers and ϕ_{sec} is secondary-minimum depths, both of which can be calculated from the DLVO interaction energy profile using equations (4-12) - (4-15) (Hogg, Healy et al. 1966; Gregory 1981).

$$\phi_t = \phi_{vdw} + \phi_{el} \quad (4-12)$$

$$\phi_{vdw} = -\frac{Aa_p}{6y} \left[1 + \left(\frac{14y}{\lambda} \right) \right]^{-1} \quad (4-13)$$

$$\phi_{el} = \pi\epsilon_0\epsilon_r a_p \{ 2\psi_p\psi_c \ln \left[\frac{1+\exp(-\kappa y)}{1-\exp(-\kappa y)} \right] + (\psi_p^2 + \psi_c^2) \ln[1 - \exp(-2\kappa y)] \} \quad (4-14)$$

$$\kappa^{-1} = \sqrt{\frac{\epsilon_0\epsilon_r k_B T}{2N_A e^2 I}} \quad (4-15)$$

where A is Hamaker constant; a_p is the particle radius; y is separation distance; λ is the characteristic wavelength of the interaction; ϵ_0 is the permittivity in the vacuum; ϵ_r is the relative dielectric permittivity; ψ_p and ψ_c are particle surface potential (bacterial surface potential in our case) and collector surface potential respectively; κ is the inverse Debye length; k_B is Boltzmann constant; T is the temperature, N_A is Avogadro number; e is the elementary charge; I is the ionic strength.

In DLVO theory, the chemical factors such as ionic strength and surface charges of bacteria and collectors change with respect to the changes in solution chemistry, therefore,

different sets of surface charge values were assigned to bacteria and collectors when solution chemistry varies, which enable the rate equation to estimate bacterial attachment rate under heterogeneous chemistry.

The combined rate equation (4-1) was applied to experimental data from Elimelech *et al.* (2000) and Redman *et al.* (2004) for its validation. The predicted attachment rates were compared with the experimentally determined rates.

4.2.2 Sensitivity analysis of bacterial attachment rate at the SWI

A two-phase Monte Carlo analysis was conducted to evaluate the relative importance of physical and chemical parameters in predicting bacterial attachment rate. The analysis of chemical variability was nested within the analysis of physical variability, as illustrated in **Figure 4-1**.

First, values were selected at random from within each distribution of the physical parameters: particle size (a_p), soil grain size (d_c), porosity (n), fluid approach velocity (U), mineral fraction (f) and temperature (T). Together these random variables defined a physical simulation scenario. Next, values were selected at random from the distributions of each of the chemical parameters: ionic strength (I) and pH. The distributions of all physical and chemical input variables and constant parameters are summarized in **Table 4-1** and **Table 4-2**, respectively. These parameters defined the chemical iteration. The selected physical and chemical parameters were input into the model, and used to calculate the bacterial attachment rate. Without changing the values of the physical parameters, a new set of chemical parameters was selected randomly and used to calculate a new bacterial attachment rate. This output value represents the 2nd chemical

iteration of the 1st physical simulation scenario. This resampling of chemical parameters was repeated 500 times, resulting in 500 chemical iterations for the physical simulation scenario. These 500 output results were analyzed statistically, resulting in a cumulative distribution function (CDF). This CDF represents the variability in model estimates of bacterial attachment rate due to the variability of chemical parameters for one physical simulation scenario. This entire process was repeated for 500 physical simulation scenarios. Each physical simulation scenario resulted in a set of 500 simulated chemical iterations, represented in a single CDF. The overall analysis resulted in a distribution of 500 CDFs. The variation within each CDF shows the effects of chemical variability on the model estimates of bacterial attachment rate while the distribution of CDFs shows the effects of physical variability on bacterial attachment rate.

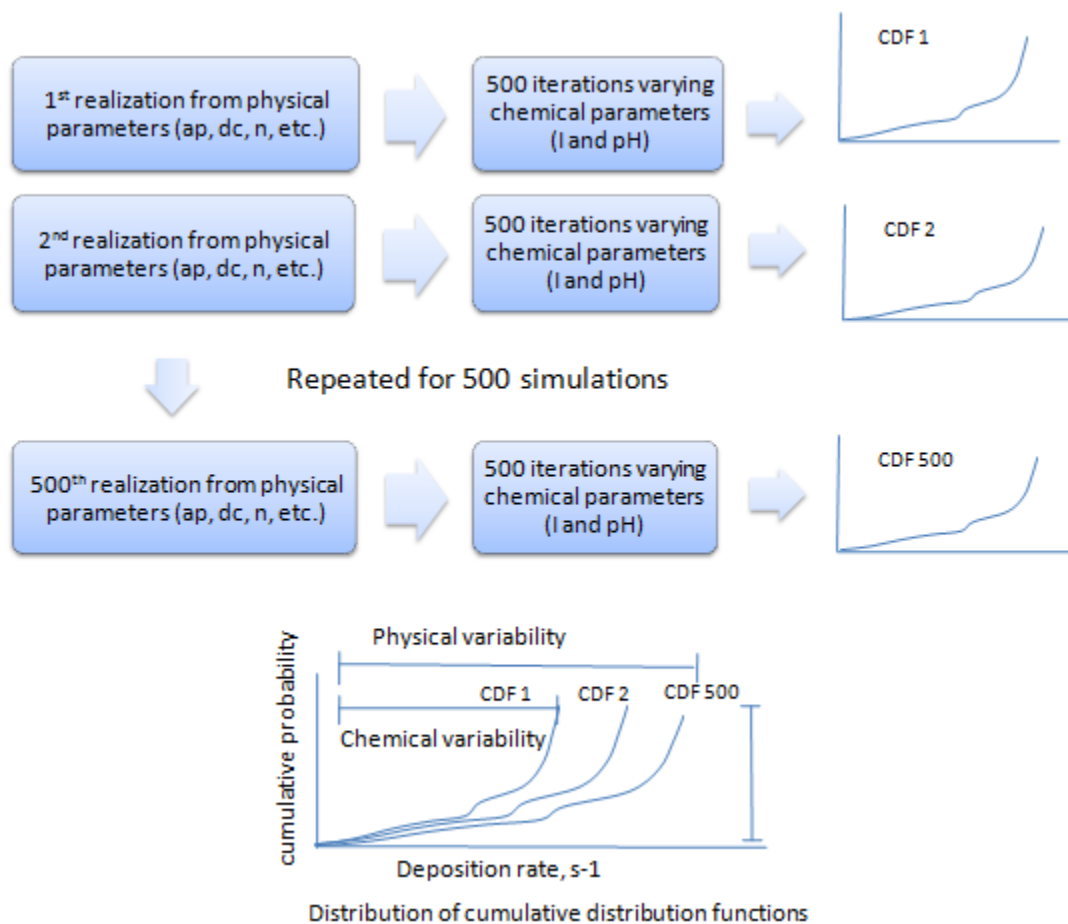


Figure 4-1. Procedure of two-phase Monte Carlo analysis

Table 4-1. Summary of input variables in rate prediction

Category	Input variables	Distribution	Unit
Chemical variables	Ionic strength, I	Uniform (0, 70)*	mol m^{-3}
	pH	Uniform (5, 9)	-
Physical variables	Fluid approach velocity, U	Uniform (5.56×10^{-8} , 8.25×10^{-5})	m s^{-1}
	Particle density, ρ_p^*	Uniform (1.105, 1.105)	g cm^{-3}
	Particle, a_p	Normal (1148, 0.1458)**	μm
	Fluid absolute temperature, T	Uniform (293, 298)	K
	Porosity, n	Uniform (0.36, 0.48)	-
	Collector diameter, d_c	Uniform (180, 600)	μm
	Mineral fraction, f	Uniform (0, 0.05)	-

* Lower bound and upper bound value are displayed in () under uniform distribution.

** Mean and standard deviation are displayed in () under normal distribution.

Table 4-2. Summary of constant parameters used in rate prediction

Constants	Value	Unit
Hamaker constant, A	6.50×10^{-21}	J
Characteristic wavelength,	100	-
Boltzmann constant, k	1.38×10^{-23}	J K ⁻¹
Permittivity in the vacuum,	8.85×10^{-12}	C · V ⁻¹ m ⁻¹
Relative dielectric permittivity,	79	-
Elementary charge, e	1.60×10^{-19}	C
Avogadro number,	6.02×10^{23}	mol ⁻¹
Gravitational acceleration, g	9.8	m s ⁻²
Fluid viscosity, μ	0.0089	g cm ⁻¹ s ⁻¹
Fluid density, ρ_f	0.988	g cm ⁻³
Attachment efficiency under favorable condition,	1	-

4.2.3 Modeling approach

A semi-reactive microbial transport model was developed to simulate scenarios with mixing water sources, as in the infiltration of stormwater runoff into a subsurface soil environment equilibrated with groundwater. A simplified infiltration basin as seen in **Figure 4-2** illustrates the environmental conditions to be simulated in the semi-reactive microbial transport model. An infiltration basin receives water from both precipitation and stormwater runoff, where bacteria and other pollutants, such as nutrients and heavy metals are present. Soil is initially covered with patch-wise mineral surfaces. During the infiltration process, the infiltrated stormwater runoff mixes with soil water/groundwater

in the subsurface. Bacteria may deposit at the soil-water interface (SWI) and the air-water interface (AWI), detach at the SWI, transport freely in the pore water or become inactivated during transport.

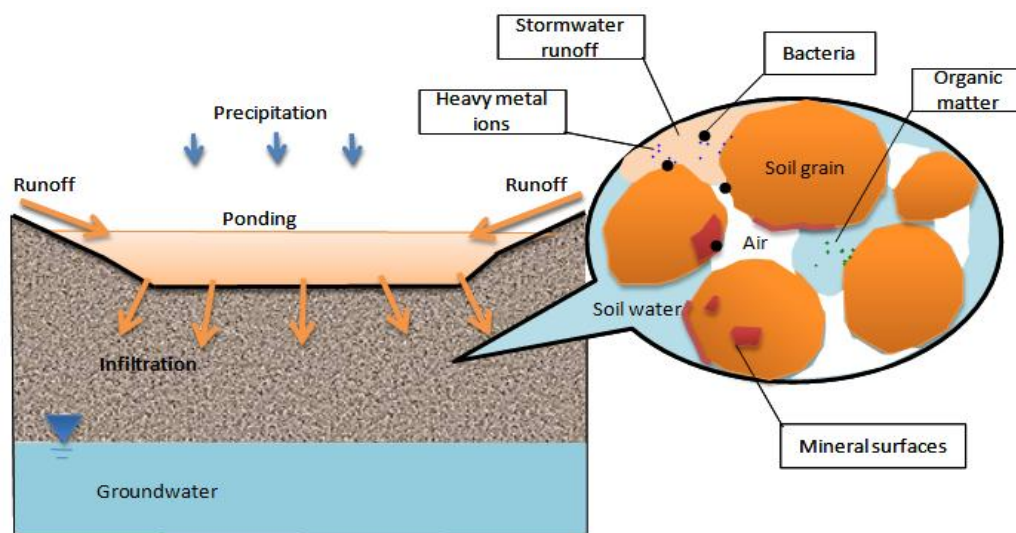


Figure 4-2. Schematic diagram of stormwater infiltration and bacterial transport and deposition in the subsurface

The model is developed within HP1 (HYDRUS1D-PHREEQC) (D.L. Parkhurst 1999; Šimůnek, Šejna et al. 2008) and includes both water flow and solute transport under transient, unsaturated flow conditions. The software package HP1 was developed by Jacques, D., and J. Šimůnek by coupling the HYDRUS-1D one-dimensional variably-saturated water flow and solute transport model with the PHREEQC geochemical code,

which has capabilities to model kinetic reactions with user defined rate expressions (Jacques and Šimůnek 2005; Jacques and Šimůnek 2010). **Figure 4-3** displays the schematic of the modeling approach of HP1.

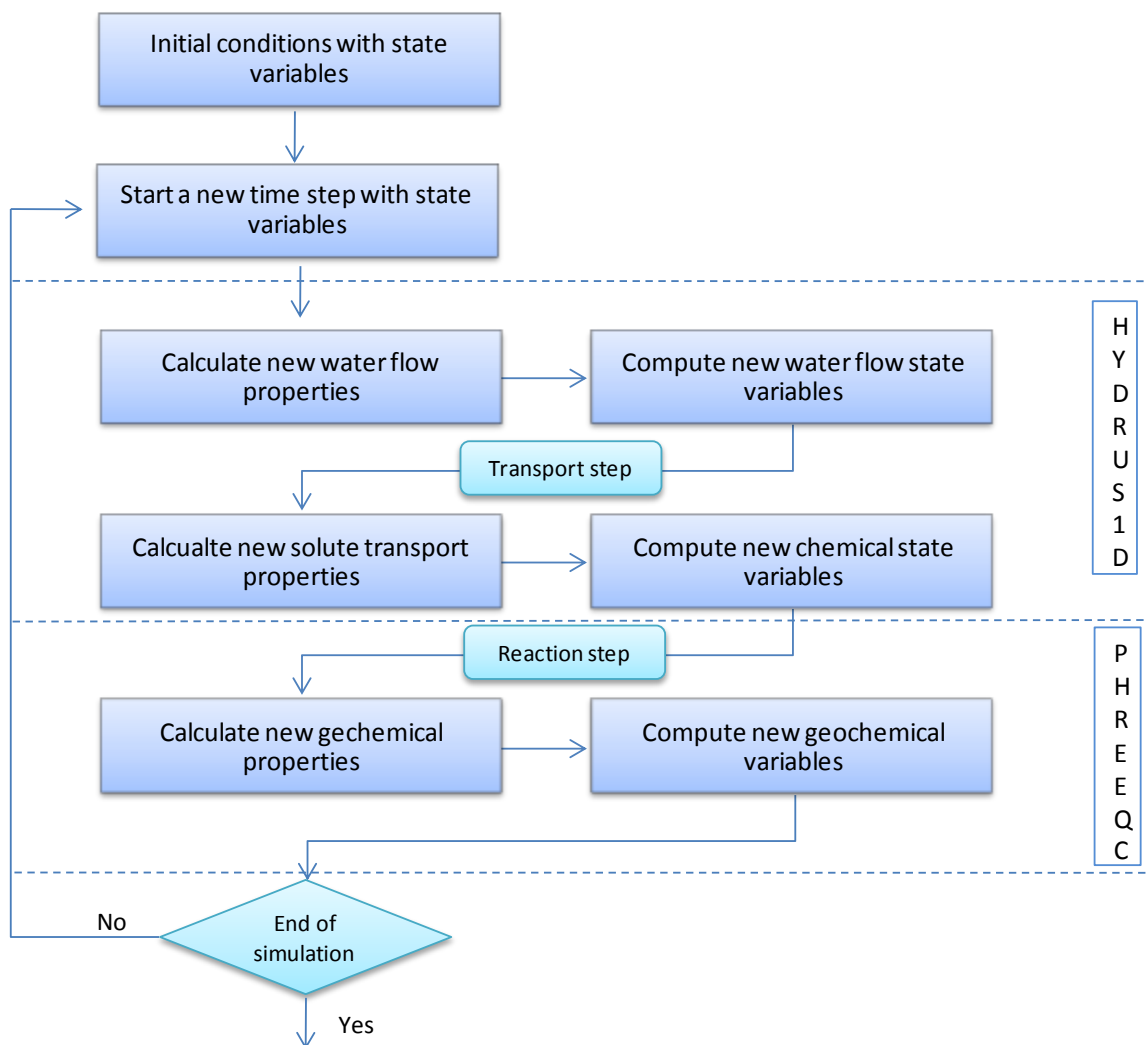


Figure 4-3. The schematic of the modeling approach of HP1, reproduced from Jacques and Šimůnek (2005).

Water flow and solute transport are simulated under the frame of HYDRUS 1D. The main inputs required for water flow are soil hydraulic parameters, and initial and boundary conditions. The main inputs required for solute transport are initial, boundary conditions and the processes involved during solute transport. Bacterial attachment at the SWI is estimated using the bacterial attachment rate equation, considering changes in solution chemistry due to mixing of the two water sources. Other transport processes such as attachment at the air-water interface (AWI), straining and inactivation are also included. Rate expressions for those processes are programmed into PHREEQC module in the form of Basic statements. Solute transport in the HYDRUS module is modeled as the transport of inert tracers (i.e., no interaction with the solid phase) because reactions are considered in the PHREEQC module. In PHREEQC, compositions of stormwater runoff and groundwater are defined to calculate solution chemistry. Bacteria are defined as an additional aqueous component.

The governing equation is a modified one dimensional advection dispersion equation, which includes bacterial attachment, detachment, straining and inactivation processes as described in equation (4-16).

$$\frac{\partial \theta C}{\partial t} = \frac{\partial}{\partial x} \left(\theta D \frac{\partial C}{\partial x} \right) - \frac{\partial q C}{\partial x} - k_{SWI} \theta C + k_{det} \rho S - k_{AWI} \theta C - \psi k_{str} \theta C - k_{decay} \theta C$$

(4-16)

where C is the aqueous concentration of the solute, S is the soil phase concentration, θ is the water content, q is the volumetric flux, D is the dispersion coefficient in the liquid phase, k_{SWI} is attachment rate at the SWI, k_{det} is detachment rate at the SWI, ρ is dry

bulk density of soil matrix, k_{AWI} is attachment rate at the AWI, ψ is dimensionless straining function, k_{str} is the straining coefficient and k_{decay} is decay/ inactivation rate.

Bacterial detachment rate from SWI (k_{det}) can be quantified using the following mass transfer equations.

$$k_{det} = \kappa_{det} A_{SWI} \quad (4-17)$$

The specific SWI area is estimated by the following equation (Fogler 1999) :

$$A_{SWI} = 6 \left(\frac{1-\theta_s}{d_c} \right) \quad (4-18)$$

Where κ_{det} is the mass transfer rate coefficient for detachment at SWI; A_{SWI} is the specific SWI area; d_c is the collector diameter; θ_s is the saturated water content.

Mass transfer coefficients for detachment at the SWI are calculated using literature values from studies of *Escherichia coli* transport through variably saturated columns (Jiang, Noonan et al. 2007) and *E. coli* O157: H7 (Bradford, Simunek et al. 2006).

Bacterial attachment rate at the air-water interface (AWI) is generally modeled using mass transfer equations.

$$k_{AWI} = \kappa_{AWI} A_{AWI} \quad (4-19)$$

Where k_{AWI} is bacterial attachment to the AWI; κ_{AWI} is liquid to AWI mass transfer coefficient; A_{AWI} is AWI area, which can be obtained by equations (4-20)-(4-21) (Faulkner, Lyon et al. 2003) .

$$A_{AWI} = \frac{\rho_f g \theta}{\alpha \sigma} \left[[S_e^{-1}]^{\frac{1}{1-n}} - 1 \right]^{\frac{1}{n}} \quad (4-20)$$

$$S_e = \frac{\theta - \theta_r}{\theta_s - \theta_r} \quad (4-21)$$

Where θ is water content; θ_s is the saturated water content; θ_r is residual water content; ρ_f is the fluid density, g is the gravitational constant, σ is the surface tension of water, S_e is the effective saturation; α, m and n are the Van Genuchten water retention function parameters.

The attachment at the AWI is considered irreversible. The AWI mass transfer coefficient (κ_{AWI}) is calculated using literature values from two transport studies on *E. coli* (Jiang, Noonan et al. 2007) and studies of virus transport in saturated and unsaturated sand (Anders and Chrysikopoulos 2009). Detachment from the AWI is assumed to be negligible because of the presence of large capillary forces (Schäfer, Ustohal et al. 1998).

Straining occurs when bacteria become trapped in down-gradient pore throats that are too small for bacteria to pass through. The magnitude of colloidal retention depends on both colloid and porous medium properties. Tien and Payatakes first suggested that straining is a dominant capture mechanism when the particle diameter is approximately 15% of the soil grain diameter (Tien and Payatakes 1979). Further research indicates that straining becomes significant when the ratio of bacterial size to collector size is larger than 0.005 (Bradford, Simunek et al. 2003; Bradford and Bettahar 2005). Bradford et al. (2003) define a correlation between straining coefficient and the bacteria : collector size ratio which can be used to predict a straining coefficient, k_{str} :

$$k_{str} = 269.7 \left(\frac{d_p}{d_{50}} \right)^{1.42} \quad (4-22)$$

The straining process is a function of distance and the dimensionless colloid straining function ψ is calculated by

$$\psi = \left(\frac{d_c + z}{d_c}\right)^{-\beta} \quad (4-23)$$

where d_c is the diameter of the sand grains, z is the down gradient distance from where straining process starts (the surface of the soil profile), and β is an empirical factor (with an optimal value of 0.43) (Bradford, Simunek et al. 2003).

Bacterial inactivation takes place during bacterial transport due to unfavorable conditions for bacterial survival and is described as first-order decay in equation (4-16).

4.2.4 Model application to lab data

Two sets of column transport experiments were conducted to evaluate bacterial transport in environments with both constant solution chemistry and variable solution chemistry, as described in **Table 4-3**. The semi-reactive microbial transport model implemented in HP1 was then applied to fit observed bacterial transport data.

Table 4-3. Summary of column transport scenarios

	Bacterial suspension	Background solution
Scenario 1	Bacteria suspended in synthetic stormwater (SSW)	AGW
Scenario 2	Bacteria suspended in artificial groundwater (AGW)	AGW

Solution preparation

Synthetic stormwater (SSW) was prepared by modifying a previously described recipe (Davis, Shokouhian et al. 2001). The formulation for SSW is as follows: 0.201 mg/L cupric sulfate (CuSO_4), 0.107 mg/L lead chloride (PbCl_2), 1.251 mg/L zinc chloride (ZnCl_2), 120 mg/L calcium chloride (CaCl_2), 12.14 mg/L sodium nitrate (NaNO_3) as well as 5.191 mg/L dibasic sodium phosphate ($\text{Na}_2\text{HPO}_4 \cdot 7\text{H}_2\text{O}$). The ionic strength of SSW was 2.9 mM and the pH was adjusted to 6. Artificial groundwater (AGW) was prepared following Mills *et al.* (Mills, Herman et al. 1994), with ionic strength of 42.3 mM and pH of 7.9. The formulation for AGW is as follows: 75.83 mg/L potassium nitrate (KNO_3), 842.58 mg/L magnesium sulfate (MgSO_4), 694.32 mg/L calcium sulfate (CaSO_4), 99.35 mg/L sodium chloride (NaCl) and 588.05 mg/L sodium bicarbonate (NaHCO_3).

Bacterial preparation

Escherichia coli (*E. coli*) K12 was selected due to its wide use as an indicator for fecal contamination. *E. coli* was cultured in 75 mL Luria-Bertani (LB) medium for 6 hours at 35 °C on an orbital shaker. Cell cultures were centrifuged at 7100 rpm for ten minutes and rinsed with deionized water (DI water). The resulting cell pellet was resuspended in either synthetic stormwater (SSW) solution or artificial groundwater (AGW) solution as prescribed for column transport experiments. Cell concentration was determined by measuring optical density at 590 nm. The cell length and width was measured via scanning electron microscopy.

Soil preparation

Field soil was collected from the top ten inches (25.4 cm) of a newly constructed bioretention basin in Philadelphia, PA and dried at 103 °C. The particle size distribution was determined and the mean grain size and coefficient of uniformity were determined. The organic matter (OM) content was determined in triplicate samples by comparing the mass difference before and after heating at 400 °C for four hours. The iron content of the soil sample was determined via EPA method 200.9. The soil properties are summarized in **Table 4-4**.

Table 4-4. The fitted soil hydraulic parameters, soil properties and bacterial properties

Parameters	Values
Saturated water content, θ_s	0.55
Residual water content, θ_r	0.015
Soil water retention parameter, α	0.038
Soil water retention parameter, n	2.33
Saturated hydraulic conductivity, k , cm/min	1.279
Soil size, d_c , μm	300
Size uniformity, -	2.36
Organic matter, -	0.062
Iron content, -	0.014
Bacterial equivalent diameter, μm	0.838 ± 0.076

Column transport experiments

The column setup for conducting bacterial transport experiments is displayed in

Figure 4-4. The acrylic column is 6 inch (15.24 cm) in height and 2 inch (5.08 cm) in

inside diameter. The bottom end plate is sealed by an o-ring. A filter membrane and a perforated aluminum plate were placed on both ends of the column. Two tensiometers were installed at depths of 1.5 inch (3.81 cm) and 4.5 inch (11.43 cm) from the top of the column to monitor the pressure head inside the column. The pressure head values were recorded by a data logger (Campbell Scientific, Inc., Logan, UT). The columns were dry packed to minimize disturbance of soil and then saturated by introducing DI water through the bottom of the column. The porosity and bulk density were obtained via mass balance. The saturated column was first flushed with enough DI water to ensure clarity of the effluent and then flushed with several pore volumes of background solution (AGW) to equilibrate the column with AGW. The saturated column was drained by gravity until no water flowed out to achieve unsaturated conditions. When simulating water flow under unsaturated conditions, AGW without bacteria was applied at constant flow rate (9ml per min) on the top of the column with a peristaltic pump for a designated duration. The pressure heads at two depths over time were recorded and used to inversely fit soil hydraulic parameters.

When simulating bacterial transport under unsaturated conditions, a saturated column was first flushed with enough DI water to ensure clarity of the effluent and then flushed with several pore volumes of background solution (AGW) to equilibrate the column with AGW. The saturated column was then drained by gravity to achieve unsaturated condition, which was used as the initial condition for bacterial transport. Two scenarios were simulated for bacterial transport as summarized in **Table 4-3**. The two types of bacterial suspensions were applied on top of the column at flow rate of 9ml per minute for at least two pore volumes (more than 35 minutes): (1) bacteria suspended in

SSW; and (2) bacteria suspended in AGW. The effluent was collected every 90 drops using a fraction collector and time was recorded.

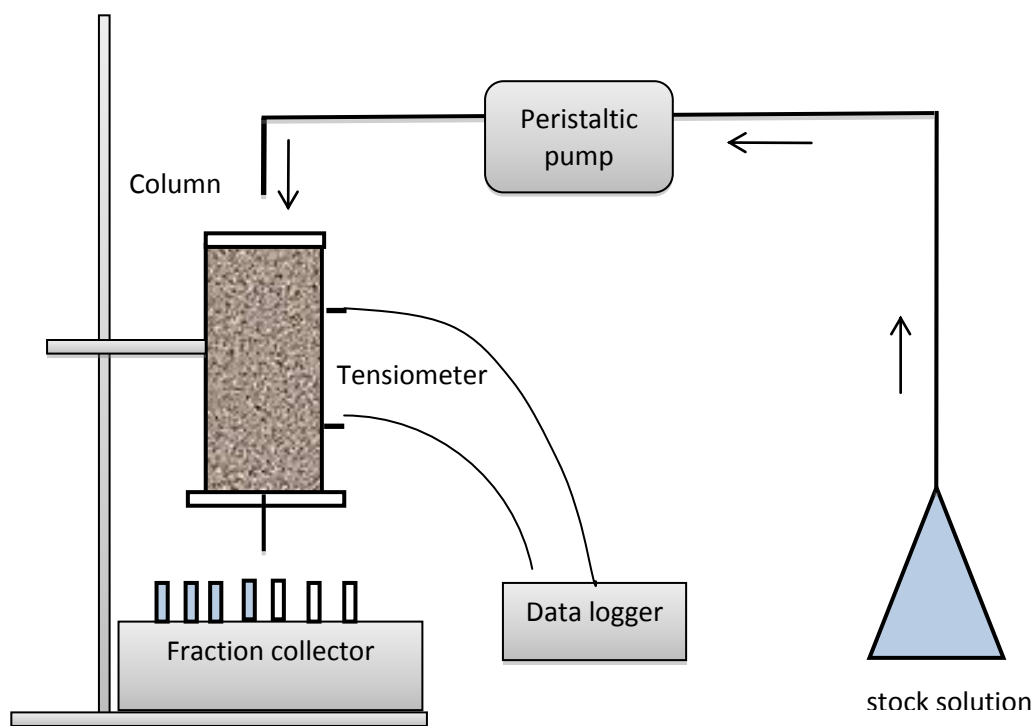


Figure 4-4. Schematic of the column setup for water flow and bacterial transport experiments

Inputs to the HYDRUS 1D Model

The initial soil profile in the column had a pressure head of $-21.26 \text{ cm H}_2\text{O}$ at the top of the column and zero $\text{cm H}_2\text{O}$ at the bottom of the column. The initial solution present in the soil was AGW with no bacteria. The upper boundary condition of the column was

input as a constant flux with bacteria suspended in either SSW or AGW. The lower boundary condition was described in HYDRUS using the seepage face boundary condition, which means that the bottom is exposed to atmosphere. This lower boundary condition is commonly used for column or lysimeter studies.

4.3 Results

4.3.1 Validation of rate equations used to predict bacterial attachment rate at the SWI

Experimental data from Elimelech *et al.* (2000) and Redman *et al.* (2004) were used to test the estimates of bacterial attachment rate predicted with the combined rate equations. In the study from Elimelech *et al.* (2000), colloidal transport in geochemically heterogeneous porous media was investigated, where clean sand grains were mixed with different fractions of aminosilane-modified sand while the ionic strength of the background solution was maintained at 1mM. The discrepancy between predicted attachment rate and experimentally determined rates was within 1.2 orders of magnitude, as seen in **Figure 4-5**. In the study from Redman *et al.* (2004), the adhesion of *E. coli* to quartz grains was studied under various ionic strengths. The discrepancy between predicted attachment rate and the experimentally determined rate was within 1.4 orders of magnitude, as shown in **Figure 4-6**.

The discrepancy between predicted and experimental attachment rates may be attributed to the Maxwell approach used to predict the attachment efficiency. Despite this discrepancy, the Maxwell approach is so far the best theoretical approach to predict attachment efficiency. A correction factor (CF) was added in equation (4-1) to account for the overestimation and to ensure that a conservative attachment rate is predicted and used in the semi-reactive microbial transport model.

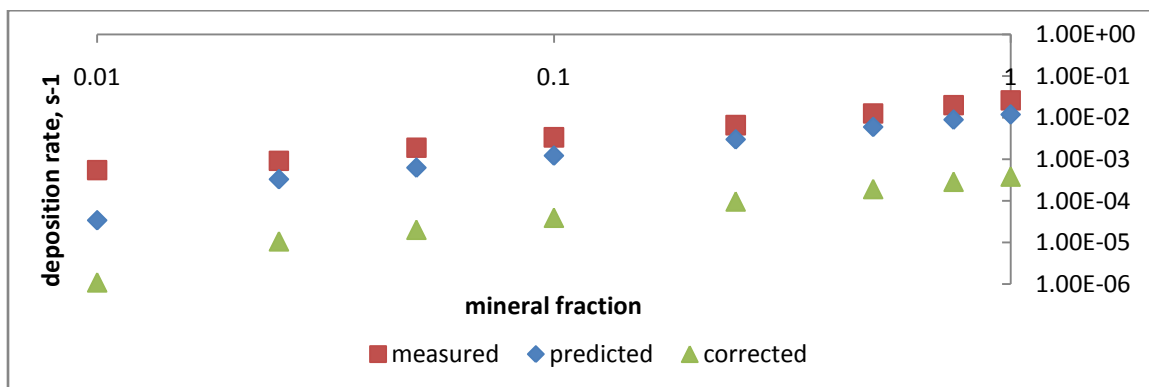


Figure 4-5. Predicted attachment rate using combined rate equations and corrected attachment rate versus the experimentally determined attachment rate from Elimelech, Magaiet *et al.* (2000). The background ionic strength is 1mM.

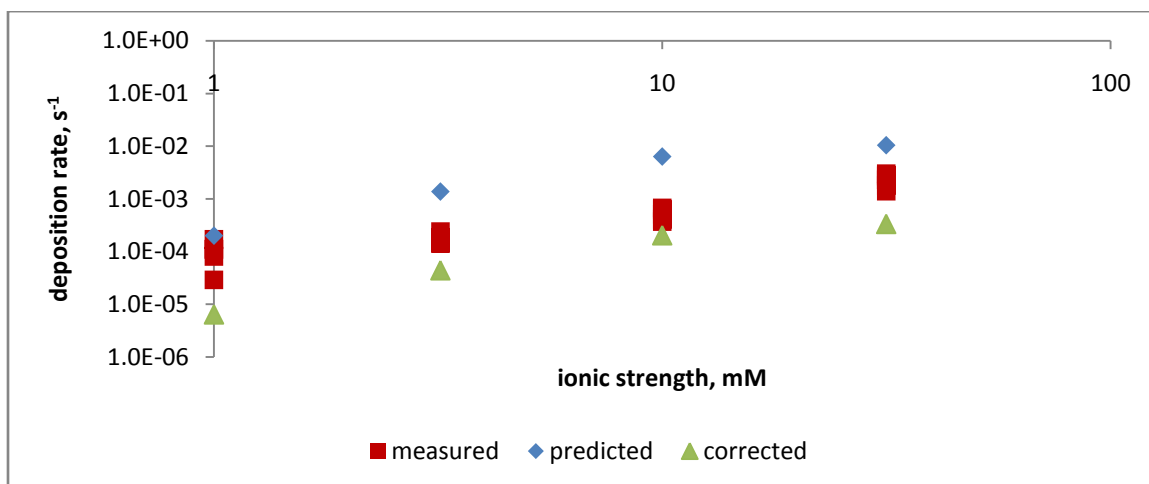


Figure 4-6. Predicted bacterial attachment rate using combined rate equations and corrected attachment rate versus experimentally determined attachment rate from Redman, Walker *et al.* (2004). The ionic strength varied from 1 mM to 100 mM.

4.3.2 Profile of attachment rate to SWI under two scenarios simulated

The validated rate equation was utilized to predict attachment rates at the SWI under two transport scenarios described in **Table 4-3**. The inputs of constant parameters, as well as fitted soil, hydraulic and bacterial properties are summarized in **Table 4-2** and **Table 4-4**, respectively. **Figure 4-7** displays changes in solution chemistry and attachment rate at the SWI 6 inches (15.24 cm) from the top of the column (at the column effluent) during a 40-minute simulation. For the AGW_AGW scenario with constant solution chemistry, the attachment rate remains unchanged throughout the simulation ($9.10 \times 10^{-3} \text{ min}^{-1}$). For the SSW_AGW scenario, in which the mixing of the two water sources results in a decrease in pH and ionic strength, the attachment rate at the SWI decreases from $9.10 \times 10^{-3} \text{ min}^{-1}$ to $3.71 \times 10^{-3} \text{ min}^{-1}$.

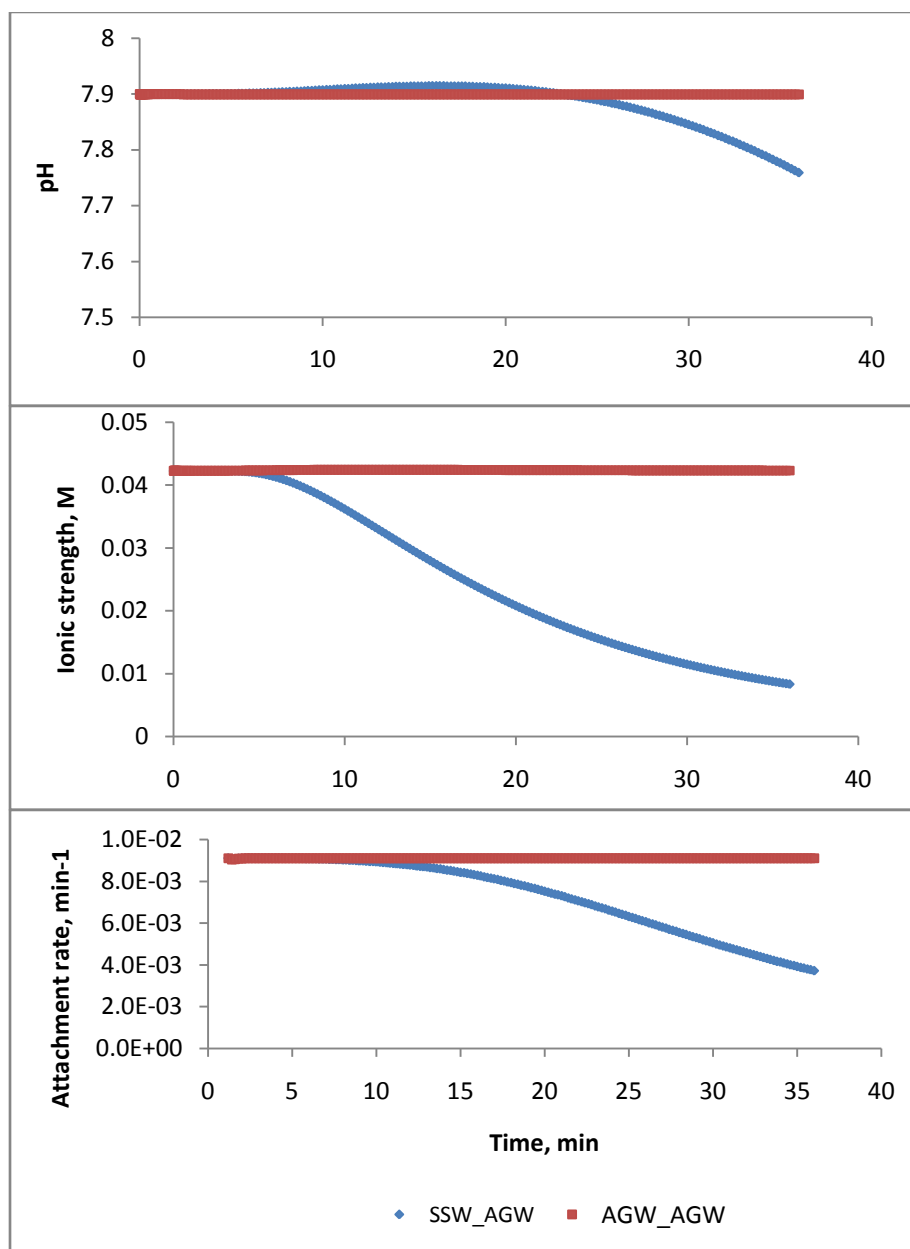


Figure 4-7. Profiles of pH, ionic strength and bacterial attachment rate at the SWI 6 inches from the top of the column under two transport scenarios: infiltration of bacteria and synthetic stormwater (SSW) into columns equilibrated with artificial groundwater (SSW_AGW, blue diamonds), and infiltration of bacteria and artificial groundwater (AGW) into columns equilibrated with AGW (AGW_AGW, red squares).

4.3.3 Sensitivity analysis of SWI attachment rate

It's important to distinguish between physical variability and chemical variability. When a distinction between physical variability and chemical variability is not maintained, their effects on estimation of attachment rate are mixed, which make it difficult to draw useful insight. A two-phase Monte Carlo analysis was conducted to evaluate the relative importance of physical and chemical parameters in predicting bacterial attachment rate.

The Monte Carlo procedure was performed using 500 physical simulations with each simulation consisting of 500 chemical iterations. Five hundred predictions of bacterial attachment rate for each physical simulation (each calculated using a different set of randomly-generated chemical input parameters) were analyzed statistically, resulting in a cumulative distribution function (CDF) of bacterial attachment rate within this physical simulation. The overall analysis (500×500 predictions) resulted in a distribution of 500 CDFs of bacterial attachment rate. For clarity, twenty of the 500 physical simulation outputs were randomly selected for presentation using boxplots. In **Figure 4-8 (a)**, each boxplot represents 500 chemical iterations within each physical simulation. The comparison across different boxplots indicates the variability of bacterial attachment rate due to physical parameters, while comparison within each physical scenario along the y-axis shows the variation due to chemical variables. In **Figure 4-8 (b)**, each CDF represents the probability that attachment rate will be found below or equal to certain values. The variation within each CDF shows the effects of chemical variability on the model estimates while the distribution of CDFs shows the effects of physical variability. **Figure 4-8 (c)** shows the 5th percentile, 50th percentile and 95th percentile of the CDFs.

Input-output correlation coefficients were calculated to quantitatively describe the importance of each variable on the prediction of bacterial attachment rate. Among physical variables, soil particle size has the highest correlation coefficient (-0.67), followed by porosity of the soil medium (-0.28), bacterial size (0.20) and flow velocity (0.17). Among chemical variables, ionic strength has the highest correlation coefficient (0.28).

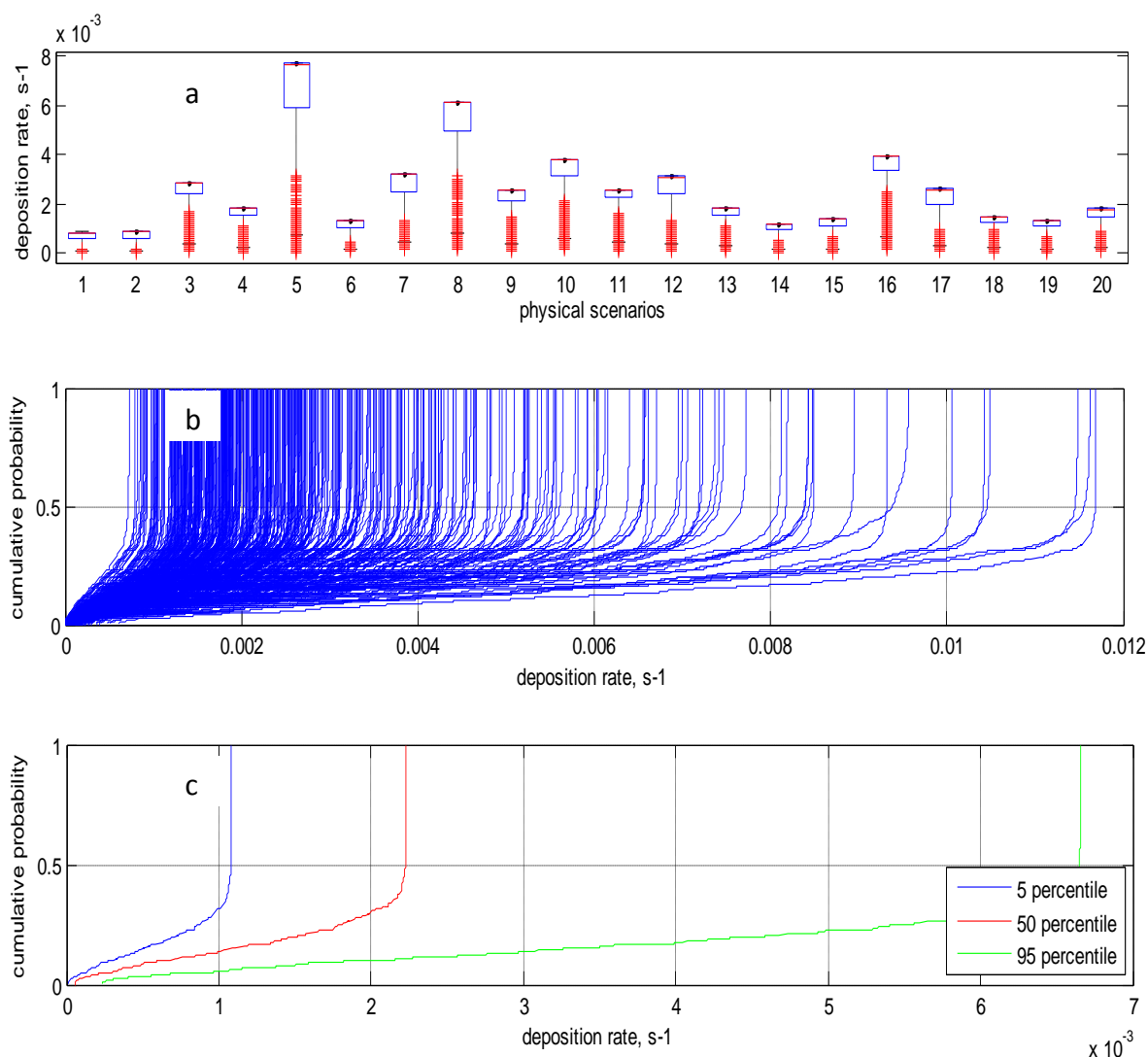


Figure 4-8. The variation of bacterial attachment rate due to physical variables (physical simulations) and chemical variables (chemical iterations within each physical simulation). (a) Boxplot of bacterial attachment rate at the SWI under different physical simulations; chemical parameters are varied within each simulation in 500 iterations; (b) distribution of CDFs of attachment rate resulting from 500 chemical iterations within 500 physical simulations; each CDF represents the distribution of attachment rate within each physical simulation resulting from variation of chemical variables; the distribution of 500 CDFs represents the variability of attachment rate due to physical variables. (c) 5th, 50th and 95th percentile of the distribution of simulated CDFs of attachment rate.

4.3.4 Inverse modeling of soil hydraulic parameters and dispersivity

Soil water pressure data from water flow experiments (pressure head at two depths vs time) were used to fit soil hydraulic parameters for field soil samples using HYDRUS 1D. The fitted soil hydraulic parameters are summarized in **Table 4-4**. Tracer (sodium chloride) transport was observed using the same column setup under saturated conditions. The tracer breakthrough curve data was used to fit the soil dispersivity. The dispersivity was determined to be 4 cm ($R^2 = 0.9996$).

4.3.5 Application of semi-reactive microbial transport model to bacterial transport data

Bacterial breakthrough curves (BTCs) under constant and variable solution chemistries are presented in **Figure 4-9**. Each observation point represents the average of triplicate experiments with error bars representing standard error. The solution chemistries of SSW and AGW are different in three aspects: pH (6 for SSW vs 7.9 for AGW), ionic strength (2.9 mM for SSW vs 42.3 mM for AGW) and solution composition (heavy metals present in SSW but not AGW). The breakthrough curve in the AGW-AGW scenario has a lower plateau ($C/C_0 = 0.532$) and effluent mass recovery (34.9%) than the SSW-AGW scenario (C/C_0 of 0.812 and mass recovery of 47.1%). Ignoring changes in solution chemistry results in erroneous predictions of bacterial transport, as demonstrated.

The mixing of SSW with AGW decreases the solution pH (which enhances bacterial attachment), decreases the ionic strength (which reduces bacterial attachment) and increases the concentration of heavy metals (which enhances bacterial attachment (Zhang and Olson 2012)). Under the combined effects of solution chemistry, the BTC in the

SSW_AGW scenario shows reduced bacterial attachment, indicating that the effects of ionic strength dominate bacterial attachment in this case.

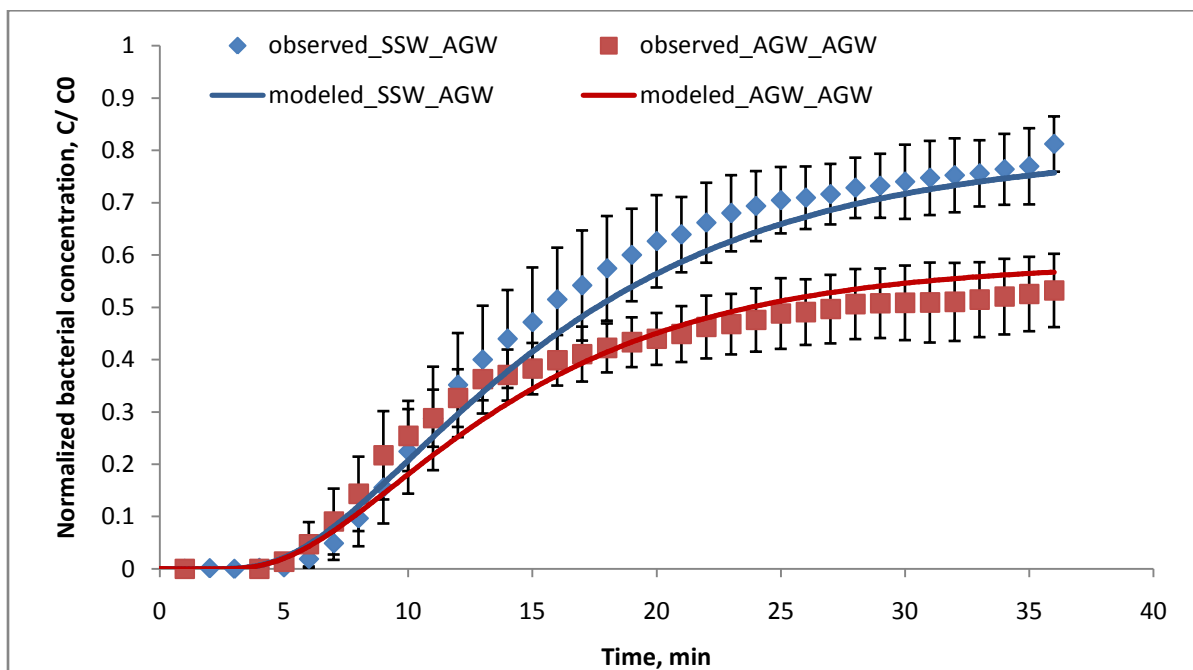


Figure 4-9. Observed (red square vs blue diamond) and modeled (red line vs blue line) bacterial breakthrough curves under constant solution chemistry (AGW_AGW, $R^2 = 0.951$) and variable solution chemistry (SSW_AGW, $R^2 = 0.986$). Each observation point represents the average of triplicate experiments with error bars representing standard error.

The semi-reactive microbial transport model was applied to fit observed BTCs.

Straining was neglected from the model because the ratio of bacterial size to average soil grain size (d_c) was smaller than 0.05 (Bradford, Simunek et al. 2003). Bacterial

inactivation was also assumed to be negligible due to the relatively short duration of the transport experiments (approximately 40 minutes). Therefore, the variation in BTCs was primarily due to bacterial attachment at the SWI, detachment at the SWI and attachment at the AWI.

The semi-reactive microbial transport model was applied to describe *E. coli* breakthrough in the AGW_AGW scenario. Attachment rate at the SWI was predicted using the combined rate equations. The mass transfer coefficient for attachment at the AWI and the mass transfer coefficient for detachment at SWI were used as fitting parameters, and optimal values were selected. The mass transfer coefficient for attachment at the AWI was $2.5 \times 10^{-8} \text{ m s}^{-1}$, within the range reported in the literature (Jiang, Noonan et al. 2007). The mass transfer coefficient for detachment at the SWI was $1.25 \times 10^{-10} \text{ m s}^{-1}$. The modeled bacterial breakthrough curve of the AGW_AGW scenario is displayed as the red solid line in **Figure 4-9**, with an R-squared value equal to 0.951.

The semi-reactive transport model was then applied to the bacterial breakthrough curve observed in the SSW_AGW scenario. Attachment at the SWI was also estimated using the combined rate equations, which take into consideration mixing of SSW and AGW. The previously fitted mass transfer coefficient at the AWI ($2.5 \times 10^{-8} \text{ m s}^{-1}$) was used, because attachment rate at the AWI is not strongly influenced by solution chemistry, as compared with SWI attachment. The mass transfer coefficient for detachment was fitted and the best value was determined to be $1.0 \times 10^{-5} \text{ m s}^{-1}$. The modeled bacterial breakthrough curve for the SSW_AGW scenario is displayed as a blue solid line in **Figure 4-9**, with an R-squared value equal to 0.986.

4.4 Discussion

The importance of solution chemistry in determining bacterial attachment has been shown extensively, yet water chemistry is generally assumed to be static when modeling bacterial transport. This assumption of constant solution chemistry does not accurately represent bacterial transport behavior when heterogeneous solution chemistries are involved, as is proven in the column transport experiments in this study. Results from column transport experiments indicate a 47.1% bacterial mass recovery in effluent from mixed synthetic stormwater and artificial groundwater (SSW_AGW) experiments, compared with 34.9% bacterial mass recovery under constant water chemistry (AGW_AGW). This increase in bacterial breakthrough under variable solution chemistry can be attributed to the decrease in attachment rate at the soil-water interface and the increase in detachment rate at the soil-water interface.

We observed a 35 percent increase in the total number of effluent bacteria in conditions with variable water chemistry, that can only be accounted for computationally when variable solution chemistry is considered in the transport model. Therefore ignoring variations in solution chemistry in bacterial transport models may result in erroneous predictions of microbial breakthrough. The semi-reactive microbial transport model introduced in this study, which estimates temporally- and spatially-variable bacterial attachment rates based on changing water chemistry, is able to accurately model and predict bacterial transport under variable solution chemistry. As such it represents a positive step towards understanding and modeling bacterial transport in complex microbial-water-soil systems.

CHAPTER 5. FIELD EVALUATION AND MODELING OF MICROBIAL POLLUTANT REMOVAL IN BIORETENTION SYSTEMS USING A SEMI-REACTIVE MICROBIAL TRANSPORT MODEL

Abstract

Research efforts on bioretention systems have historically concentrated on the removal of physical and chemical pollutants. The removal of biological contaminants in bioretention systems is studied to a lesser extent, particularly under heterogeneous field conditions. In this study, influent and effluent water samples from bioretention areas in New York City were analyzed for fecal indicator *E. coli* in order to assess the bacterial removal efficiency of the bioretention systems. During three storm events monitored, reduction in bacterial concentrations in effluent samples was observed, except for one storm on July 20th, 2012, where an increase in the effluent bacterial concentration was observed. Even when bacterial concentrations in the effluent were reduced, approximately 87.5% of the total effluent samples exceeded the primary contact recreation standard of 126 CFU/100ml. Bacterial removal was found to be affected by the antecedent field conditions, specifically the number of dry days. The presence of preferential flow paths in bioretention areas was shown to negatively affect bacterial removal. A semi-reactive microbial transport model, capable of estimating bacterial attachment at the soil-water-interface using aqueous chemical data, was applied to test its ability to capture bacterial transport data in heterogeneous field conditions. The modeled bacterial removal efficiency agrees well with observed values. The measured bacterial removal efficiency was 66% for storm event on August 15th, 2012, while the modeled removal efficiency

was 71%. A slight overestimation of the removal efficiency may be due to the presence of preferential flow paths in the field, which are not considered in the semi-reactive microbial transport model. In addition to bacteria removal, turbidity, total nitrogen and total phosphorous were also analyzed to evaluate their removal efficiencies in bioretention areas. Most effluent samples had higher turbidity, total nitrogen and total phosphorous readings than their corresponding influent samples, which may be a result of organic matter and debris washing off from the bioretention areas.

Keyword: stormwater runoff, bioretention, bacterial removal, antecedent dry period, preferential flow

5.1 Introduction

Urbanization, and the associated increase in impervious surfaces, reduces natural groundwater recharge while increasing the volume of urban stormwater runoff. The stormwater runoff available for recharge contains high levels of pollutants, including total suspended solids, nutrients, heavy metals, organics as well as pathogenic microorganisms (Pitt, Clark et al. 1999; Davies and Bavor 2000; Prestes, Anjos et al. 2006; Brownell, Harwood et al. 2007; Helmreich, Hilliges et al. 2010). Contamination of groundwater by pathogenic microorganisms threatens the safety of groundwater as a potable water resource.

To mitigate increases in storm-water runoff, stormwater BMPs have been applied by many communities to control and treat stormwater runoff. Bioretention systems are one of the best BMPs to treat stormwater runoff, as recommended by the U.S. EPA. Research on the effectiveness of bioretention systems has concentrated on physical and chemical contaminants such as total suspended solids, nutrients and metals, while considerably less effort has been devoted to the investigation of microorganism removal from stormwater runoff. Many studies on bacterial removal in bioretention systems are limited to the lab scale (Rusciano and Obropta 2007; Zhang, Seagren et al. 2010; Zhang, Seagren et al. 2011; Zhang, Seagren et al. 2012) while field studies are very few (Hunt, Smith et al. 2008; Hathaway, Hunt et al. 2009; Zhang, Seagren et al. 2012). The highly variable effectiveness of bacterial removal in bioretention systems summarized in **Table 2-1** indicates that a variety of conditions affect microbial removal and transport and thus the performance of bioretention systems.

In a study of five pilot bioretention units with different vegetation types, the highest bacterial removal efficiency was observed in a control unit where no vegetation was planted. This result was attributed to a high hydraulic retention time in the control unit, where soil particle size was uniform and no preferential flow paths were created from the root system (Kim, Sung et al. 2012). The bacterial removal efficiency was found to be independent of temperature, although the influent bacterial concentration was related to daily temperature (Zhang, Seagren et al. 2012). Other factors influencing the performance of bioretention areas include precipitation intensity and duration, antecedent number of dry days, land use, geographic characteristics and maintenance practices. The roles of those factors in determining bacterial removal in bioretention systems are not clear, because of the limited number of field studies available, which is likely due in part to the difficulty of collecting effluent water samples following infiltration into the underlying soil. A better understanding of the factors affecting bacterial removal could provide useful information in the design of urban bioretention systems.

In light of frequent detection of bacteria in stormwater runoff, it is increasingly important to consider the removal of bacterial, as well as physical and chemical, pollutants when evaluating the effectiveness and sustainability of bioretention systems operating under heterogeneous field conditions (O'Shea and Field 1992; Arnone 2005; Selvakumar and Borst 2006). A semi-reactive microbial transport model was developed, and described in Chapter 4, to model bacterial transport in the subsurface with variable water chemistry, as is common when surface water mixes with groundwater. This chapter presents a field validation of the model. Two bioretention areas (Nashville and Colfax) located in New York City were monitored over the summer of 2012 to determine their

bacterial removal efficiency. The collected bacterial transport data from the bioretention areas were used to test the performance of the semi-reactive microbial transport model in the field condition.

The overall objectives of this chapter are: (1) to evaluate the performance of bioretention areas in removing microbial pollutants (fecal indicator *Escherichia coli* in this study); (2) to model bacterial transport through a bioretention system using a semi-reactive microbial transport model.

5.2 Methods

5.2.1 Site description

Two bioretention areas were investigated in this study, both located in Queens, NY, and termed “Nashville” and “Colfax”, based on their cross-streets. The Nashville bioretention area was designed to collect and treat stormwater runoff while the Colfax bioretention area was designed to receive precipitation only. Schematic diagrams of the two bioretention areas and site images are illustrated in **Figure 5-1** and **Figure 5-2**, respectively.

Nashville bioretention area is located at 116th Avenue and Nashville Boulevard, Queens, NY. The site area is about 223.5 m². The bioretention area (from top to bottom) consists of 0.075 m of mulch, 0.6 m of bioretention soil mix and 0.3 m of 20 mm crushed blue stone below the native soil. The area is planted with native trees and plants. To analyze effectiveness of the bioretention area on bacterial removal, two housings (influent housing and effluent housing) and a weighing lysimeter were installed onsite. Stormwater runoff is introduced into the bioretention area via a flume and then diverted at the still pond. Part of stormwater runoff is diverted to the lysimeter to simulate the

runoff conditions while the remaining runoff is spilled into the bioretention area other than the lysimeter. The influent housing positioned between the still pond and the lysimeter while the effluent housing is placed after the lysimeter. Both housings have ISCO water samplers installed and programmed to sample the influent to the lysimeter and the effluent from the lysimeter. The circular lysimeter has a diameter of approximately 1 m and a depth of 0.75 m. The soil profile in the lysimeter is nearly identical to the rest of the bioretention area with 0.075 m of mulch, 0.6 m of bioretention soil mix and 0.15 m of a crushed stone drainage layer. A scale was put at the bottom of the lysimeter to monitor changes in lysimeter mass resulting from the gain and loss of water. Five soil moisture sensors were installed inside the lysimeter at five different depths: 5 cm, 10 cm, 20 cm, 30 cm and 50 cm from the top. A weather station is located at the center of the bioretention area which captures the wind speed and direction, air temperature and relative humidity. Rain gauges and a rain collector were also installed on site.

Colfax bioretention area is located at 210th Street and Colfax Street, Queens, NY. The site area is approximate 113 m². The setup of the bioretention area is similar to Nashville, except there is no influent housing in the Colfax bioretention area, because it is designed to receive precipitation only.

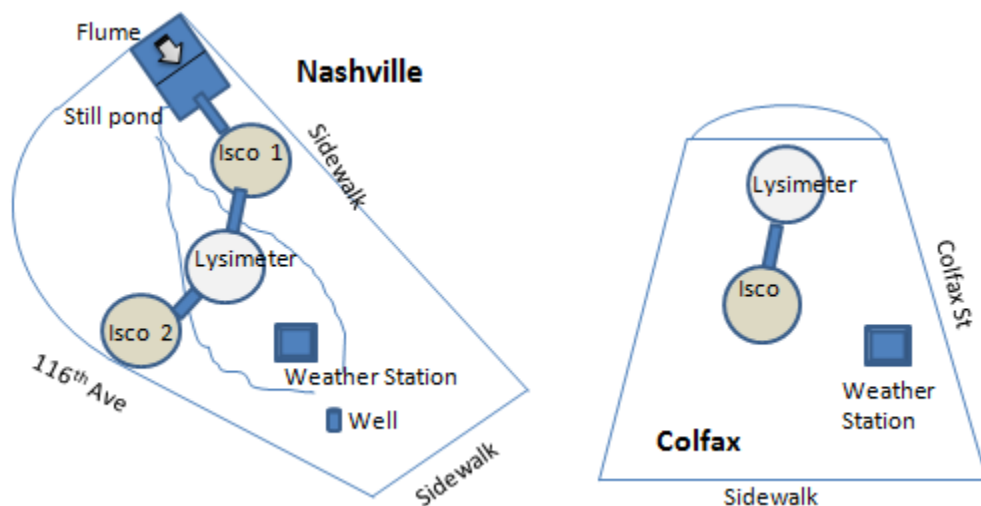


Figure 5-1. Schematic of Nashville bioretention area and Colfax bioretention area



Figure 5-2. Site setup of Nashville basin (A-E) and Colfax bioretention area (F). (A) overview of Nashville bioretention area; (B) the flume and the still pond; (C) the influent housing; (D) the weighing lysimeter; (E) the effluent housing; (F) overview of Colfax bioretention area with the weighing lysimeter and the effluent housing.

5.2.2 Soil characterization

The bioretention soil mix (0.6 m) at both bioretention areas was analyzed to determine soil classification. Soil samples were collected from six or seven discrete depths. The particle size distribution, organic matter content as well as iron content of the soil mix at Nashville were also determined. The particle size distribution was determined by passing the soil mix through series of sieves. The mean grain size and coefficient of uniformity were determined. The organic matter content was determined in triplicate samples by comparing the mass difference before and after heating at 400 °C for four hours. The iron content of the soil mix was determined using EPA method 200.9.

5.2.3 Water sampling

The water sampling for both Nashville and Colfax bioretention areas took place during the storm events in the summer of 2012. The amount of precipitation required was no less than 0.5 inch (1.27 cm) due to the desire to get effluent from the lysimeter in the Nashville bioretention area. Only eligible storm events were sampled and analyzed.

At the Nashville bioretention area, three types of water sample were collected during three storm events in the summer of 2012: rain water, influent water to the lysimeter (stormwater runoff), and effluent water from the lysimeter (treated stormwater runoff). Rain water was collected in an on-site rain collector. Influent and effluent water samples were collected by two ISCOs. ISCO 1 in the influent housing was set to be enabled when the water level in the influent pipe rose above half of the pipe diameter and the flow velocity is larger than zero; the sampler was otherwise disabled. ISCO 2 in the effluent housing was programmed to be enabled when the water level in a collection beaker triggered a water-sensitive actuator (the level actuator was positioned at a certain depth to

ensure enough effluent could be sampled) and disabled otherwise. When the water sampler was continually activated, it sampled every 15 minutes.

At the Colfax bioretention area, two types of water samples were collected during each storm event: rain water and effluent water from the lysimeter. Rain water was collected using the rain collector. The effluent was collected via ISCO sampler whose setting was the same as ISCO 2 at Nashville.

The collected water samples were cooled with ice packs and transported to laboratory immediately for water quality analysis. The water quality parameters analyzed were fecal indicator (*E. coli*), turbidity, pH, total nitrogen and total phosphorus. *E. coli* concentration was determined via EPA method 1603 (Modified mTEC membrane filtration method). Turbidity and pH were measured using a turbidity meter and pH meter, respectively. Total nitrogen and total phosphorous were determined using HACH method 10071 and HACH method 8189, respectively.

The precipitation, soil volumetric water content at five depths and lysimeter mass were continually monitored and recorded using a data logger (Campbell scientific CR1000) during the period of this study.

5.3 Data Analysis

The bacterial removal efficiency was also calculated as:

$$Bacterial\ removal\ efficiency = 1 - \frac{\sum(C_{out,i} \times V_{out,i})}{\sum(C_{in,i} \times V_{in,i})} \quad (5-1)$$

Where $C_{out,i}$ is the *E. coli* concentration of i^{th} effluent sample, $V_{out,i}$ is the corresponding effluent volume; $C_{in,i}$ is the *E. coli* concentration of i^{th} influent sample; $V_{in,i}$ is the corresponding influent volume.

5.4 Application of the Semi-reactive Microbial Transport Model

The semi-reactive microbial transport model described in Chapter 4 was used to model bacterial transport at Nashville bioretention area. The inputs required to run the model include the initial soil moisture profile, the water flow boundary conditions and the solute transport boundary conditions, the soil hydraulic parameters, bacterial properties and solution chemistry.

Soil moisture data at five different depths were continually monitored via moisture sensors. The upper boundary condition for water flow was set as variable water flux and lower boundary condition for water flow was set as seepage face, which means that the bottom is open to atmosphere. The surface water flux was calculated by dividing the total influent water volume by the cross-sectional area of the lysimeter, where the total influent volume to the lysimeter was determined based on the changes in lysimeter mass and the effluent volume. The change in the lysimeter mass was the mass difference between influent water and effluent water. The total influent volume was then obtained by adding up the volume difference (converted from the mass difference of the lysimeter) and the effluent volume.

The upper boundary condition for solute transport was concentration flux, where solution composition of the infiltrating water was specified using characteristics of synthetic stormwater runoff described in section 4.2.4 in Chapter 4 (the infiltrating water

was collected, but not yet analyzed by a collaborator). The lower boundary condition is a zero concentration gradient.

The soil particle size and iron content of the soil mix were determined as described in section 5.2.2. The *E. coli* properties were adopted from **Table 4-1** in section 4.2.2 and **Table 4-4** in section 4.2.4 in Chapter 4. The soil hydraulic parameters were inversely fitted in HYDRUS 1D using the soil moisture data collected during each storm event. The hydraulic model selected in HYDRUS 1D is van Genuchten (1980).

Using these inputs, modeled bacterial breakthrough curves were generated using the semi-reactive microbial transport model and compared with the observed bacterial transport data.

5.5 Results

5.5.1 Soil properties

The soil samples collected from six discrete depths at the Nashville bioretention area (0-6.5 cm, 6.5-13 cm, 13-19.5 cm, 19.5-25 cm, 30-44 cm, 44-60 cm) and seven depths at the Colfax bioretention area (0-6.5 cm, 6.5-13 cm, 13-19.5 cm, 19.5-26 cm, 23-28 cm, 28-33 cm and 33-38 cm) indicate that the majority of bioretention soil mix is sand, with a small portion of loamy sand. The presence of a high percentage of sand can increase the infiltration capacity, which is desirable from the perspective of controlling stormwater runoff volume. Further soil characterization was conducted on soil mix collected from the Nashville bioretention area. The soil particle size distribution (**Figure 5-3**) demonstrates that over 78% of the soil particles are larger than 425 μm , with a median soil particle size of 850 μm and a uniformity coefficient of 2.85. The soil properties are summarized in **Table 5-1**.

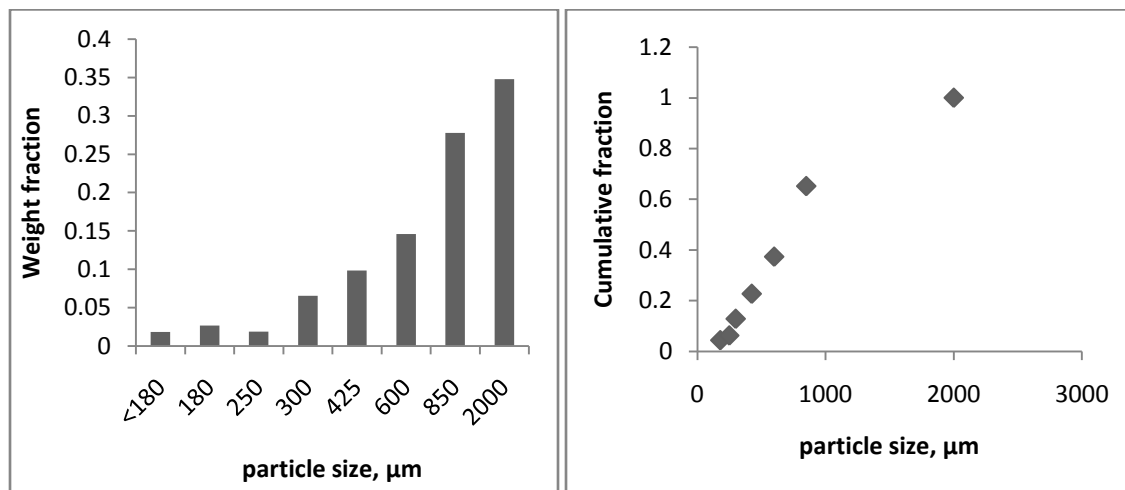


Figure 5-3. The particle size distribution of soil mix from Nashville bioretention area

Table 5-1. The soil properties at Nashville bioretention area

Parameters	Soil
Soil classification	sand
Soil size, d_c , μm	850
Size uniformity coefficient, -	2.85
Organic matter, -	0.030
Iron content, -	0.013
Bacterial equivalent diameter, μm	0.838

5.5.2 Storm event characteristics

Three complete storm events were sampled at the Nashville bioretention area and two storm events at the Colfax bioretention area (**Table 5-2**). The total precipitation varied from 10.67 mm to 40.26 mm over the entire day of the sampling events, and the antecedent number of dry days ranged from 1 day to 12.

Table 5-2. Characteristics of storm events

Storm number	Date	Total precipitation, mm	Antecedent number of dry days	Sampling Sites
1	7/20/2012	10.67	1	*N only
2	8/15/2012	26.93	4	N, C
3	9/18/2012	40.26	12	N, C

*N stands for Nashville bioretention area; C stands for Colfax bioretention area.

5.5.3 Water quality analysis

Bacterial analysis

No *E. coli* was detected in rain water collected from either bioretention areas during the three storm events, which suggests that there are no bacteria present in the rain water. The effluent *E. coli* concentrations at the Colfax bioretention area ranged from zero to very low (20 CFU/100ml) as observed during two storm events monitored.

In contrast, high levels of *E. coli* concentration were detected from both influent and effluent samples at the Nashville bioretention area for each storm, as seen in **Figure 5-4**, **Figure 5-5** and **Figure 5-6**. The *E. coli* concentrations in influent samples (stormwater

runoff) to Nashville show substantial variability, with a range from as low as 20 CFU/100ml to as high as 1.0×10^5 CFU/100ml. The *E. coli* concentration in the influent samples on September 18th, 2012 reach as high as two orders of magnitude higher than the maximum concentrations recorded from the other two events. Among all influent samples analyzed, approximately 79% exceed the primary contact recreational standard (126 CFU/100ml). The *E. coli* concentration in effluent samples also varies substantially, ranging from 80 CFU/100ml to 6.0×10^4 CFU/100ml. Reduction in *E. coli* concentration was observed after flowing through bioretention soil mix for two storm events, but not for the storm event on July 20th, 2012, when a relatively high increase of *E. coli* concentration in effluent was observed. Although the concentrations of *E. coli* were reduced in the effluent, they do not necessarily achieve the primary contact standard (126 CFU/100ml). Instead, approximately 88% of the total effluent samples analyzed exceeded the standard, which might be due to the high bacterial inputs from the influent.

Higher bacterial counts was observed in effluent from the Nashville bioretention area, which received both runoff and precipitation, compared to zero or low bacterial counts in effluent from the Colfax bioretention area, which received precipitation only. It indicates that the bacterial loads to bioretention areas are primarily from stormwater runoff.

The bacterial removal efficiency for the bioretention area was calculated using Equation (5-1) for the storm event on August 15th. The bacterial removal efficiency was 66%.

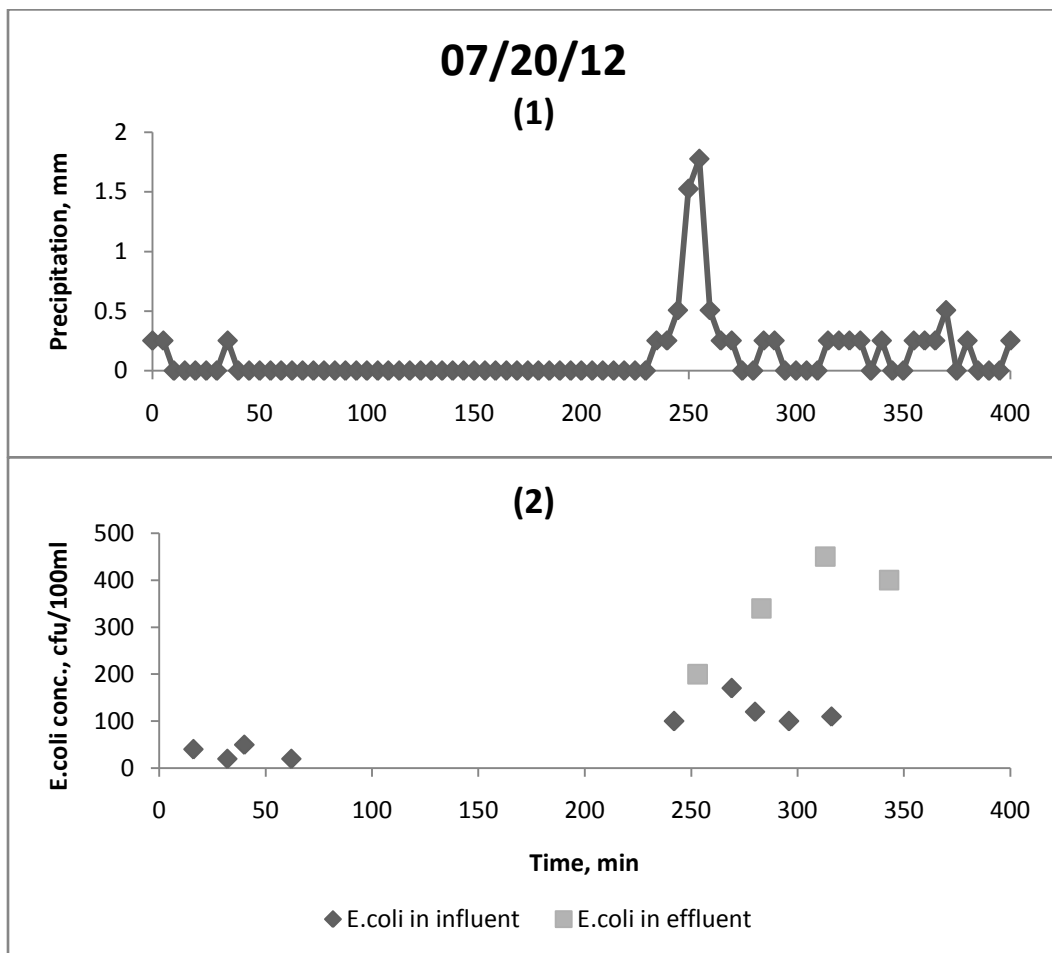


Figure 5-4. Precipitation and bacterial concentration in water samples collected at the Nashville bioretention area for the storm event on 20th, July 2012: (1) precipitation; (2) *E.coli* concentrations in the lysimeter influent and effluent.

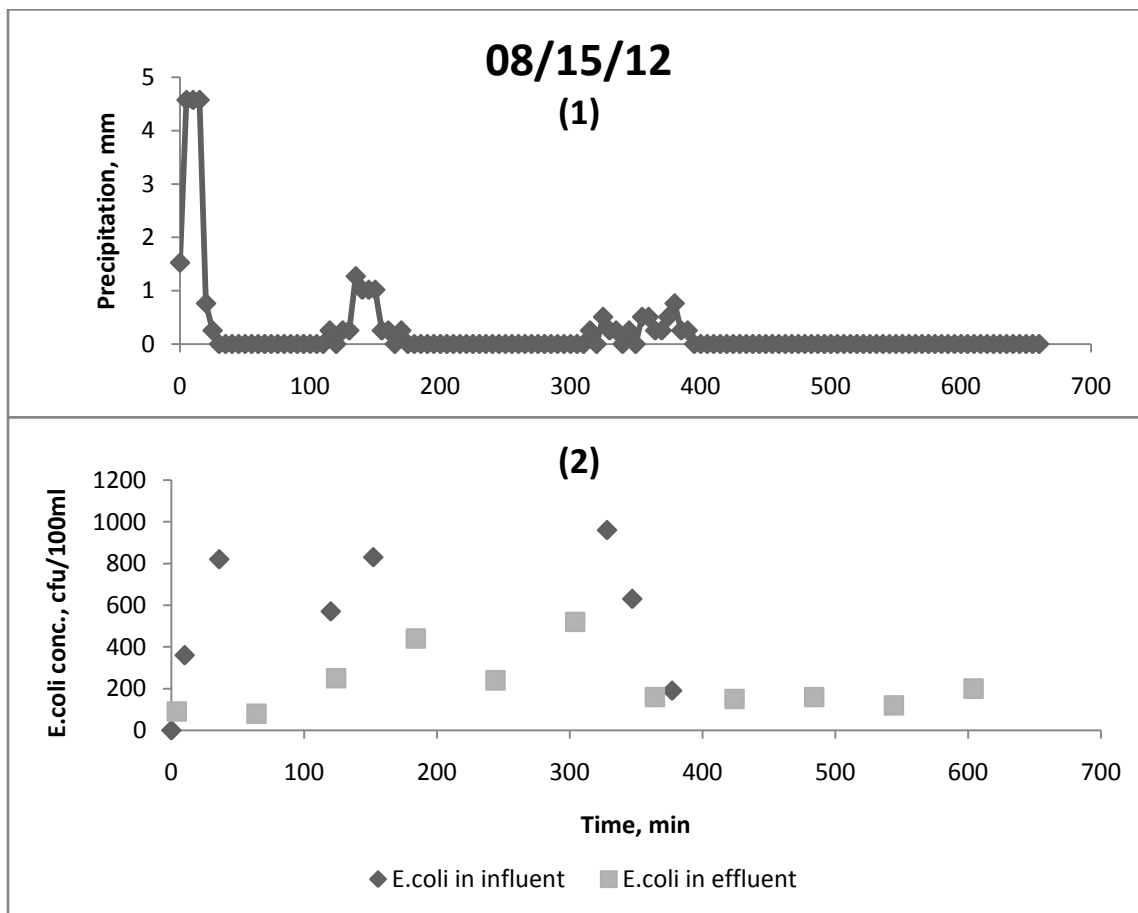


Figure 5-5. Precipitation and bacterial concentration in the water samples collected at the Nashville bioretention area for the storm event on 15th, August, 2012: (1) precipitation; (2) *E. coli* concentrations in the lysimeter influent and effluent.

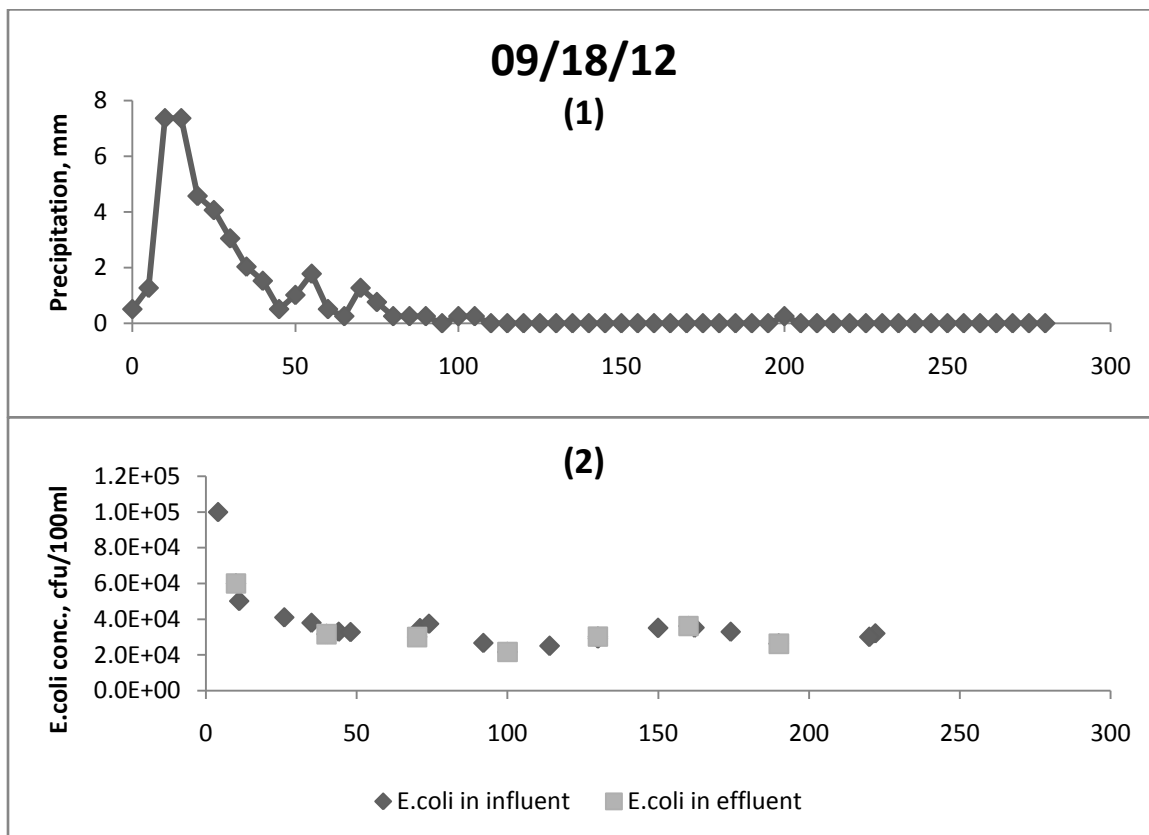


Figure 5-6. Precipitation and bacterial concentration in water samples collected at the Nashville bioretention area for the storm event on 18th, September, 2012: (1) precipitation; (2) *E. coli* concentrations in the lysimeter influent and effluent.

Turbidity and pH

For Nashville bioretention area receiving stormwater runoff, the influent turbidity ranged from 1.22 NTU to 56.10 NTU with a median value of 4.86 NTU while the effluent turbidity ranged from 14.30 NTU to 35.40 NTU with a median value of 22.70 NTU. In contrast, the turbidity readings were much lower at Colfax, which receives only

precipitation. The influent turbidity ranged from 0.94 NTU to 1.87 NTU while effluent turbidity ranged from 3.07 NTU to 5.39 NTU. The difference between the two sites illustrates the contribution of stormwater runoff to turbidity.

At both bioretention areas, the turbidity of effluent water samples was consistently higher than that of influent water samples as shown in **Figure 5-7**, **Figure 5-8**, **Figure 5-9** and **Figure 5-10**. This effect may be due to soil particles and other debris washing off from the lysimeter during infiltration.

The influent pH at Nashville was relatively stable, ranging from 6.0 to 7.2. The effluent pH values were slightly higher than those of influent samples. A similar trend was observed at Colfax, where the effluent pH was slightly higher than influent water.

Nutrient analysis

Total nitrogen and total phosphorous were analyzed to determine the nutrient removal through the bioretention areas. **Table 5-3** summarizes the concentration range of total nitrogen and total phosphorous in influent samples (stormwater runoff) to and effluent samples from the Nashville bioretention area. As shown in **Figure 5-7**, **5-8**, and **5-9**, the concentrations of nitrogen in effluent samples were higher than the concentrations of most influent samples, excluding the first flush. A similar trend was observed for total phosphorous, where the concentrations of total phosphorous in effluent samples were substantially higher than those in influent samples. The increase in nutrient concentration is attributed to the organic debris washed off from the lysimeter, which is supported by the increase in turbidity observed in all effluent samples.

Figure 5-10 displays results of the nutrient analysis for Colfax bioretention basin which receives precipitation only. The total nitrogen, total phosphorous and turbidity in effluent samples are all much higher than those in influent samples. This suggests that organic matter and debris in the lysimeter are contributing to the increase in nutrients in observed in effluent samples, even though no runoff was collected for the Colfax bioretention area, the one designed to receive precipitation only.

Table 5-3. Concentrations of total nitrogen and total phosphorous in stormwater runoff and lysimeter effluent samples collected from the Nashville bioretention area for all sampled storm events

Sample ID	Concentration, mg/L		
	Max.	Min.	Median
Total nitrogen			
Stormwater runoff	7.13	0.07	0.93
Effluent	6.93	0.80	2.45
Total phosphorous			
Stormwater runoff	1.87	0.25	0.42
Effluent	1.50	0.72	0.97

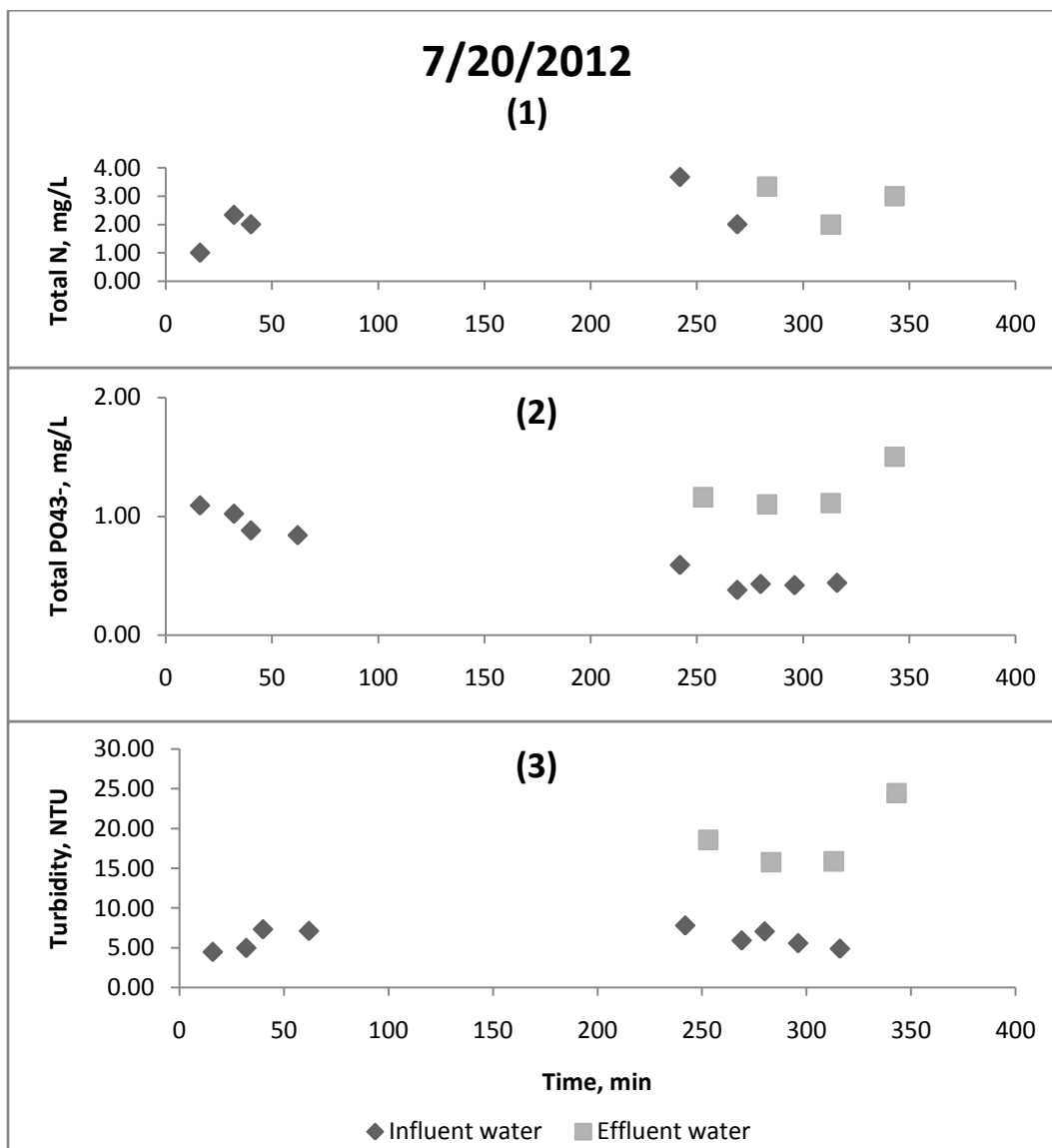


Figure 5-7. Chemical properties of water samples collected at the Nashville bioretention area for the storm event on 20th, July, 2012: (1) total nitrogen; (2) total phosphorous; (3) turbidity in both influent and effluent.

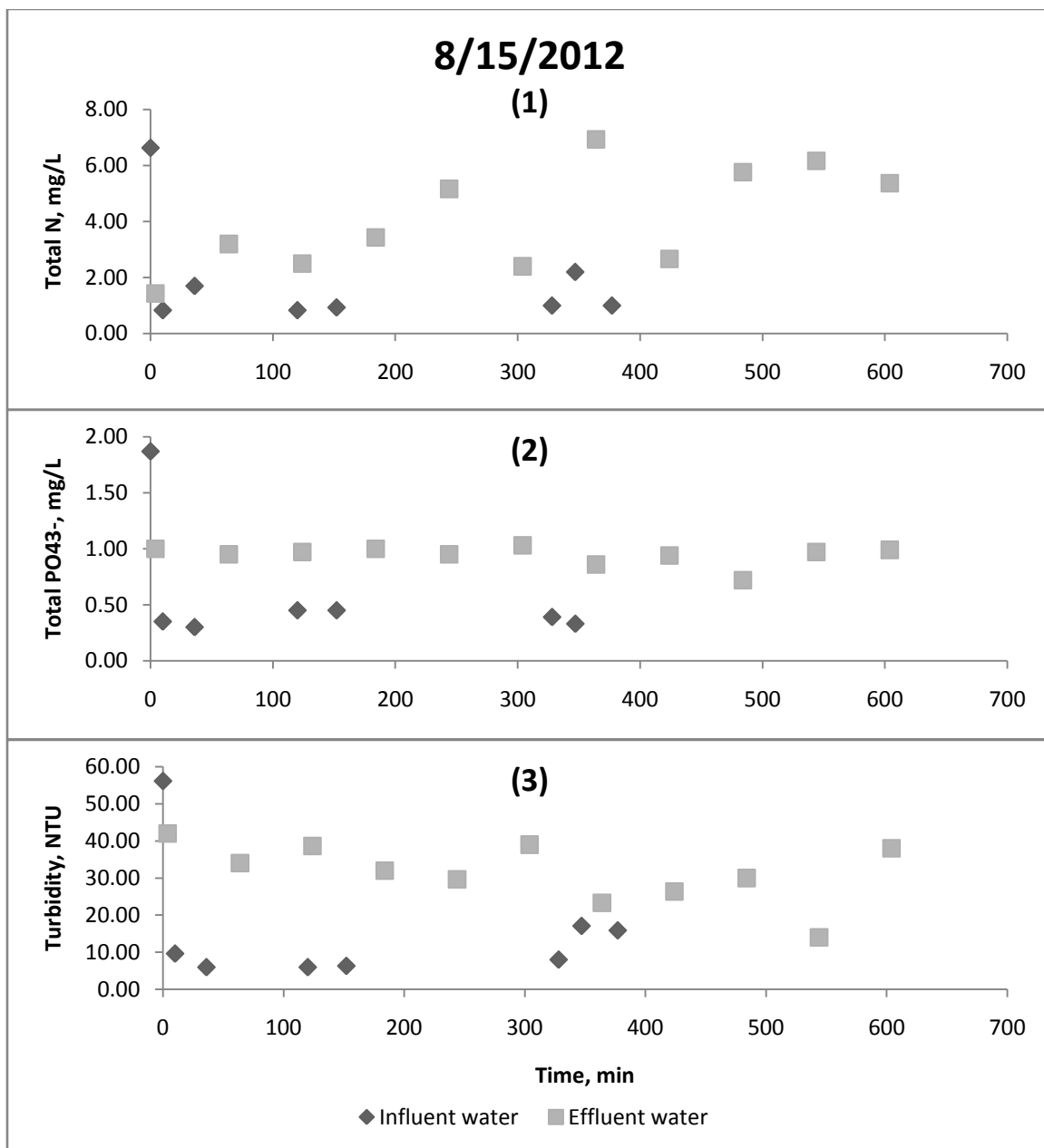


Figure 5-8. Chemical properties of water samples collected at the Nashville bioretention area for the storm event on 15th, August, 2012: (1) total nitrogen; (2) total phosphorous; (3) turbidity in both influent and effluent.

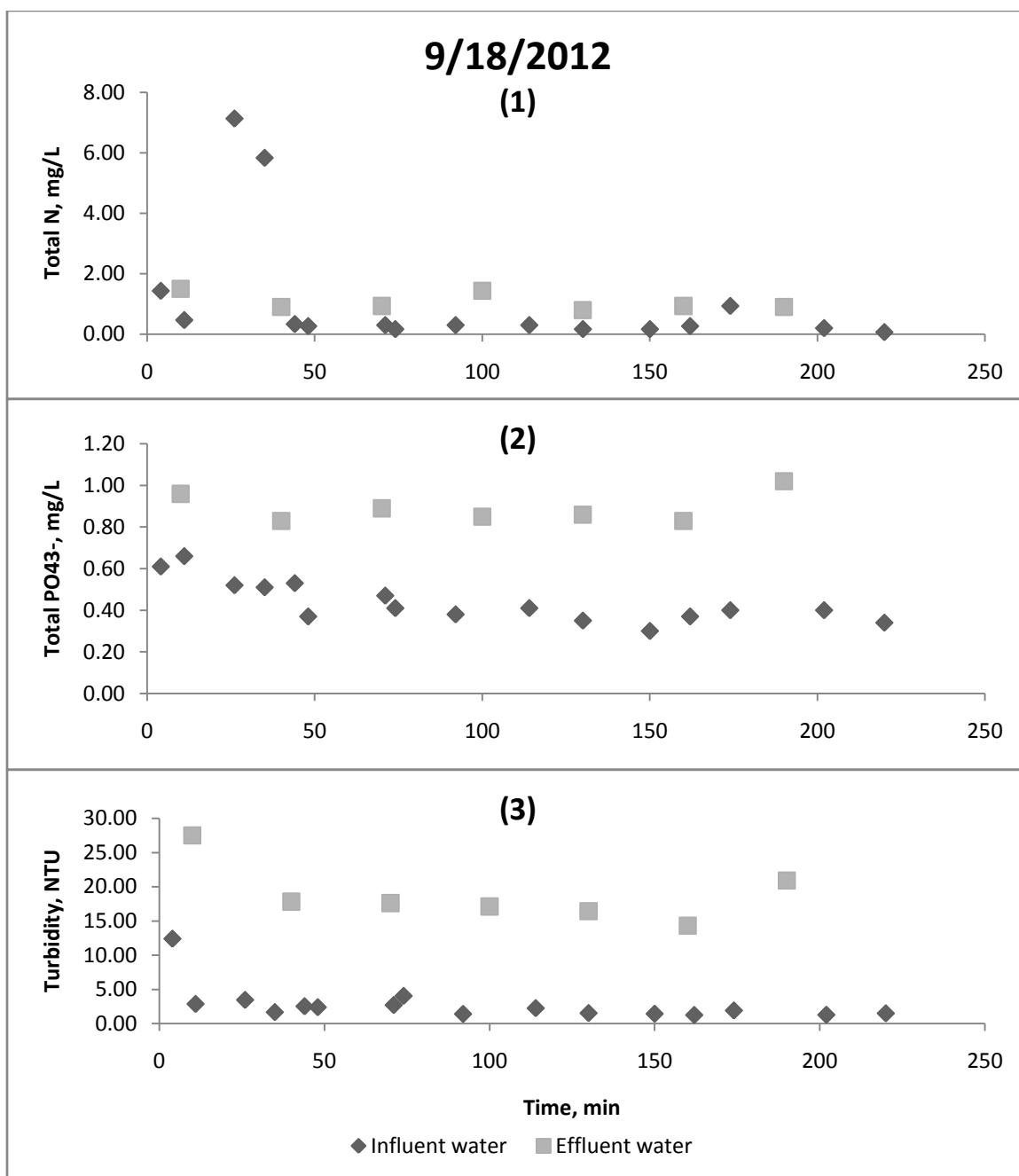


Figure 5-9. Chemical properties of water samples collected at the Nashville bioretention area for the storm event on 18th, September, 2012: (1) total nitrogen; (2) total phosphorous; (3) turbidity in both influent and effluent

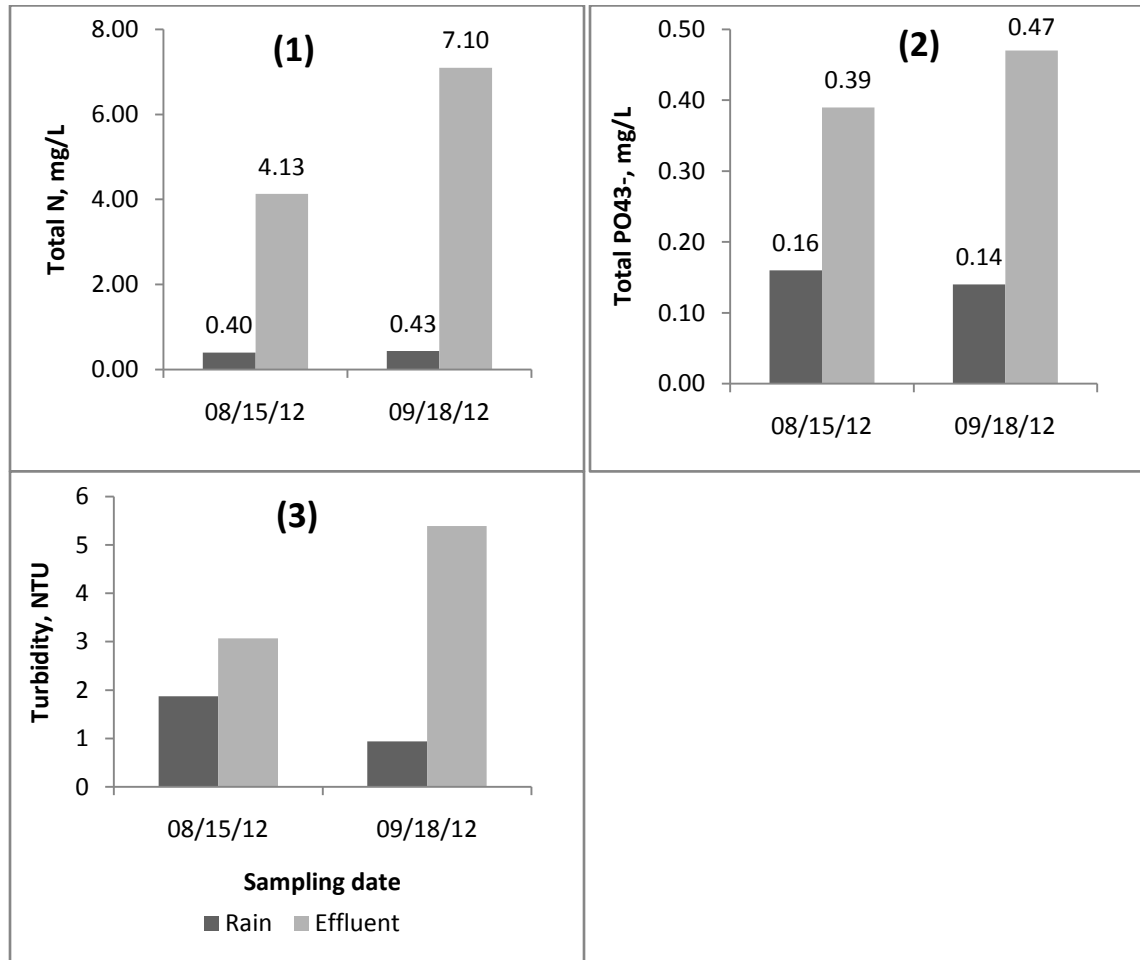


Figure 5-10. Chemical properties of water samples collected at the Colfax bioretention area for the storm event on 15th, August, 2012 and 18th, September, 2012: (1) total nitrogen; (2) total phosphorous; (3) turbidity.

5.5.4 Application of the semi-reactive microbial transport model

The semi-reactive microbial transport model was applied to describe the transport of *E. coli* through the Nashville bioretention system during a storm event on August 15th, 2012.

Inverse fitting of soil hydraulic parameters

Soil hydraulic parameters were inversely fitted in HYDRUS 1D using soil moisture data from August 15th, 2012. The initial soil water content at five depths (5cm, 10cm, 20cm, 30cm and 50cm) are directly read from data logger (**Table 5-4**). The soil water contents at other depths are interpolated according to the linear relationship between soil water content and soil depth, as demonstrated in **Figure 5-11**. The upper boundary condition is variable flux and the values are summarized in **Table 5-5**. The lower boundary condition is seepage face, which means the bottom of lysimeter is open to the atmosphere. With the initial condition, upper/lower boundary conditions determined, the changes of soil water content for a certain period were used to inversely fit the soil hydraulic parameters using van Genuchten-Mualem model (van Genuchten 1980). The monitored and fitted soil water contents over time are displayed in **Figure 5-12**. The fitted soil hydraulic parameters are summarized in **Table 5-6**. The R squared value for the fitting of predicted vs observed values is 0.55.

Table 5-4. Initial soil moisture profile for the lysimeter at Nashville bioretention area on August 15th, 2012

Depth, cm	Volumetric water content, -	Data acquisition
5	0.134	Monitored
10	0.147	
20	0.151	
30	0.184	
50	0.309	
0	0.097	Interpolated
60	0.277	

Table 5-5. The surface flux to the lysimeter at Nashville bioretention area on August 15th, 2012

Time, min	*flux, cm/min	Time, min	flux, cm/min	Time, min	flux, cm/min	Time, min	flux, cm/min
0.2	-0.0009	105	0	210	-0.0856	315	-0.0010
5	0	110	0	215	-0.1204	320	0
10	0	115	0	220	-0.0998	325	0
15	0	120	0	225	0	330	-0.0002
20	-0.0006	125	0	230	0	335	0
25	-0.0232	130	0	235	0	340	0
30	-1.0618	135	0	240	0	345	-0.0019
35	-1.0230	140	0	245	0	350	0
40	0	145	0	250	0	355	-0.2311
45	0	150	-0.0822	255	0	360	-1.0460
50	0	155	-0.1792	260	0	365	-0.2557
55	0	160	-0.9111	265	0	370	0
60	0	165	-0.8782	270	0	375	0
65	-0.0617	170	-0.0459	275	0	380	-0.1210
70	0	175	-0.0181	280	0	385	-0.4814
75	0	180	-0.1522	285	0	390	-0.2689
80	0	185	-0.2622	290	0	395	0
85	0	190	-0.1904	295	0	400	0
90	0	195	-0.1434	300	0	405	-0.0583
95	0	200	-0.1848	305	0	410	0
100	0	205	-0.0739	310	0	**685	0

* The negative sign means water flows into the lysimeter.

** The surface flux from time 410min to 685min is zero.

Table 5-6. Fitted soil hydraulic parameters for Nashville bioretention area

Parameters	Value
Saturated water content, θ_s , -	0.44
Residual water content, θ_r , -	0.0285
Soil water retention parameter, α , -	0.0542
Soil water retention parameter, n , -	1.36
Saturated hydraulic conductivity, k , cm/min	6.4

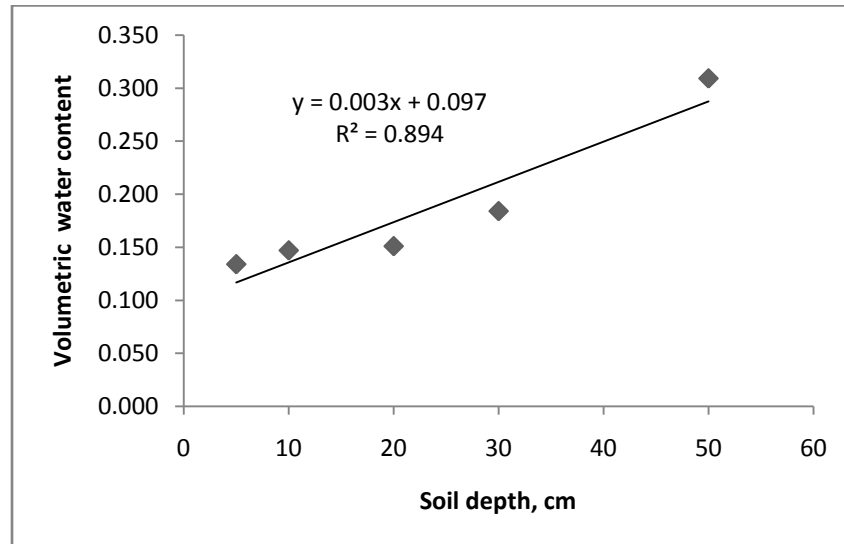


Figure 5-11. The monitored soil water content at five discrete depths (5 cm, 10 cm, 20 cm, 30 cm and 50 cm) right before the storm occurred on August 15th, 2012. A linear trend line was established and used to estimate soil water content at other soil depths.

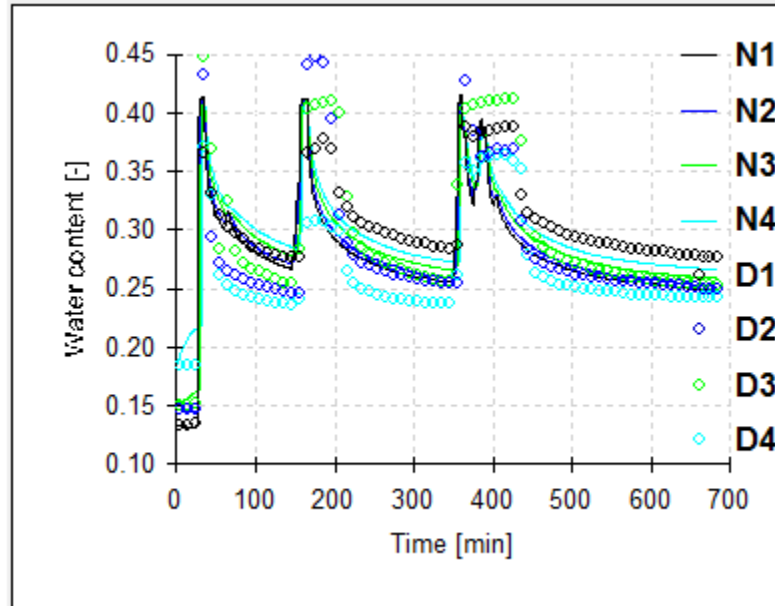


Figure 5-12. The observed (D, circle) and fitted (N, solid line) volumetric water content at different depths during the storm event on August 15th, 2012. Number 1, 2, 3 and 4 represent depths of 5 cm, 10 cm, 20 cm and 30 cm.

Results of model application

Four processes are included in the model: attachment and detachment at the soil-water interface, attachment at the air-water interface, and inactivation. Physical straining is neglected from the model, because the ratio of bacterial size to the average soil grain size (d_c) was smaller than 0.5% (Bradford, Simunek et al. 2003), indicating that straining is not an important removal mechanism in this situation.

In the model, attachment rate at the soil-water interface was estimated using the combined rate equation (4-1) described in Chapter 4. The mass transfer coefficient for attachment at the air-water interface and the mass transfer coefficient for detachment at soil-water interface were used as fitting parameters, and optimal values were selected. The fitted mass transfer coefficient for attachment at the air-water interface was $2.5 \times 10^{-11} \text{ m s}^{-1}$. The fitted mass transfer coefficient for detachment at the soil-water interface was $5.0 \times 10^{-9} \text{ m s}^{-1}$. Non-zero bacterial numbers in soil were assumed with a total initial bacterial loading of 3×10^5 CFU distributed evenly over the lysimeter. The modeled and observed bacterial breakthrough curves are shown in **Figure 5-13**. The predicted *E. coli* breakthrough curve follows the general trend of the observed breakthrough data. However, apparent delays are observed for two peaks in the modeled breakthrough curves. The early breakthrough of the observed bacterial data is likely due to the presence of preferential flow paths which is not incorporated in the semi-reactive microbial transport model.

The observed bacterial removal efficiency calculated using equation (5-1) is 66% while the modeled bacterial removal efficiency is 71%, as shown in **Figure 5-14**.

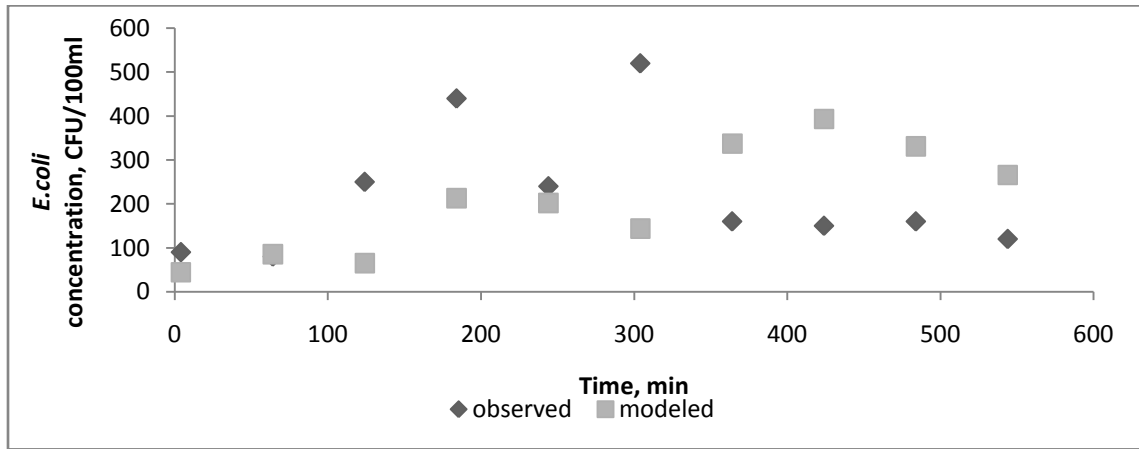


Figure 5-13. The observed (diamond) bacterial breakthrough data and modeled (square) bacterial breakthrough data at Nashville bioretention area for the storm event on August 15th, 2012.

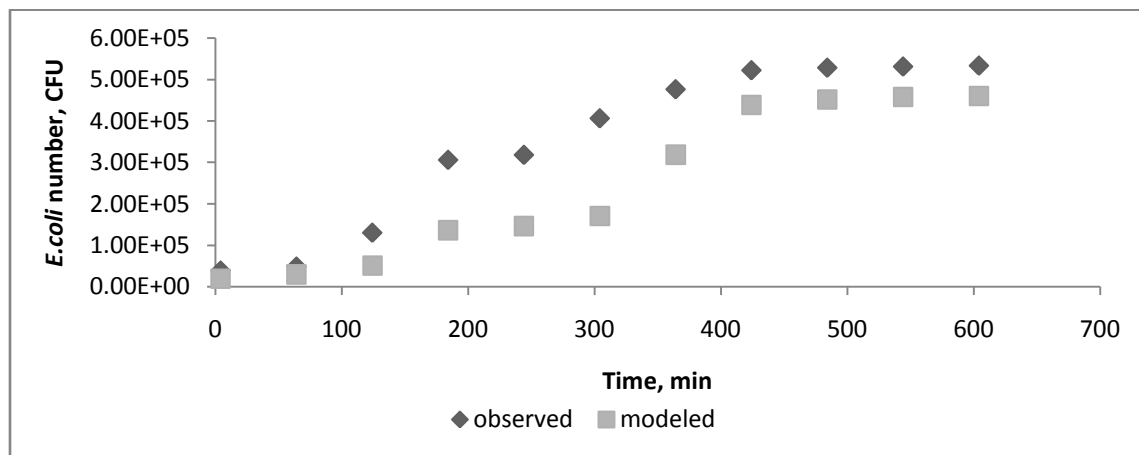


Figure 5-14. The observed (diamond) and modeled (square) cumulative bacterial counts in effluent samples at Nashville bioretention area for the storm event on August 15th, 2012.

5.6 Discussion

5.6.1 The effect of antecedent conditions on bacterial removal

Observed data from storm events on August 15th and September 18th, 2012 suggest that the bioretention area at Nashville is effective in reducing bacterial concentrations in stormwater runoff, which is seen in the apparent decrease in bacterial concentration in effluent samples as compared with influent samples. A contradicting trend was observed for the storm event on July 20th, 2012, which showed an increase in bacterial concentration in the effluent. The number of antecedent dry days is one day for the storm on July 20th, 2012, compared to more than four days for the other two storm events. A plausible explanation for the discrepancy is that *E. coli* retained in the soil from a previous storm were still present, and flushed into the effluent with infiltrating water, which contributed to the observed increase in *E. coli* in the effluent. The antecedent dry period affects bacterial removal in two ways. The bacterial concentration in stormwater runoff increases with the number of antecedent dry days, as shown in all three storm events monitored. This is presumably due to the accumulation of bacterial sources on the street and soil surfaces during dry days. On the other hand, the effluent bacterial concentration could be largely affected by the bacteria retained in the soil from previous storm events when the antecedent dry period is short. The survival of *E. coli* in soil is positively correlated with the soil moisture (Bitton and Gerba 1984; Mubiru, Coyne et al. 2000; Sinegani and Maghsoudi 2011). *E. coli* may persist in soil more than ten days depending on the temperature, the strains of *E. coli* and the soil composition (Topp, Welsh et al. 2003). At the same time, shorter antecedent dry period implies more frequent storm events and therefore bacterial inputs to the bioretention areas, which is also responsible to the increase of effluent bacterial concentration during the following storms.

Therefore, antecedent conditions are an important factor to be considered when evaluating the performance of BMPs. And the effectiveness of bioretention areas can not be simply determined by a single storm event, because of the variability in the efficiency of bacterial removal observed among the three storm events.

5.6.2 The effect of preferential flow paths on bacterial removal

The peaks of the modeled bacterial breakthrough were delayed compared to those of the observed bacterial breakthroughs, which was likely a result of the presence of preferential flow paths. The ideal travel time and actual travel time of bacteria were compared to confirm the existence of preferential paths. The ideal solute travel time was calculated using the Green Ampt model, where the infiltration rate was equal to surface flux when the soil was not saturated. The ideal travel time was then calculated by dividing the depth of the lysimeter by the infiltration rate. The actual travel time was obtained by determining the time lag between the peaks of influent water volume and effluent water volume. The ideal travel time through the lysimeter ranged from 57min to 394,837min under the variable surface flux conditions of the field precipitation pattern. However, the actual travel time observed was less than 25min (**Figure 5-15**), which suggests the presence of preferential flow paths during storm event on August 15th.

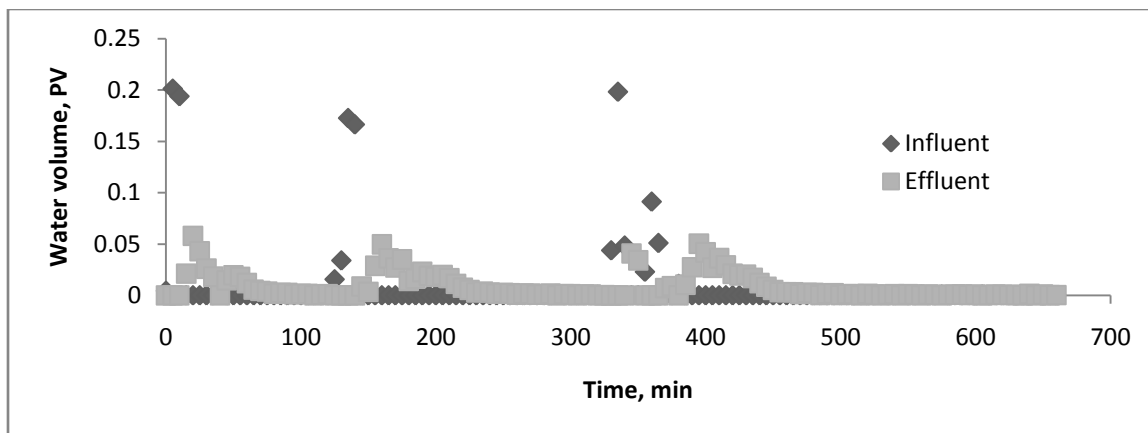


Figure 5-15. The water volume of influent and effluent during the storm event on August 15th, 2012

Bacterial concentrations in effluent samples were slightly lower than influent concentrations during September 18th storm event. The variation of volumetric water content at different depths on September 18th was much lower than the changes during the storm event on August 15th, given the higher precipitation on September 18th. The volumetric water content values recorded at five depths were all below the saturated water content (**Figure 5-16**), indicating that the lysimeter was not saturated during the storm event on September 18th, despite the high input of water flux on the surface. The unsaturated condition was further confirmed by the mass of the lysimeter (**Figure 5-17**), which was 96 lbs less than the mass of the saturated lysimeter (1941 lbs). Based on the evidence of the unsaturated lysimeter, we can conclude that preferential flow paths were

also present in the lysimeter during the storm event on September 18th. The runoff was not fully contacted with the soil mix and bacterial removal was minimal.

It has been suggested that *E. coli* removal has a positive correlation with hydraulic retention time in the bioretention systems when adsorption is the major removal mechanism (Kim, Sung et al. 2012). The longer the hydraulic retention time, the better bacterial removal efficiency is likely to be achieved. In this study, the presence of preferential flow paths in the Nashville bioretention area was reflected on the shorter travel time (equivalent to the hydraulic retention time), which negatively affected the bacterial removal efficiency. The development of preferential flow paths can be caused by the rooting effect of different vegetation as they have various root growth and depth (Li, Sung et al. 2011) or the improper construction of the bioretention areas.

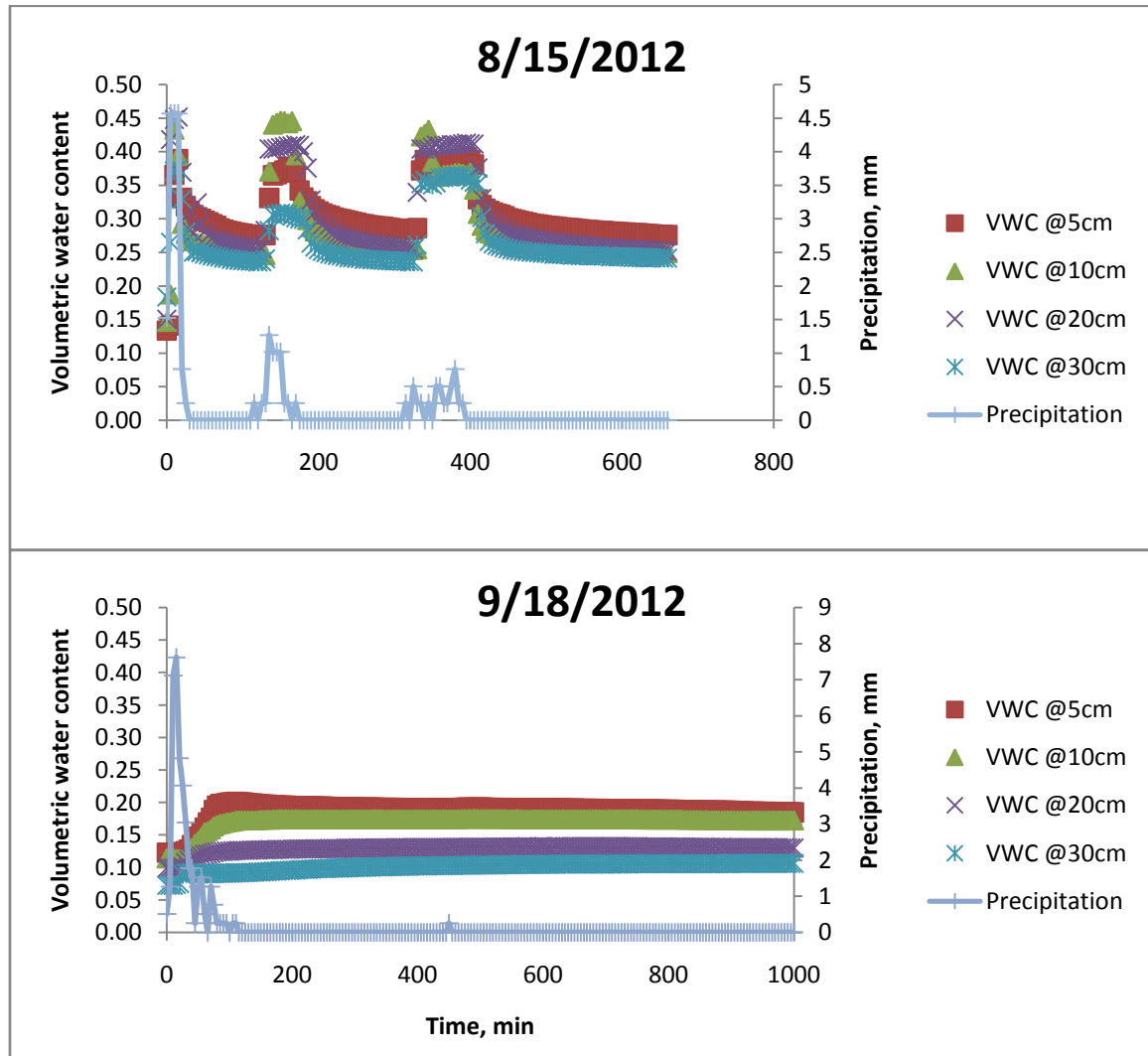


Figure 5-16. The changes of volumetric water content (VWC) at different depths corresponding to the precipitation on August 15th, 2012 and September 18th, 2012

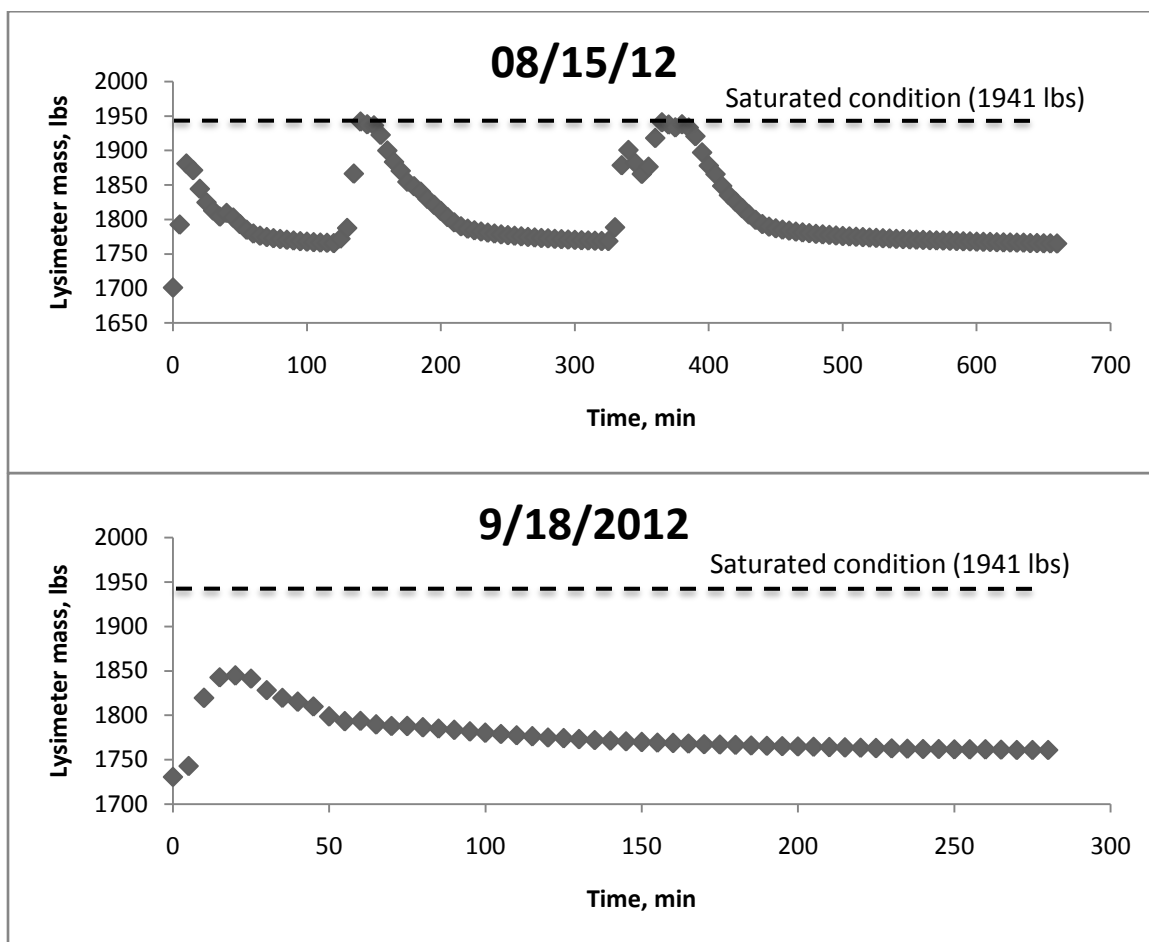


Figure 5-17. The changes of lysimeter mass over time during the storm events on August 15th and September 18th, 2012.

CHAPTER 6. CONCLUSIONS AND FUTURE RESEARCH

6.1 Conclusions

This work can be summarized as (1) investigation of stormwater runoff composition on bacterial attachment, particularly focusing on the effect of heavy metals; (2) development of a semi-reactive microbial transport model that can be used to predict bacterial transport in the subsurface under heterogeneous water chemistries and quantitative evaluation on relative importance of physical and chemical parameters on bacterial attachment; (3) field evaluation and modeling of microbial pollutant removal in bioretention areas using the semi-reactive microbial transport model and investigation of factors affecting microbial pollutant removal.

This work investigated the influence of heavy metals in solution on bacterial attachment to soil surfaces, which has historically been overlooked in the literature, despite frequent detection of heavy metals in stormwater runoff. This study examined changes in bacterial surface charge and soil surface composition following exposure to synthetic stormwater amended with heavy metals. The adsorption of heavy metal ions onto bacterial cell surfaces tends to make the surface less negatively charged while the accumulation of metals onto soil particle surfaces tends to create favorable conditions for bacterial attachment. The combined effect is that bacterial attachment is enhanced in the presence of heavy metal. This effect was confirmed in carefully planned column transport experiments. In terms of protecting underlying ground water during stormwater infiltration, the presence of heavy metals seems to decrease the transport capacity of viable bacteria, primarily by increasing bacterial attachment to the soil surfaces.

The second significant contribution of this work is the development and validation of a semi-reactive microbial transport model. Variable solution chemistry, which has been demonstrated to significantly influence bacterial attachment and transport, has been incorporated into a bacterial transport model to estimate bacterial attachment at the soil-water interface. The bacterial attachment at the soil-water interface varies with respect to changes in solution chemistry both spatially and temporally. The model can be applied to describe bacterial transport scenarios with the presence of heterogeneous water chemistries, such as bioretention areas and infiltration basins, where the mixing of stormwater runoff with groundwater occurs in the subsurface. More importantly, the model is implemented in HP1, a user-friendly software package, providing users a convenient interface to apply this model to various scenarios with heterogeneous water chemistry. Model inputs including water application, soil properties, bacterial properties and solution chemistries can be easily adjusted according to the scenarios to be simulated. To our best knowledge, this is the first study to quantitatively evaluate the relative importance of physiochemical factors on bacterial attachment. Two-phase Monte Carlo analysis was conducted and correlation coefficient was calculated to quantitatively describe the importance of physiochemical variation on the estimates of attachment rate. Among physical variables, soil particle size has the highest correlation coefficient, followed by porosity of the soil media, bacterial size and flow velocity. Among chemical variables, ionic strength has the highest correlation coefficient.

The third contribution of this work is the field evaluation and modeling of bioretention areas in terms of microbial pollutant removal, and the investigation of factors that influence microbial removal. Reduction of bacterial concentration in effluent

was observed in two of three storm events monitored over the summer of 2012. Even though the effluent bacterial concentration were reduced, there are still 87.5% of the total effluent samples exceeded the primary contact recreation standard of 126 CFU/100ml. Bacterial removal was found to be negatively affected by the antecedent dry period. The shorter antecedent dry period results in higher moisture in the soil matrix, which provides a favorable environment for bacteria retained in soil to persist. The observed bacterial removal efficiency by the bioretention area was 66% while the modeled removal efficiency was 71%. The slight overestimation of removal efficiency was attributed to the presence of preferential flow paths that are not incorporated in the model. The presence of preferential flow paths in the bioretention area substantially reduced the travel time (retention time) of stormwater runoff in the system, and therefore the bacterial removal. Due to the variability of bacterial removal efficiency observed from all three storm events, the performance of bioretention areas on bacterial removal can not be simply evaluated from single storm.

6.2 Future Research

In the semi-reactive microbial transport model, bacterial attachment at the soil water interface was estimated with respect to the changes in solution chemistry. The detachment rate at the soil water interface was selected from an optimized value. Further study may be dedicated to estimate bacterial detachment rate under transient solution chemistry. The incorporation of bacterial detachment estimation into HP1 can largely improve the accuracy of the model.

The semi-reactive microbial transport model has its limitations. The model assumes that there are no preferential flow paths in the subsurface and the infiltrating water has

opportunities to mix with the soil water/groundwater. However, when preferential flow paths are present in the subsurface, plug flow conditions may shield the effects of solution chemistry on bacterial attachment. It is of interest to investigate the influence of heterogeneous flow conditions on the performance of the semi-reactive transport model.

The semi-reactive microbial transport model developed within HYDRUS 1D provides a user-friendly interface to model bacterial transport under heterogeneous water chemistries. The required inputs for bacteria, soil and solution properties can be updated easily in the PHREEQC module while the solute transport conditions can be conveniently specified in HYDRUS 1D. There are, however, limitations in using this software package. Only one single value can be assigned to each parameter, rather than a distribution. In other words, only one outcome can be generated from each simulation performed by the semi-reactive microbial transport model. In order to view the variation of outcomes due to the variation of parameter inputs (as in Chapter 4), multiple simulations need to be carried out, which is time consuming. Therefore, further efforts can be put into incorporating the current code of HYDRUS 1D and PHREEQC into a programming environment where more sophisticated distributions can be assigned to certain parameters.

This work also investigated bacterial removal by bioretention systems in the field. Effluent bacterial concentrations leaving the bioretention system were higher than influent concentrations following a storm event with a short antecedent dry period. Shorter antecedent dry period results in higher moisture in the soil matrix, which is a favorable condition for bacteria to persist. Those bacteria retained in the soil from a previous storm were then flushed into the effluent with infiltrating water, which

contributed to the increase in effluent bacterial concentration. The observations are based on a limited numbers of storm events due to time, cost, and logistical constraints. Thus, it is desirable to include more storm events to further confirm the observed phenomena. With a larger sample size, statistical analysis may be conducted to quantitatively evaluate the correlation between the numbers of antecedent dry days with the increase in effluent bacterial concentration. In addition, research efforts should be dedicated to quantifying bacterial survival in the field to understand the fate and transport of the retained bacteria in soil, which could provide useful information when evaluating the performance of bioretention systems on bacterial removal. The following experiments (in the field and laboratory scales) are suggested:

- (1) The field experiment proposed is to observe the fate and transport of bacteria retained in the soil from previous storm events. Synthetic stormwater without bacteria may be applied to a lysimeter in the days following a real storm event to simulate repeated storm events. The effluent samples can be collected each day and for enumeration of bacteria. This outcome would provide useful information regarding the survival and transport of retained bacteria in soil. There are other factors affecting the outcome which need to be considered when planning the experiments, such as the duration of the storm event, volume of the stormwater runoff, the temperature, solution composition and the repeated days of storm events simulated.
- (2) The laboratory experiment proposed is to determine the contribution of retained bacteria from previous storm events to the effluent bacterial concentration in the following storm events. The repeated storm events can be simulated in lab

columns, whose setup mimic field experiments. The key part is that bacteria for the first storm and the repeated storms are labeled differently. There are some methods available, such as staining with multi-color fluorochromes (Drevets and Elliott 1995; Nebe-von-Caron, Stephens et al. 2000) and nanoparticles or quantum dots labeling (Lian, Litherland et al. 2004; Hahn, Tabb et al. 2005). Distinct genotypes could also be used and then enumerated via PCR using different PCR primers (Sharma, Dean-Nystrom et al. 1999). We are able to tell the source of the bacteria when enumerating bacteria in the effluent and further calculate the contribution of retained bacteria to the effluent bacterial concentration.

LIST OF REFERENCES

- Abudalo, R. A., Y. G. Bogatsu, et al. (2005). "Effect of Ferric Oxyhydroxide Grain Coatings on the Transport of Bacteriophage PRD1 and *Cryptosporidium parvum* Oocysts in Saturated Porous Media†." Environmental Science & Technology **39**(17): 6412-6419.
- Akthar, M. N., K. S. Sastry, et al. (1996). "Mechanism of metal ion biosorption by fungal biomass." BioMetals **9**(1): 21-28.
- Anders, R. and C. Chrysikopoulos (2009). "Transport of Viruses Through Saturated and Unsaturated Columns Packed with Sand." Transport in Porous Media **76**(1): 121-138.
- Arnone, R. D., M. Borst, et al. (2005). Investigation of *Cryptosporidium* and *Giardia* concentrations in combined sewer overflow and stormwater runoff, Reston, VA 20191-4400, United States, American Society of Civil Engineers.
- Arnone, R. D., Borst, M. and Walling, J.P. (2005). Investigation of *Cryptosporidium* and *Giardia* Concentrations in Combined Sewer Overflow and Stormwater Runoff. Impacts of Global Climate Change: 1-14.
- Becker, M. W., S. A. Collins, et al. (2004). "Effect of cell physicochemical characteristics and motility on bacterial transport in groundwater." Journal of Contaminant Hydrology **69**(3-4): 195-213.
- Bitton, G. and C. P. Gerba (1984). Groundwater Pollution Microbiology. New York, Wiley.
- Blackburn, B. G., G. F. Craun, et al. (2004). "Surveillance for Waterborne-Disease Outbreaks Associated with Drinking Water --- United States, 2001--2002." Morbidity and Mortality Weekly Report **53**(SS08): 23-45.
- Bolster, C. H., A. L. Mills, et al. (2001). "Effect of surface coatings, grain size, and ionic strength on the maximum attainable coverage of bacteria on sand surfaces." Journal of Contaminant Hydrology **50**(3-4): 287-305.
- Bradford, S. A. and M. Bettahar (2005). "Straining, Attachment, And Detachment Of Oocysts In Saturated Porous Media." Journal of Environmental Quality **34**(2): 469-478.

Bradford, S. A., J. Simunek, et al. (2003). "Modeling Colloid Attachment, Straining, and Exclusion in Saturated Porous Media." Environmental Science & Technology **37**(10): 2242-2250.

Bradford, S. A., J. Simunek, et al. (2006). "Transport and straining of E. coli O157:H7 in saturated porous media." Water Resources Research **42**(12): W12S12.

Bradford, S. A., S. Torkzaban, et al. (2012). "Modeling colloid and microorganism transport and release with transients in solution ionic strength." Water Resources Research **48**(9): W09509.

Brown, D. G. (2007). "Adaptable method for estimation of parameters describing bacteria transport through porous media from column effluent data: Optimization based on data quality and quantity." Colloids and Surfaces A: Physicochemical and Engineering Aspects **296**(1-3): 19-28.

Brown, J. N. and B. M. Peake (2006). "Sources of heavy metals and polycyclic aromatic hydrocarbons in urban stormwater runoff." Science of the Total Environment **359**(1-3): 145-155.

Brownell, M. J., V. J. Harwood, et al. (2007). "Confirmation of putative stormwater impact on water quality at a Florida beach by microbial source tracking methods and structure of indicator organism populations." Water Research **41**(16): 3747-3757.

Camesano, T. A. and B. E. Logan (1998). "Influence of Fluid Velocity and Cell Concentration on the Transport of Motile and Nonmotile Bacteria in Porous Media." Environmental Science & Technology **32**(11): 1699-1708.

Chapman, C. and R. R. Horner (2010). "Performance Assessment of a Street-Drainage Bioretention System." Water Environment Research **82**(2): 109-119.

Chrysikopoulos, C. V., P. K. Kitanidis, et al. (1990). "Analysis of one-dimensional solute transport through porous-media with spatially-variable retardation factor." Water Resources Research **26**(3): 437-446.

Chrysikopoulos, C. V., P. K. Kitanidis, et al. (1992). "Macrodispersion of sorbing solutes in heterogeneous porous formations with spatially periodic retardation factor and velocity-field." Water Resources Research **28**(6): 1517-1529.

Chu, Y., Y. Jin, et al. (2003). "Effect of Soil Properties on Saturated and Unsaturated Virus Transport through Columns." Journal of Environmental Quality **32**(6): 2017-2025.

Clement, T. P., B. M. Peyton, et al. (1997). "Microbial growth and transport in porous media under denitrification conditions: experiments and simulations." Journal of Contaminant Hydrology **24**(3-4): 269-285.

Collins, Y. E. and G. Stotzky (1992). "Heavy metals alter the electrokinetic properties of bacteria, yeasts, and clay minerals." Applied and Environmental Microbiology **58**(5): 1592-1600.

Cunningham, A. B., R. R. Sharp, et al. (2007). "Effects of starvation on bacterial transport through porous media." Advances in Water Resources **30**(6-7): 1583-1592.

D.L. Parkhurst, V. A. (1999). "User Guide to PHREEQC (Version 2)--A Computer Program for Speciation, Batch-Reaction, One-Dimensional Transport, and Inverse Geochemical Calculations." US Geological Survey Water-Resources Investigations Report 99-4259: 44.

David, A., F. Jeremy, et al. (2004). "Experimental Measurements of the Adsorption of *Bacillus subtilis* and *Pseudomonas mendocina* Onto Fe-Oxyhydroxide-Coated and Uncoated Quartz Grains." Geomicrobiology Journal **21**: 511-519.

Davies, C. M. and H. J. Bavor (2000). "The fate of stormwater-associated bacteria in constructed wetland and water pollution control pond systems." Journal of Applied Microbiology **89**(2): 349-360.

Davis, A. P. (2007). "Field performance of bioretention: Water quality." Environmental Engineering Science **24**(8): 1048-1064.

Davis, A. P., M. Shokouhian, et al. (2001). "Laboratory Study of Biological Retention for Urban Stormwater Management." Water Environment Research **73**(1): 5-14.

Davis, A. P., Shokouhian, M and Sharma, H (2003). "Water quality improvement through bioretention: Lead, copper, and zinc removal." Water Environment Research **75**(1): 73-82.

Davis, A. P., Shokouhian, M., Sharma, H. and Minami, C. (2006). "Water quality improvement through bioretention media: Nitrogen and phosphorus removal." Water Environment Research **78**(3): 284-293.

Drevets, D. A. and A. M. Elliott (1995). "Fluorescence labeling of bacteria for studies of intracellular pathogenesis." Journal of Immunological Methods **187**(1): 69-79.

Elimelech, M., M. Nagai, et al. (2000). "Relative Insignificance of Mineral Grain Zeta Potential to Colloid Transport in Geochemically Heterogeneous Porous Media." Environmental Science & Technology **34**(11): 2143-2148.

Faulkner, B. R., W. G. Lyon, et al. (2003). "Modeling leaching of viruses by the Monte Carlo method." Water Research **37**(19): 4719-4729.

Fein, J. B. (2000). "Quantifying the effects of bacteria on adsorption reactions in water-rock systems." Chemical Geology **169**(3-4): 265-280.

Fein, J. B., Daughney, C.J., Yee, N. and Davis, T. A. (1997). "A chemical equilibrium model for metal adsorption onto bacterial surfaces." Geochimica et Cosmochimica Acta **61**(16): 3319-3328.

Fogler, H. S. (1999). Elements of Chemical Reaction Engineering. Prentice Hall: New Jersey; 707.

Fontes, D. E., A. L. Mills, et al. (1991). "Physical and chemical factors influencing transport of microorganisms through porous media." Applied and Environmental Microbiology **57**(9): 2473-2481.

Franchi, A. and C. R. O'Melia (2003). "Effects of Natural Organic Matter and Solution Chemistry on the Deposition and Reentrainment of Colloids in Porous Media." Environmental Science & Technology **37**(6): 1122-1129.

Gannon, J. T., V. B. Manilal, et al. (1991). "Relationship between Cell Surface Properties and Transport of Bacteria through Soil." Applied and Environmental Microbiology **57**(1): 190-193.

Gargiulo, G., S. Bradford, et al. (2007). "Bacteria transport and deposition under unsaturated conditions: the role of the matrix grain size and the bacteria surface protein." Journal of Contaminant Hydrology **92**(3-4): 255-273.

Geosyntec Consultants and Wright Water Engineers. (2012). "International Stormwater Best Management Practices (BMP) Database Pollutant Category Summary Statistical

Addendum: TSS, Bacteria, Nutrients and Metals." Retrieved September, 2012, from <http://www.bmpdatabase.org/BMPPerformance.htm>.

Glass, C. and S. Bissouma (2005). "Evaluation of a parking lot bioretention cell for removal of stormwater pollutants." Ecosystems and Sustainable Development V(81): 699-708.

Greene, G. (1992). "Ozone disinfection and treatment of urban storm drain dry-weather flows: A pilot treatment plant demonstration project on the Kenter Canyon storm drain system in Santa Monica."

Gregory, J. (1981). "Approximate expressions for retarded van der waals interaction." Journal of Colloid and Interface Science **83**(1): 138-145.

Hahn, M. A., J. S. Tabb, et al. (2005). "Detection of Single Bacterial Pathogens with Semiconductor Quantum Dots." Analytical Chemistry **77**(15): 4861-4869.

Hahn, M. W. and C. R. O'Melia (2003). "Deposition and Reentrainment of Brownian Particles in Porous Media under Unfavorable Chemical Conditions: Some Concepts and Applications." Environmental Science & Technology **38**(1): 210-220.

Harper, H. H. (1985). "Fate of Heavy Metals from Highway Runoff in Stormwater Management System." PhD Dissertation, University of Central Florida.

Harper, H. H. (1985). Fate of Heavy Metals from Highway Runoff in Stormwater Management Systems, University of Central Florida.

Harvey, R. W. and S. P. Garabedian (1991). "Use of colloid filtration theory in modeling movement of bacteria through a contaminated sandy aquifer." Environmental Science & Technology **25**(1): 178-185.

Hassanizadeh, S. M. and J. F. Schijven (2000). "Use of bacteriophages as tracers for the study of removal of viruses." Proceeding of TRAM'2000 held in Liege, Belgium: 167-174.

Hathaway, J. M., W. F. Hunt, et al. (2009). Field evaluation of indicator bacteria removal by stormwater BMPs in North Carolina. World Environmental and Water Resources Congress 2009: Great Rivers, May 17, 2009 - May 21, 2009, Kansas City, MO, United states, American Society of Civil Engineers.

Helmreich, B., R. Hilliges, et al. (2010). "Runoff pollutants of a highly trafficked urban road--correlation analysis and seasonal influences." Chemosphere **80**(9): 991-997.

Hogg, R., T. W. Healy, et al. (1966). "Mutual coagulation of colloidal dispersions." Transactions of the Faraday Society **62**: 1638-1651.

Hong, E. Y., Seagren, E. A. and Davis, A. P. (2006). "Sustainable oil and grease removal from synthetic stormwater runoff using bench-scale bioretention studies." Water Environment Research **78**(2): 141-155.

Hornberger, G. M., A. L. Mills, et al. (1992). "Bacterial transport in porous media: Evaluation of a model using laboratory observations." Water Resources Research **28**(3): 915-938.

Hsieh, C. and A. Davis (2005). "Evaluation and optimization of bioretention media for treatment of urban storm water runoff." Journal of Environmental Engineering **131**: 1521.

Hunt, W., A. Jarrett, et al. (2006). "Evaluating Bioretention Hydrology and Nutrient Removal at Three Field Sites in North Carolina." Journal of Irrigation and Drainage Engineering **132**(6): 600-608.

Hunt, W., J. Smith, et al. (2008). "Pollutant Removal and Peak Flow Mitigation by a Bioretention Cell in Urban Charlotte, N.C." Journal of Environmental Engineering **134**(5): 403-408.

Hyun Jung, K., S. S. Tazehkand, et al. (2006). E. coli deposition and transport in porous media: Influence of solution chemistry and bacterial surface polymers. 2006 AIChE Annual Meeting, Nov 12 - 17 2006, San Francisco, CA, United states, American Institute of Chemical Engineers.

Jacobs, A., F. Lafolie, et al. (2007). "Kinetic adhesion of bacterial cells to sand: cell surface properties and adhesion rate." Colloids and Surfaces B: Biointerfaces **59**(Copyright 2007, The Institution of Engineering and Technology): 35-45.

Jacques, D. and J. Šimůnek (2005). User Manual of the Multicomponent Variably-Saturated Flow and Transport Model HP1, Description, Verification and Examples, Version 1.0, SCK•CEN-BLG-998, Waste and Disposal, SCK•CEN. Mol, Belgium: 79 pp.

Jacques, D. and J. Šimůnek (2010). Notes on HP1 – a software package for simulating variably-saturated water flow, heat transport, solute transport and biogeochemistry in porous media, HP1 Version 2.2, SCK•CEN-BLG-1068, Waste and Disposal, SCK•CEN. Mol, Belgium: 113 pp.

Jaffe, P. and S. Taylor (1990). "Substrate and Biomass Transport in a Porous Medium." Water Resources Research WRERAQ **26**(9).

Jiang, G., M. J. Noonan, et al. (2007). "Transport of Escherichia coli through variably saturated sand columns and modeling approaches." Journal of Contaminant Hydrology **93**(1-4): 2-20.

Jiang, S. and W. Chu (2004). "PCR detection of pathogenic viruses in southern California urban rivers." Journal of Applied Microbiology **97**(1): 17-28.

Johnson, W. P. and B. E. Logan (1996). "Enhanced transport of bacteria in porous media by sediment-phase and aqueous-phase natural organic matter." Water Research **30**(4): 923-931.

Johnson, W. P., M. J. Martin, et al. (1996). "Facilitation of bacterial transport through porous media by changes in solution and surface properties." Colloids and Surfaces A: Physicochemical and Engineering Aspects **107**(0): 263-271.

Kim, H. N., S. A. Bradford, et al. (2009). "Escherichia coli O157:H7 transport in saturated porous media: Role of solution chemistry and surface macromolecules." Environmental Science and Technology **43**(12): 4340-4347.

Kim, M.-K., S.-B. Kim, et al. (2008). "Bacteria transport in an unsaturated porous media: Incorporation of air-water interface area model into transport modelling." Hydrological Processes **22**(13): 2370-2376.

Kim, M., S. A. Boone, et al. (2009). "Factors that Influence the Transport of Bacillus cereus Spores through Sand." Water Air and Soil Pollution **199**(1-4): 151-157.

Kim, M. H., C. Y. Sung, et al. (2012). "Bioretention for stormwater quality improvement in Texas: Removal effectiveness of Escherichia coli." Separation and Purification Technology **84**: 120-124.

- Kim, S.-B., S.-J. Park, et al. (2008). "Bacteria transport through goethite-coated sand: Effects of solution pH and coated sand content." Colloids and Surfaces B: Biointerfaces **63**(2): 236-242.
- Kim, S.-B., S.-J. Park, et al. (2008). "Transport and retention of Escherichia coli in a mixture of quartz, Al-coated and Fe-coated sands." Hydrological Processes **22**(18): 3856-3863.
- Kuznar, Z. A. and M. Elimelech (2004). "Role of Surface Proteins in the Deposition Kinetics of Cryptosporidium parvum Oocysts." Langmuir **21**(2): 710-716.
- Lenhart, J. J. and J. E. Saiers (2003). "Colloid Mobilization in Water-Saturated Porous Media under Transient Chemical Conditions." Environmental Science & Technology **37**(12): 2780-2787.
- Li, M.-H., C. Sung, et al. (2011). "Assessing Performance of Bioretention Boxes in Hot and Semiarid Regions." Transportation Research Record: Journal of the Transportation Research Board **2262**(-1): 155-163.
- Lian, J. Y., T. Y. Liu, et al. (2011). "Experimental Investigation and Numerical Simulation for Bacteria Transport in Soil." Chinese Journal of Chemical Engineering **19**(2): 327-333.
- Lian, W., S. A. Litherland, et al. (2004). "Ultrasensitive detection of biomolecules with fluorescent dye-doped nanoparticles." Analytical Biochemistry **334**(1): 135-144.
- Lipson, S. M. and G. Stotzky (1983). "Adsorption of Reovirus to Clay-Minerals - Effects of Cation-Exchange Capacity, Cation Saturation, and Surface-Area." Applied and Environmental Microbiology **46**(3): 673-682.
- Logan, B. E., D. G. Jewett, et al. (1995). "Clarification of Clean-Bed Filtration Models." Journal of Environmental Engineering **121**(12): 869-873.
- Martinez-Salas, E., J. A. Martin, et al. (1981). "Relationship of Escherichia coli density to growth rate and cell age." Journal of Bacteriology **147**(1): 97-100.
- May, D. B. and M. Sivakumar (2009). "Prediction of heavy metal concentrations in urban stormwater." Water and Environment Journal **23**(4): 247-254.

McCaulou, D. R., R. C. Bales, et al. (1994). "Use of short-pulse experiments to study bacteria transport through porous media." Journal of Contaminant Hydrology **15**(1-2): 1-14.

McClaine, J. W. and R. M. Ford (2002). "Characterizing the adhesion of motile and nonmotile *Escherichia coli* to a glass surface using a parallel-plate flow chamber." Biotechnology and Bioengineering **78**(2): 179-189.

Mergeay, M., Nies, D., Schlegel, H. G., Gerits, J., Charles, P. and Van Gijsegem, F (1985). "*Alcaligenes eutrophus* CH34 is a facultative chemolithotroph with plasmid-bound resistance to heavy metals." Journal of Bacteriology **162**(1): 328-334.

Mills, A. L., J. S. Herman, et al. (1994). "Effect of solution ionic strength and iron coatings on mineral grains on the sorption of bacterial cells to quartz sand." Applied and Environmental Microbiology **60**(9): 3300-3306.

Moore, R. S., Taylor, D. H., Reddy, M. M. M. and Sturman, L. S. (1982). "Adsorption of Reovirus by Minerals and Soils." Applied and Environmental Microbiology **44**(4): 852-859.

Morales, V. L., W. Zhang, et al. (2011). "Impact of dissolved organic matter on colloid transport in the vadose zone: deterministic approximation of transport deposition coefficients from polymeric coating characteristics." Water Research **45**(4): 1691-1701.

Mubiru, D. N., M. S. Coyne, et al. (2000). "Mortality of *Escherichia coli* O157:H7 in Two Soils with Different Physical and Chemical Properties." Journal of Environmental Quality **29**(6): 1821-1825.

Muthanna, T. M., M. Viklander, et al. (2007). "Heavy metal removal in cold climate bioretention." Water Air and Soil Pollution **183**(1-4): 391-402.

National Ground Water Association. (2010). "Groundwater Facts." Retrieved January, 2012, from <http://www.ngwa.org/Fundamentals/use/Pages/Groundwater-facts.aspx>.

Nebe-von-Caron, G., P. J. Stephens, et al. (2000). "Analysis of bacterial function by multi-colour fluorescence flow cytometry and single cell sorting." Journal of Microbiological Methods **42**(1): 97-114.

O'Shea, M. and R. Field (1992). "Detection and disinfection of pathogens in storm-generated flows." Canadian Journal of Microbiology **38**(4): 267-276.

Olivieri, A. W., Boehm, A., Sommers, C. A., Soller, J. A., Eisenberg, J. N. and Danielson, R. (2007). "Development of a protocol for risk assessment of microorganisms in separate stormwater system." Water Environment Research Foundation.

Pitt, R., S. Clark, et al. (1999). "Groundwater contamination potential from stormwater infiltration practices." Urban Water **1**(3): 217-236.

Prestes, E. C., V. E. d. Anjos, et al. (2006). "Copper, lead and cadmium loads and behavior in urban stormwater runoff in Curitiba, Brazil." Journal of the Brazilian Chemical Society **17**: 53-60.

Rasmussen, P. P. (1998). "Concentrations, loads, and yields of selected water-quality constituents during low flow and stormwater runoff from three watersheds at Fort Leavenworth, Kansas, May 1994 through September 1996." US Geological Survey Water-Resources Investigations Report 98-4001.

Reddy, H. L. and R. M. Ford (1996). "Analysis of biodegradation and bacterial transport: Comparison of models with kinetic and equilibrium bacterial adsorption." Journal of Contaminant Hydrology **22**(3-4): 271-287.

Redman, J. A., S. L. Walker, et al. (2004). "Bacterial Adhesion and Transport in Porous Media: Role of the Secondary Energy Minimum." Environmental Science and Technology **38**(6): 1777-1785.

Roy-Poirier, A., P. Champagne, et al. (2010). "Review of Bioretention System Research and Design: Past, Present, and Future." Journal of Environmental Engineering **136**(9): 878-889.

Rusciano, G. M. and C. C. Obropta (2007). "Bioretention column study: Fecal coliform and total suspended solids reductions." Transactions of the ASABE **50**(4): 1261-1269.

Schäfer, A., P. Ustohal, et al. (1998). "Transport of bacteria in unsaturated porous media." Journal of Contaminant Hydrology **33**(1-2): 149-169.

Schijven, J. F. and J. Šimůnek (2002). "Kinetic modeling of virus transport at the field scale." Journal of Contaminant Hydrology **55**(1-2): 113-135.

Schillinger, J. E. and J. J. Gannon (1985). "Bacterial Adsorption and Suspended Particles in Urban Stormwater." Journal (Water Pollution Control Federation) **57**(5): 384-389.

Schinner, T., A. Letzner, et al. (2010). "Transport of selected bacterial pathogens in agricultural soil and quartz sand." Water Research **44**(4): 1182-1192.

Selvakumar, A. and M. Borst (2004). Land use and seasonal effects on Urban stormwater runoff microorganism concentrations, New York, NY 10016-5990, United States, American Society of Mechanical Engineers.

Selvakumar, A. and M. Borst (2006). "Variation of microorganism concentrations in urban stormwater runoff with land use and seasons." Journal of Water and Health **4**(1): 109-124.

Sharma, V. K., E. A. Dean-Nystrom, et al. (1999). "Semi-automated fluorogenic PCR assays (TaqMan) for rapid detection of Escherichia coli O157:H7 and other Shiga toxinogenic E. coli." Molecular and Cellular Probes **13**(4): 291-302.

Shen, C., B. Li, et al. (2007). "Kinetics of coupled primary- and secondary-minimum deposition of colloids under unfavorable chemical conditions." Environmental Science and Technology **41**(20): 6976-6982.

Šimůnek, J., M. Šejna, et al. (2008). The Hydrus-1D Software Package for Simulating the Movement of Water, Heat, and Multiple Solutes in Variably Saturated Media, Version 4.0, HYDRUS Software Series 3. Department of Environmental Sciences, University of California Riverside, Riverside, California, USA, pp. 315.

Sinegani, A. A. S. and J. Maghsoudi (2011). "The effect of soil water potential on survival of fecal coliforms in soil treated with organic wastes under laboratory conditions." African Journal of Microbiology Research **5**(3): 229-240.

Tien, C. and A. C. Payatakes (1979). Advances in deep bed filtration, AIChE Journal.

Topp, E., M. Welsh, et al. (2003). "Strain-dependent variability in growth and survival of Escherichia coli in agricultural soil." FEMS Microbiology Ecology **44**(3): 303-308.

Tosco, T., A. Tiraferri, et al. (2009). "Ionic Strength Dependent Transport of Microparticles in Saturated Porous Media: Modeling Mobilization and Immobilization

Phenomena under Transient Chemical Conditions." Environmental Science & Technology **43**(12): 4425-4431.

Tufenkji, N. (2006). "Modeling microbial transport in porous media: Traditional approaches and recent developments." Advances in Water Resources **30**(6-7): 1455-1469.

Tufenkji, N. and M. Elimelech (2004). "Correlation Equation for Predicting Single-Collector Efficiency in Physicochemical Filtration in Saturated Porous Media." Environmental Science & Technology **38**(2): 529-536.

USEPA (1986). Ambient Water Quality Criteria for Bacteria - 1986. EPA 440/5-84-002. Office of Water, Washington, DC.

van Genuchten, M. T. (1980). "A Closed-form Equation for Predicting the Hydraulic Conductivity of Unsaturated Soils1." Soil Sci. Soc. Am. J. **44**(5): 892-898.

Vaughn, J. M., E. F. Landry, et al. (1978). "Survey of human virus occurrence in wastewater-recharged groundwater on Long Island." Applied and Environmental Microbiology **36**(1): 47-51.

Walker, S. L., Redman, J. A., Elimelech, M. (2004). "Role of Cell Surface Lipopolysaccharides in Escherichia coli K12 Adhesion and Transport." Langmuir **20**(18): 7736-7746.

Walker, W. J., McNutt, R. P. and Maslanka, C. K. (1999). "The potential contribution of urban runoff to surface sediments of the Passaic River: Sources and chemical characteristics." Chemosphere **38**(2): 363-377.

Weiss, T. H., A. L. Mills, et al. (1995). "Effect of bacterial cell shape on transport of bacteria in porous media." Environmental Science and Technology **29**(7): 1737-1740.

Wilson, L., M. Osborn, et al. (1990). "The Ground Water Recharge and Pollution Potential of Dry Wells in Pima County, Arizona." Ground Water Monitoring & Remediation **10**(3): 114-121.

Yee, N. and J. B. Fein (2002). "Does metal adsorption onto bacterial surfaces inhibit or enhance aqueous metal transport? Column and batch reactor experiments on Cd-Bacillus subtilis-quartz systems." Chemical Geology **185**(3-4): 303-319.

Yee, N., J. B. Fein, et al. (2000). "Experimental study of the pH, ionic strength, and reversibility behavior of bacteria-mineral adsorption." Geochimica et Cosmochimica Acta **64**(4): 609-617.

Yousef, Y. A., T. Hvitved-Jacobsen, et al. (1990). "Heavy metal accumulation and transport through detention ponds receiving highway runoff." Science of the Total Environment **93**: 433-440.

Yousef, Y. A., Wanielista, M. P., Hvitved-Jacobsen, T. and Harper, H. H. (1984). "Fate of heavy metals in stormwater runoff from highway bridges." Science of the Total Environment **33**(1-4): 233-244.

Yukselen, Y. and A. Kaya (2003). "Zeta Potential of Kaolinite in the Presence of Alkali, Alkaline Earth and Hydrolyzable Metal Ions." Water, Air, & Soil Pollution **145**(1): 155-168.

Zgheib, S., Moilleron, R. and Chebbo, G. (2011). "Influence of the land use pattern on the concentrations and fluxes of priority pollutants in urban stormwater." Water Science and Technology **64**(7): 1450-1458.

Zhang, H. and M. Olson (2012). "Effect of Heavy Metals on Bacterial Attachment in Soils." Journal of Environmental Engineering **138**(11): 1106-1113.

Zhang, L., E. Seagren, et al. (2011). "Long-Term Sustainability of Escherichia Coli Removal in Conventional Bioretention Media." Journal of Environmental Engineering **137**(8): 669-677.

Zhang, L., E. A. Seagren, et al. (2010). "The Capture and Destruction of Escherichia coli from Simulated Urban Runoff Using Conventional Bioretention Media and Iron Oxide-coated Sand." Water Environment Research **82**(8): 701-714.

Zhang, L., E. A. Seagren, et al. (2012). "Effects of Temperature on Bacterial Transport and Destruction in Bioretention Media: Field and Laboratory Evaluations." Water Environment Research **84**(6): 485-496.

Appendix A: List of Symbols

Variables

A : Hamaker constant

A_s : porosity dependent parameter

A_{AWI} : air-water interface area

A_{SWI} : specific soil-water interface area

a_p : particle radius

C : number of free bacteria per unit volume in the aqueous phase

c_0 : initial bacteria concentration

d_c : collector diameter

D : hydrodynamic dispersion coefficient

e : elementary charge

f : faction of mineral surface

g : gravitational constant

I : ionic strength

k_B : Boltzmann constant

k_{SWI} : bacterial attachment to liquid-solid interface

k_{det} : bacterial detachment to liquid-solid interface

k_{AWI} : bacterial attachment to liquid-air interface

k_{str} : bacterial straining rate

k_{decay} : bacterial decay rate

k_{AWI} : bacterial attachment to the air-water interface

L : length of the soil column

m : parameter of van Genuchten water retention function

n : porosity of the soil column; parameter of van Genuchten water retention function

N_R : aspect ratio

N_{Pe} : Peclet number

N_{vdW} : van der Waals number

N_A : attraction number; Avpgadro number

N_G : new gravity number

q : volumetric flux

S : attached bacteria in soil

S_e : effective saturation

t_0 : injection time

t : time

T : temperature

v : interstitial fluid velocity

y : separation distance

z : down gradient distance from where straining process starts

Greek Symbols

α : attachment efficiency; parameter of van Genuchten water retention function

α_u : attachment efficiency under unfavorable conditions

α_f : attachment efficiency under favorable condition

β : empirical factor in the straining function developed by Bradford et.al (2003)

ϵ_0 : permittivity in the vacuum

ϵ_0 : relative dielectric permittivity

ρ : dry bulk density

ρ_f : fluid density

σ : surface tension of water

θ : water content

θ_s : saturated water content.

θ_r : residual water content

ψ_p : article surface potential(bacterial surface potential in our case)

κ : the inverse debye length

κ_{AWI} : liquid to the air-water interface mass transfer coefficient

λ : characteristic wavelength of the interaction

$\Delta\phi$: sum of ϕ_{\max} and ϕ_{\sec}

ϕ_{\max} : maximum energy barriers

ϕ_{\sec} : secondary-minimum depths

η : single collector contact efficiency

ψ_c : collector surface potential respectively

Appendix B: List of Abbreviation and Acronyms

AGW	Artificial groundwater
AWI	Air-water interface
AODC	Acridine orange direct counts
BNS-U	Bacterial suspended in nutrient buffer with untreated soil
BNS-T	Bacteria suspended in nutrient buffer with treated soil
BSS-U	Bacteria suspended in synthetic stormwater with untreated soil
BSS-T	Bacteria suspended in synthetic stormwater with treated soil
BTC	Breakthrough curve
BMP	Best management practice
CDF	Cumulative distribution function
DI water	Deionized water
EDS	Energy dispersive X-ray spectroscopy
IFBL	Interaction force boundary layer model
MICs	Minimum inhibitory concentrations
MR	Mass recovery
SEM	Scanning electron microscopy
SWI	Soil-water interface
SSW	Synthetic stormwater

Appendix C: Experimental Protocols

Preparation of bacterial growth medium (Luria-Bertani medium)

- Dissolve those three components (Tryptone 10 g; Yeast extract 5 g; Sodium Chloride 10 g) into 1 liter of distilled or deionized water and mix thoroughly
- Sterilize the medium by autoclaving at 15 psi, from 121-124 °C for 15 minutes.

Measurement of bacterial zeta potential via Zeta Meter 3.0+

- Fill the cell with bacterial suspension to be tested;
- Insert the electrodes into the cell and connect them to the Zeta Meter 3.0+ unit;
- Select voltage and energize the electrodes;
- Watch bacteria as they move across a grid in the microscope;
- Track each bacteria by pressing the button and holding on until the bacteria move cross the grid;
- The zeta potential of the bacteria is instantly displayed when releasing the button.

Determine *E. coli* in water by membrane filtration methods (EPA method 1603)

- Mark the petri dishes with sample identification and sample volumes.
- Place a sterile membrane filter on the filter base, grid-side up and attach the funnel to the base
- Shake the sample bottle vigorously about 25 times to distribute the bacteria uniformly

- Measure the desired volume of sample or dilution into the funnel. Sample volumes of 1-100 mL are normally tested at half log intervals (e.g., 100, 30, 10, 3 mL).
- Filter the sample, and rinse the sides of the funnel at least twice with 20-30 mL of sterile buffered rinse water.
- Turn off the vacuum and remove the funnel from the filter base.
- Use sterile forceps to aseptically remove the membrane filter from the filter base, and roll it onto the modified mTEC Agar to avoid the formation of bubbles between the membrane and the agar surface. Reseat the membrane if bubbles occur. Run the forceps around the edge of the filter to be sure that the filter is properly seated on the agar.
- Close the dish, invert, and incubate 35 ± 0.5 °C for 2 h.
- After a 2 h incubation at 35 ± 0.5 °C, transfer the plate to a Whirl-Pak® bag, seal the bag, place the bag with the plate inverted in a test-tube rack, and put the rack in a 44.5 ± 0.2 °C water bath for 22-24 h.
- After 22-24 h, remove the plate from the water bath, count and record the number of red or magenta colonies (if practical, 20-80) with the aid of an illuminated lens with a 2-5x magnification or a stereoscopic microscope.
- Select the membrane filter with an acceptable number of colonies and calculate the number of *E. coli* per 100 mL according to the following general formula:

$$(E. coli) / 100ml = \frac{\text{Number of } E. coli \text{ colonies}}{\text{Volume of sample filtered (ml)}} \times 100$$

Appendix D: PHREEQC Programming for the Semi-reactive Microbial Transport Model

```

#define bacteria as a new aqueous species
SOLUTION_MASTER_SPECIES
Bac Bac 0.0 Bac 1.0

SOLUTION_SPECIES
Bac=Bac; log_k 0

#Bacteria attachment, detachment, staining and inactivation are
defined in RATES section.
RATES
Bacsolid # At the soil-water interface
-start
#parameters to calculate DLVO interaction energies
10 e0=8.854E-12 # C/V/m, the permittivity in vacuum
20 er=79 #dimensionless, the relative dielectric prmittivity
30 kb=1.38065E-23 # J/K, Boltzmann constant
40 T=298 # K, temp
50 na=6.02214E+23 # mol-1, Avogadro constant
60 el=1.60218e-19 # C, elemental charge
70 A=9.3e-21 # J, Hamaker constant
80 lamda=100 # nm, the characteristic wavelength of the
interaction
90 ap=419 # nm, particle radius
91 pi=3.1415926

# parameters to calculate single collector efficiency
92 theta=0.41 # represents porosity in bac_solid calculation
93 dp=2*ap*10e-3 #um, particle diameter
94 dc=225.098 # um, collector diameter
95 pp=1.105 #g/cm3, particle density
96 vis=0.0089 # g/cm/s, fluid viscosity
97 pf=0.988 # g.cm-3, fluid density
98 g=9.8 # m/s2, gravitational acceleration
99 pi=3.1415926
100 Dd=(kb*T)/(3*pi*vis*dp)*1e+11 # cm2/s, Bulk diffusion
coefficient
101 U=abs(water_flux(cell_no)/conv_x("meters")*conv_t("seconds"))
#m/s, fluid approach velocity

130 REM Define value of zetac(V) & zetap(V) at various solution
chemistry
140 if (-LA("H+"))>=5 and (-LA("H+"))<6 then goto 145 else goto
210
145 if (MU >= 5E-3) then GOTO 165
150 zetac=-0.0385 # V, zeta potential of collector surface
155 zetap =-0.0614 # V, zeta potential of particle surface

```

```

156 goto 300
165 if (MU>= 15E-3) then GOTO 185
170 zetac=-0.0222
175 zetap=-0.0488
176 goto 300
185 if (MU>= 100E-3) then goto 197
190 zetac=-0.0136
195 zetap=-0.0384
196 goto 300
197 zetac=-0.0116
198 zetap=-0.0215
199 goto 300

210 if (-LA("H+"))>= 6 and (-LA("H+"))<7 then goto 212 else goto
250
212 if (MU >= 5E-3) then GOTO 220
214 zetac=-0.048
216 zetap=-0.045
217 goto 300
220 if (MU>= 15E-3) then GOTO 228
222 zetac=-0.048
224 zetap=-0.0321
225 goto 300
228 if (MU>= 100E-3) then goto 240
230 zetac=-0.035
238 zetap=-0.0179
239 goto 300
240 zetac=-0.0227
241 zetap=-0.0215
242 goto 300

250 if (-LA("H+"))>= 7 and (-LA("H+"))<8 then goto 252
252 if (MU >= 5E-3) then GOTO 260
254 zetac=-0.057
256 zetap=-0.045
257 goto 300
260 if (MU>= 15E-3) then GOTO 268
262 zetac=-0.0418
264 zetap=-0.0338
265 goto 300
268 if (MU>= 100E-3) then goto 280
270 zetac=-0.0418
272 zetap=-0.0338
273 goto 300
280 zetac=-0.0237
285 zetap=-0.02

```

#parameters used of algorithm for finding the roots

```
300 e = 1E-8
```



```

301 max = 100

310 if (get(1)<0.0001) then x0 = .001 else x0=get(1) #nm
320 x1 = 0.95*x0

330 gosub 3000 #calculate general variables

#Determination of maximum using first derivative
410 choice = 2 #derivative
420 GOSUB 5000 #algorithm to find root
425 choice=1
430 on choice gosub 4000, 6000 #calculate y
460 upper = y # maximum phi_tot
465 if upper<0 then goto 780 # cases when no energy barriers
exist

#determination of root of total function starting from maximum
500 x0 = x
510 x1 = x0+0.5*x0
525 choice=1
530 gosub 5000
540 on choice gosub 4000, 6000

#Determination of minimum using first derivative starting from
root
600 x0 = x
610 x1 = x0+0.5*x0
625 choice=2
630 gosub 5000
635 choice=1
640 on choice gosub 4000, 6000
660 lower = y #local minimum phi_tot

700 REM Calculation of bacterial attachment efficiency
710 x = (ABS(lower))^0.5 # lower integration bound
720 gosub 7000 # Function call of equation to be calculated
730 fa= yout
735 x1=upper-lower # for cases when no energy barrier exist
736 if x1<0 then goto 780
740 x = (upper-lower)^0.5 #upper integration bound
750 gosub 7000
760 fb = yout
770 att=1-(fb-fa) # attachment efficiency
775 fra=0 # fraction of mineral surfaces
776 att1=att*(1-fra)+fra*1 # attachment efficiency is 1 under
the favorable condition

771 goto 800

780 att=1 # The attachment is assumed to be favorable when no
energy barrier exists

```

```

# kdet is the detachment rate between liquid-solid interface
800 kdet_coe=5e-9 # mass transfer coefficient, m s-1
801 f=tot("water")
803 SWI=6*(1-f)/(dc*1e-6) # soil water interface area, m-1
805 kdet=kdet_coe*SWI # s-1, detachment rate between liquid-solid
interface
806 kdet=kdet*60 #min

810 gosub 8100 #calculate general variables for eta and katt
820 eta=2.4*AS^(1/3)*NR^(-0.081)*NPE^(-
0.715)*NVDW^(0.052)+0.55*AS*NR^(1.675)*NA^(0.125)+0.22*NR^(-
0.24)*NG^(1.11)*NVDW^(0.053) # single collector contact
efficiency

900 REM Calculation of attachment rate in liquid-solid interface
960 katt=3*(1-theta)*eta*att1*U/(2*theta*dc*1E-6) # 1/s,
attachment rate
965 katt=katt*60/100 # min-1

970 REM rate calculations
1100 rate=-katt*mol("Bac")+kdet*(m)
1200 moles=rate*time
1400 save moles

1500 end

3000 REM General Variables
3010 D = (zetac^2 + zetap^2) # zeta potential unit, V
3020 P = pi*e0*er*ap*1E-9*D
3030 Q = 2*zetac*zetap/D
3050 muvalue = MU*1000 # ionic strength, mol/m3
3060 kdeb = ((2*na*muvalue*el^2)/(e0*er*kb*T))^0.5 # the
inverse Debye length 1/m
3100 Aq = A*ap*1E-9/6
3110 B = 14/(lamda*1E-9)
3120 num = kb*T
3130 der1 = 2*P*kdeb
3990 return

4000 REM Total function
4010 sepm = x*(1E-9) #separation distance, m
4020 Xd =-kdeb*sepm
4030 p1 = log((1+exp(Xd))/(1-exp(Xd)))
4040 p2 = log(1-exp(2*Xd))
4050 phi_el = P*(Q*p1+p2) #the electrical double layer
interaction energy
4100 phi_vdw = -Aq/(sepm*(1+B*sepm)) # Van der Waals attractive
interaction energy
4200 y = (phi_el + phi_vdw)/num # total interaction energy
4990 return

```

```

5000  n=0
      # 'Start iteration
5010  x=x0
5020  on choice gosub 4000, 6000
5030  y0=y
5040  x=x1
5050  on choice gosub 4000, 6000
5060  y1=y
5070  if ABS(y1-y0)<1E-24 then y1=y0+1E-24
5080  x=(x0*y1-x1*y0)/(y1-y0)
5090  n=n+1
      # 'Test for convergence
5100  if n>=max then return
5105  if (x<0) then goto 5150
5110  if ABS((x1-x0))<e then return
5111  if x>300 then return # let the algorithm stop when the
separation distance is over 300nm
      # 'Update positions
5120  x0=x1
5125  y0=y1
5130  x1=x
5140  goto 5030
5150  x0=0.9*x0
5160  x1=0.9*x1
5170  goto 5010
5990  return

6000  REM First derivative
6010  sepm = x*(1E-9)
6020  Xd =-kdeb*sepm
6030  exp1 = exp(Xd)
6040  p1 = der1*exp1*(Q-exp1)
6070  exp1 = exp(2*Xd)
6080  p2 = (exp1-1)
6090  term1 = p1/p2
6100  p1 = 2*B*sepm+1
6110  p2 = sepm*sepm*(B*sepm+1)^2
6130  term2 = Aq*p1/p2
6200  y = term1 + term2
6990  return

7000  REM Function of Maxwell model
7010  t = 1/(1+0.47047*x)
7020  exp1 = exp(-x*x)
7030  erf = 1 - (0.3480242 * t - 0.0958798 * t*t + 0.7478556 *
t*t*t)*exp1
7040  yout = erf - 1.128379*x*exp1
7050  return

REM general variables for eta
8100  gama=(1-theta)^(1/3)

```

```

8110 AS=2*(1-gama^5)/(2-3*gama+3*gama^5-2*gama^6) # porosity
dependent parameter
8120 NR=dp/dc # aspect ratio
8130 NVDW=A/(kb*T) # van der Waals number
8140 NPE=U*dc/Dd/100 #the Peclet number
8150 NA=A*1000/(12*pi*vis*100*((dp/2000000)^2)*U) # the
attraction number
8160 NG=(2/9)*(dp/2000000)^2*(pp-pf)*g/(vis*U)*10000 #the new
gravity number
8300 return

-end

Bacair # at the air-water interface
-start
#parameters for air-liquid interface attachment rate
10 REM kair is the attachment rate between air-liquid interface
20 k_coe=2.5e-11 # m/s, liquid to liquid-air interface mass
transfer coefficient
30 sigma=71.97 # g/s2, surface tension of water
45 theta=tot("water") # water content
50 pf=0.988 # g.cm-3, fluid density
60 g=9.8 # m/s2, gravitational acceleration

100 REM calculating kair
105 choice=2 # select the soil type; choice 1(sand), 2(loamy
sand), 3(loam)...
110 on choice gosub 2000,3000,4000
120 gosub 1000
130 kair=k_coe*at #mass transfer between liquid-air interface

135 kair=kair*60 # min-1

200 REM m=current number of moles of reactants
210 rate=-kair*mol("Bac")
220 moles=rate*time
240 save moles

400 end

1000 REM general variables for kair
1010 Se=(theta-theta_r)/(theta_s-theta_r)
1020 Sel=((se^(-1))^(n/(n-1))-1)^(1/n)
1040 pgt=(pf*1E+6)*g*theta # unit g/s^2/m^2
1060 at=pgt*Sel/(alpha*sigma) # unit 1/m
1080 return

2000 REM hydraulic parameters of sand
2005 alpha=0.145 # 1/m, water retention curve fitting
parameter

```

```

2010 n=2.68          # water retention curve fitting parameter
2020 theta_r=0.045   # residual soil water content
2030 theta_s=0.43    # water content in saturated porous media
2040 return

3000 REM hydraulic parameters of loamy sand
3005 alpha=0.124     # 1/m, water retention curve fitting
parameter
3010 n=2.28          # water retention curve fitting parameter
3020 theta_r=0.057   # residual soil water content
3030 theta_s=0.412   # water content in saturated porous media
3040 return

4000 REM hydraulic parameters of loam
4005 alpha=0.075     # 1/m, water retention curve fitting
parameter
4010 n=1.89          # water retention curve fitting parameter
4020 theta_r=0.065   # residual soil water content
4030 theta_s=0.41    # water content in saturated porous media
4040 return

-end

Bacstr #straining process
-start
10 ap=1148 #nm, particle radius
15 dp=2*ap*10e-3 #um, particle diameter
20 dc=225.098 # um, collector diameter
30 beta=0.43 # optimized value for blocking coefficient
calculation
40 L=1 #m, column length
50 totn=101 # total node number
51 c=cell_no
55 psi=(1+((c-1)*L/(totn-1))/(dc*1e-6))^(-beta) # depth

60 rsize=dp/dc #ratio of paticle size to grain size
70 if rsize>0.005 then goto 200 # Staining is considered when the
ratio of particle to soil grain is larger than 0.005

80 kstr=0
90 goto 300

dependent blocking coefficient
200 kstr=269.7*(dp/dc)^1.42 #min-1
300 rate=-psi*kstr*mol("Bac")
400 moles=rate*time
500 save moles
600 end
-end

```

```

Bacdecay #bacterial inactivation
-start
5 REM E coli decay rate is defined based on temperature
10 if TC<=10 then goto 100 else goto 110
100 kdec=7.61e-4 #bacterial decay rate, min-1
105 goto 300
110 if TC<=20 then goto 130 else goto 150
130 kdec=7.97e-4 #min-1
135 goto 300
150 if TC<=37 then goto 175
175 kdec=1.10e-3 #min-1

300 rate=-psi*kstr*mol("Bac")
400 moles=rate*time
500 save moles
600 end
-end

```

#Solution chemistry of stormwater and groundwater

```

SOLUTION 1001 groundwater
  temp      25
  pH 7.9
  units      mmol/kgw
  K          0.75
  Mg         7
  Ca         5.1
  Na         8.7
  N(5)       0.75
  S(6)       12.1
  Cl         1.7
  C(4)       7

```

end

```

SOLUTION 1001 groundwater
  temp      25
  pH 7.9
  units      mmol/kgw
  K          0.75
  Mg         7
  Ca         5.1
  Na         8.7
  N(5)       0.75
  S(6)       12.1
  Cl         1.7
  C(4)       7

```

end

```

SOLUTION 3001 Stormwater
  temp      25

```

```

pH          6
units       mmol/kgw
Cu(2)       0.001259
Pb          0.000386
Zn          0.009177
Na          0.162231
Ca          1.081229
    P       0.019374
    S(6)    0.001259
    Cl      1.090712
    N(5)    0.142857
    Bac    0.36
end

```

```

SOLUTION 4001 Stormwater
temp     25
pH       6
units    mmol/kgw
Cu(2)    0.001259
Pb       0.000386
Zn       0.009177
Na       0.162231
Ca       1.081229
    P    0.019374
    S(6) 0.001259
    Cl   1.090712
    N(5) 0.142857
    Bac  0.82
end

```

```

SOLUTION 5001 Stormwater
temp     25
pH       6
units    mmol/kgw
Cu(2)    0.001259
Pb       0.000386
Zn       0.009177
Na       0.162231
Ca       1.081229
    P    0.019374
    S(6) 0.001259
    Cl   1.090712
    N(5) 0.142857
    Bac  0.57
end

```

```

SOLUTION 6001 Stormwater
temp     25
pH       6
units    mmol/kgw
Cu(2)    0.001259
Pb       0.000386

```

```

Zn      0.009177
Na      0.162231
Ca      1.081229
  P      0.019374
  S(6)   0.001259
  Cl     1.090712
  N(5)   0.142857
  Bac    0.83
end

```

```

SOLUTION 7001 Stormwater
  temp    25
  pH      6
  units   mmol/kgw
Cu(2)    0.001259
Pb       0.000386
Zn       0.009177
Na       0.162231
Ca       1.081229
  P       0.019374
  S(6)    0.001259
  Cl      1.090712
  N(5)    0.142857
  Bac     0.96
end

```

```

SOLUTION 8001 Stormwater
  temp    25
  pH      6
  units   mmol/kgw
Cu(2)    0.001259
Pb       0.000386
Zn       0.009177
Na       0.162231
Ca       1.081229
  P       0.019374
  S(6)    0.001259
  Cl      1.090712
  N(5)    0.142857
  Bac     0.63
end

```

```

SOLUTION 9001 Stormwater
  temp    25
  pH      6
  units   mmol/kgw
Cu(2)    0.001259
Pb       0.000386
Zn       0.009177
Na       0.162231

```



```

Ca      1.081229
P       0.019374
S(6)    0.001259
Cl      1.090712
N(5)    0.142857
Bac 0.19
end

KINETICS 1-61 @Layer 1@ # layer number need to be updated
according to the total node used during the simulation
Bacsolid
-formula Bac
-m 0.0005
Bacair
-formula Bac
-m 0
Bacstr
-formula Bac
-m 0
Bacdecay
-formula Bac
-m 0

SELECTED_OUTPUT
-molalities      Bac

USER_punch
-headings      Bac_solid Bac_air Bac_staining Bac_decay
-start
110 punch kin("Bacsolid")
120 punch kin("Bacair")
140 punch kin("Bacstr")
150 punch kin("Bacdecay")
-end

```

VITA

Name Haibo Zhang

Education

- Ph.D. in Environmental Engineering, Drexel University, March 2013.
Dissertation topic: “Investigating the Effects of Variable Water Chemistry on Bacterial Transport during Stormwater Infiltration”. Advisor: Dr. Mira S. Olson
- M.S. in Civil & Environmental Engineering, Carnegie Mellon University, May 2008
- B.S in Environmental Engineering, Beijing Tech. & Business University, July 2007

Honors and Activities

- Homeland Security Philadelphia Student Chapter Research Day Specialty Award, Drexel University, 2009
- Civil Engineering Scholarship, Carnegie Mellon University, 2007-2008
- Academic Scholarship in Beijing Technology and Business University, 2004-2007
- Research assistant in Drexel University, 2012-2013
- Teaching assistant in Drexel University, 2008- 2012

Selected Publications

Zhang, H. and M.S. Olson, (2012). "Effect of heavy metals on bacterial attachment in soils", *Journal of Environmental Engineering*, 138(11): 1106-1113.

Teng, J., Kumar, A., Zhang, H., Olson, M.S., and P.L. Gurian. (2012). "Determination of Critical Rainfall Events for Quantitative Microbial Risk Assessment of Land-Applied Soil Amendments", *Journal of Hydrologic Engineering*, Vol 17, No. 3, pp. 437-444.

